

THERMOCOUPLE SIGNAL CONDITIONING USING ARTIFICIAL NEURAL NETWORKS

Moses Linda Maseko

A thesis submitted in fulfillment of the requirement for the degree of

MASTERS OF SCIENCE IN ENGINEERING

(ELECTRONIC ENGINEERING)



College of Agriculture, Engineering and Science

University of KwaZulu-Natal

Durban, South Africa

February 2022

Supervisor: Prof. J. Agee

As the candidate's Supervisor I agree to the submission of this thesis

Signed: Date: 17th March, 2022.....

Name: Prof. John Agee

DECLARATION 1 - PLAGIARISM

I,MOSES LINDA MASEKO....., declare that

1. The research reported in this thesis, except where otherwise indicated, is my original research.
2. This thesis has not been submitted for any degree or examination at any other university.
3. This thesis does not contain other persons' data, pictures, graphs or other information, unless specifically acknowledged as being sourced from other persons.
4. This thesis does not contain other persons' writing, unless specifically acknowledged as being sourced from other researchers. Where other written sources have been quoted, then:
 - a. Their words have been re-written but the general information attributed to them has been referenced
 - b. Where their exact words have been used, then their writing has been placed in italics and inside quotation marks, and referenced.
5. This thesis does not contain text, graphics or tables copied and pasted from the Internet, unless specifically acknowledged, and the source being detailed in the thesis and in the References sections.

Signed

.....

..... Date ...24/01/2022.....

ACKNOWLEDGMENTS

First, I would like to express sincere gratitude to my supervisor Prof. J. Agee for his guidance, support, and wisdom; it would not have been possible to complete the project without his assistance. I would like to thank my mother Maggie Lukhele and friends for their undying support throughout this project.

ABSTRACT

Thermocouples are probably the most widely used temperature sensing devices in industrial applications. This is due to their relatively high accuracy. Thermocouples sense temperature using thermoelectric voltages arising due to temperature differences between the hot and cold junctions of the thermocouple. The generated thermoelectric voltage is nonlinear in form. Linear approximations in the conversion of thermoelectric voltages into temperature readings compromise the accuracy of the derived temperature values: requiring further processing of the thermocouple voltage for improved temperature measurements. Moreover, undetected variations in the cold junction temperature could further worsen the accuracy of the temperature sensor. The current study researched the enhancement of the accuracy of thermocouple temperature measurement subjected to both random variations in the reference junction temperature and nonlinearities, with a validation of the design process using T, R, E, and J, thermocouples. To this end, the ITS-90 thermocouple tables based on a fixed 0°C reference junction temperature were not adequate for use in the study, so the thermocouple polynomial equations for the T, R, E, and J thermocouples were simulated in MATLAB, with randomly generated cold-junction temperature values, to produce augmented ITS-90 tables for the four thermocouples studied. Results show that the augmented thermocouple tables accurately compared with the ITS-90 tables when the reference junction temperature was set to 0°C. Data samples were generated from each of the augmented thermocouple tables for neural network studies. Half of the data samples for each of the thermocouples was used to train 'table-lookup' Multilayer Perceptron (MLP) neural networks in MATLAB. Each neural network used the cold-junction temperatures and thermoelectric voltages as inputs, while the corresponding hot-junction temperatures were used as the target outputs. The validation process for the augmented ITS-90 thermocouple tables showed that the E, T, R, and J thermocouples could all reproduce the hot junction temperature within 0.01% of the results found on the ITS-90 tables. The performance results for the neural networks showed that the E-type thermocouple neural network has a worst-case error within 0.2% in reproducing the hot junction temperature. The J-type thermocouple neural network showed a worst-case error within 0.1%, while the T and R-type thermocouple neural network produced worst error case within 0.04% of the results generated by the augmented ITS-90 tables. For the practical validation of the development presented in this thesis, the structure of each of the trained MLP neural networks was coded as a subroutine within an Arduino Uno microprocessor. The hot junction of the thermocouple was placed in a TTM-004 controller or oven. The cold junction of the thermocouple was located in the ambient of the used laboratory and monitored by an LM 35 temperature sensor connected to one of the inputs of the microcontroller. The experimental results showed that temperature of the TTM-004 controller or oven was evaluated to within 2%, 4% and 3% by the signal conditioning unit using T-type, J-type and E-type thermocouple respectively.

TABLE OF CONTENTS

	Page
ACKNOWLEDGMENTS	ii
ABSTRACT	iii
LIST OF FIGURES	vii
LIST OF TABLES	ix
LIST OF ABBRAVIATIONS	x
1. INTRODUCTION	1
1.1 Motivation	1
1.2 Significance of the study and scope	2
1.3 Study approach, aim & objective of the study	3
1.4 Thesis outline	4
1.5 Conclusion	5
1.6 References	6
2. LITERATURE REVIEW	8
2.1 Introduction	8
2.2 Thermocouple drift errors	9
2.3 Nonlinearity of thermocouple	11
2.4 Variation in thermocouple junction temperature	12
2.5 Summary and conclusion	14
2.6 References	15
3. THEORETICAL FRAMEWORK.....	20
3.1 Introduction	20
3.2 Thermocouple: Physics of thermoelectric energy conversion	20
3.3 Thermocouple linearization	23

3.4	Artificial Neural networks	24
3.4.1	Perceptron	24
3.4.2	Back propagation	27
3.5	Instrumentation amplifiers	28
3.5.1	Merits of using instrumentation amplifiers in signal conditioning.....	30
3.6	Microcontroller	30
3.6.1	Merits of microcontrollers	32
3.7	Conclusion	32
3.8	References.....	33
4.	METHODOLOGY	37
4.1	Introduction.....	37
4.2	Thermocouple ITS-90 table augmentation	38
4.2.1	Thermocouple polynomial function.....	39
4.2.2	Testing of thermocouple augmented ITS-90 table	40
4.3	Implementation of the instrumentation amplifier circuit	41
4.3.1	Performance of the instrumentation amplifier.....	43
4.4	Neural Network design: thermocouple linearization and compensation using a neural network.....	44
4.4.1	Neural network design and training.....	46
4.4.2	MLP neural network pruning.....	49
4.4.3	Generalization of neural networks testing	55
4.5	References.....	58
5.	EXPERIMENTAL WORK, RESULTS AND DISCUSSIONS	60
5.1	Introduction.....	60
5.2	Circuit implementation	60

5.3	Experimental results.....	62
5.3.1	Type T thermocouple experimental results and analysis.....	63
5.3.2	Type J thermocouple experimental results and analysis.....	65
5.3.3	Type E thermocouple experimental results and analysis.....	67
5.4	Results analysis and conclusion.....	68
6.	CONCLUSION AND RECOMMANDATIONS.....	69
6.1	Introduction.....	69
6.2	Conclusion	69
6.3	Recommendations for further study.....	70
7.	Bibliography.....	71
	Appendix A	78
	Appendix B.....	79
	Appendix C.....	81
	Appendix D	84
	Appendix E.....	86
	Appendix F.1	88
	Appendix F.2	90
	Appendix F.3	92
	Appendix F.4.....	94
	Appendix G	96
	Appendix H	97

LIST OF FIGURES

Figure 2-1 Type K Thermocouple drift with time [14]	9
Figure 3-1 Thermocouple Seebeck Coefficient vs. temperature [40]	21
Figure 3-2 Simple Thermocouple [13].....	22
Figure 3-3 Thermocouple with hot and cold junction [13]	22
Figure 3-4 Perceptron.....	24
Figure 3-5 Neural Network Structure.....	25
Figure 3-6 Sigmoid activation function	26
Figure 3-7 Hyperbolic tangent activation function	26
Figure 3-8 Rectified linear units (ReLU)	26
Figure 3-9 Inverse tangent function	26
Figure 3-10 Instrumentation amplifier	29
Figure 3-11 Atmega32 microcontroller [36]	31
Figure 3-12 Pushbutton [38]	32
Figure 4-1 Block diagram of the proposed thermocouple signal conditioning system	37
Figure 4-2 Type T Thermoelectric voltage at 0°C reference temperature	40
Figure 4-3 Type R Thermoelectric voltage at 0°C reference temperature	40
Figure 4-4 Type J Thermoelectric voltage at 0°C reference temperature	41
Figure 4-5 Type E Thermoelectric voltage at 0°C reference temperature	41
Figure 4-6 Instrumentation amplifier	41
Figure 4-7 Instrumentation amplifier with Gain =41	43
Figure 4-8 In-Amp performance with Gain of 41	44
Figure 4-9 Block diagram of ANN design, train, and testing process	45
Figure 4-10 Type E Thermocouple Neural Network structure	47
Figure 4-11 Type J, R, T Thermocouple Neural Network structure	47

Figure 4-12 Type J: NN training error	48
Figure 4-13 Type R: NN training error	48
Figure 4-14 Type E: NN training error	48
Figure 4-15 Type T: NN training error	48
Figure 4-16 Type J Thermocouple neural network Structure with weights and biases	49
Figure 4-17 Type J Thermocouple: Neural Network training error with two hidden neurons.....	50
Figure 4-18 Type R Thermocouple neural network Structure with weights and biases	51
Figure 4-19 Type R Thermocouple: Neural Network training error with two hidden neurons	52
Figure 4-20 Type T Thermocouple neural network Structure with weights and biases.....	52
Figure 4-21 Type T Thermocouple: Neural Network training error with two hidden neurons.....	53
Figure 4-22 Type E Thermocouple neural network Structure with weights and biases.....	54
Figure 4-23 Type E Thermocouple: Neural Network training error with two hidden neurons.....	55
Figure 4-24 Type E: NN generalization error	56
Figure 4-25 Type J: NN generalization error	56
Figure 4-26 Type R: NN generalization error	56
Figure 4-27 Type T: NN generalization error	56
Figure 5-1 Flow Chart of the Proposed Software Design	60
Figure 5-2 Instrumentation amplifier PCB.....	61
Figure 5-3 Experimental setups at Chemical Engineering Laboratory	62
Figure 5-4 Type T: Temperature evaluated by neural network and TTM-004 Oven.....	64
Figure 5-5 Type J: Temperature evaluated by neural network and TTM-004 Oven	66
Figure 5-6 Type E: Temperature evaluated by neural network and TTM-004 Oven.....	68

LIST OF TABLES

Table 1-1 Typical Thermocouple types [22].....	1
Table 4-1 Instrumentation Amplifier Measurements Gain= 41	43
Table 4-2 Type J Thermocouple weights and biases	50
Table 4-3 Type R Thermocouple weights and biases	51
Table 4-4 Type T Thermocouple weights and biases.....	53
Table 4-5 Type E Thermocouple weights and biases.....	54
Table 5-1 Experimental results for TTM-004 temperature (°C) measurement using type T thermocouple.....	63
Table 5-2 Experimental results for TTM-004 temperature (°C) measurement using type J thermocouple.....	65
Table 5-3 Experimental results for TTM-004 temperature (°C) measurement using type E thermocouple.....	67

LIST OF ABBRAVIATIONS

ADC	Analog to Digital Conversion
ANN	Artificial Neural Network
CMR	Common-mode rejection
CMRR	Common-mode rejection ratio
DE	Differential Evolution
GRNN	Generalized regression neural network
LCD	Liquid Crystal Display
NIST	National Institute of Standards and Technology
NTC	Negative temperature coefficient
PC	Personal Computer
RBF	Radial Basics function
RBFNN	Radial Basis Function Neural Network
RTD	Resistance temperature devices CJC
EMF	Electromotive Force
IC	Integrated Circuit
IR	Infrared Thermometer
MLP	Multilayer Perceptron
PCB	Printed Circuit Board
RC	Resistor-Capacitor
RTM	Resin flow in transfer moulding
NN	Neural Network
CJC	Cold Junction Compensation
ITS -90	International Temperature Scale of 1990

1. INTRODUCTION

A number of processes in nature involve energy flow or energy exchange, whether the process is a biological process in living organisms, a chemical process, power generation, or a mechanical process. Subsequently, energy changes are accompanied by temperature changes due to that temperature is the most measured quantity in this era. However, this quantity has a significant influence on industrial applications or processes. The introduction chapter outlines the motivation for the current study, the significance of the study, the aim and objectives of the study, as well as the methodology.

1.1 Motivation

A thermocouple is defined as a temperature-sensing device with a number of industrial applications. A thermocouple is made by joining the ends of two dissimilar metals (conductors) to form two junctions, known as the cold (reference) junction and the hot (measuring) junction, respectively [8]. The commonly used thermocouples are listed in Table 1-1 below, with the composition of the metals used.

Table 1-1 Typical Thermocouple types [22]

Type	Positive Material	Negative Material	Accuracy	Range °C
R	Pt, 13%Rh	Pt	0.25% or 1.5°C	-50 to 1768
T	Cu	Cu, 45%Ni	0.75% or 1.0°C	-270 to 400
E	Ni, 10%Cr	Cu, 45%Ni	0.5% or 1.7°C	-270 to 1000
J	Fe	Cu, 45%Ni	0.75% or 2.2°C	-210 to 1200
B	Pt, 30%Rh	Pt, 6%Rh	0.5%, >800°C	50 to 1820
P	Platinel II	Platinel II	1.0%	0 to 1395
K	Ni, 10%Cr	Ni,2%Al,2%Mn 1%Si	0.75% or 2.2°C	-270 to 1372
S	Pt, 10%Rh	Pt	0.25% or 1.5°C	-50 to 1768

Once the two junctions (cold and hot) are at different temperatures, current flows through the circuit resulting in electromotive force (EMF) produced in the circuit. The resulting EMF is a nonlinear function of the temperature difference between the hot junction and cold junction temperatures. The EMF can be represented in the form [20];

$$V = a_0 + a_1(T_H - T_{ref}) + a_2(T_H^2 - T_{ref}^2) + \dots + a_n(T_H^n - T_{ref}^n) \quad (1.1)$$

Where a_0, a_1, \dots, a_n ; are thermocouple constant of type T, E, J, B, R or S, etc.

T_H ; the hot/measuring junction temperature and

T_{ref} ; the reference/cold junction temperature.

Thermocouple devices generate a small dc voltage in millivolts and microvolts [10]. For purposes of sensitivity enhancement and accuracy improvement, this voltage must be amplified to a level beyond that produced by white noise so that the output of the thermocouple could be processed by microcontrollers or microprocessors with fidelity. Thermocouples have limitations arising from unwanted variations in the cold junction temperature [13], which can affect both the accuracy and sensitivity of the thermocouple. Thermocouple output voltages are also affected by hysteresis and parameter drift with time.

1.2 Significance of the study and scope

Earlier industrial solutions to the problem of variable cold- junction temperature involved keeping the reference junction temperature in ice, regulated at 0°C. The other critical limitation is the nonlinearity of thermocouple output voltage with respect to temperature [2-3]; there has been research on both software and hardware thermocouple linearization methods, including the use of neural networks [12-20]. Thermocouples have issues of drift voltage and pressure-induced errors. This study will only focus on cold junction compensation, dc offset, and nonlinearity. In this research work, the proposed solution will be to design a system that will solve all three problems, namely, dc bias, cold junction compensation, and nonlinearity, to improve the accuracy of thermocouples. Solving the three problems will significantly improve thermocouple temperature measurement as these three problems contribute greatly to measurement accuracy. Moreover, the cost of using thermocouples in industrial applications will reduce as there will be no need for reference junction temperature monitoring systems.

1.3 Study approach, aim & objective of the study

Aim and Study Approach

The main aim of this study is to approach the enhancement of the accuracy of thermocouple temperature measurement in a manner that is independent of the particular type of thermocouple used. In this approach, a temperature-to-voltage sensor located in proximity to the thermocouple reference junction will be used to monitor variations in the temperature of the reference junction. This sensor shall generate proportional voltage outputs. An instrumentation amplifier with a negligible dc bias/offset will be used to amplify the microvolts or millivolts output voltage of the thermocouple. A microcontroller will be used to read off the output voltages from both the thermocouple and the sensor monitoring reference junction. The voltage reading from the sensor will be converted to temperature ($^{\circ}\text{C}$), and the voltage from the thermocouple will be divided by the gain of the instrumentation amplifier to normalize the reading. Both the converted sensor and thermocouple readings will be used as input to the neural network. The standard ITS-90 tables for thermocouple types show thermoelectric voltage in mV at various measured/hot junction temperature(s) with reference junction at 0°C . Thereof, the thermocouple polynomial equation;

$$V = a_0 + a_1(T_H - T_{ref}) + a_2(T_H^2 - T_{ref}^2) + \dots + a_n(T_H^n - T_{ref}^n) \quad (1.2)$$

Will be used to generate augmented ITS-90 tables with variations in the reference junction temperature [21]. Thereafter, one neural network will be designed, trained, and tested for each thermocouple type to approximate the measured temperature of a thermocouple given sensor ($^{\circ}\text{C}$) and thermocouple voltage (mV) readings. The neural network will be trained and tested using data from the augmented ITS-90 table(s) as training data (inputs and target). The process will be repeated for the other thermocouple types sampled for this study, namely: T, R, E, and J thermocouples.

Objectives

The aim of this study will be achieved by pursuing the objectives as outlined by the following points:

1. Generate new ITS-90 tables referred to as augmented ITS-90 tables in this study for each thermocouple type with random variations in reference junction temperature using the thermocouple polynomial equation in MATLAB:

$$V = a_0 + a_1(T_H - T_{ref}) + a_2(T_H^2 - T_{ref}^2) + \dots + a_n(T_H^n - T_{ref}^n) \quad (1.3)$$

2. Design and test an instrumentation amplifier with negligible dc offset to amplify the mV reading of thermocouples.
3. Design and train Neural Network; to explore a neural network for function approximation to linearize thermocouple characteristics and compensate the variation in reference junction temperature. The augmented ITS-90 tables are used as inputs (thermoelectric voltage and reference junction temperature) and targets (measured temperature) during the training.
4. Test Neural Network for generalization with data not used for training from the augmented ITS-90 tables. Suppose targeted performance is not reached, redesign, train, and test the neural network until performance target is met.
5. Repeat steps 2 – 4 for T, R, E, and J type thermocouples.
6. Write a microcontroller program; for reading off both the output voltage of the thermocouple and temperature sensor. Convert the output voltage of the sensor into temperature ($^{\circ}\text{C}$) and divide the voltage of the thermocouple by the gain of the instrumentation amplifier. Select thermocouple type connected; as a result, call the neural network for that specific thermocouple to compute the measured temperature and display it on LCD/PC.

1.4 Thesis outline

This thesis is divided into six chapters as follows; Chapter 1 of the thesis gives a general introduction of the principle and characteristics of thermocouple and cold junction compensation methods. Moreover, it introduces the topic of the research and outlines the objectives, methodology, and scope of the research. Chapter 2 is a literature review of thermocouple cold junction compensation methods used in the past and currently for measuring temperature using thermocouples and present literature on artificial neural networks for cold junction compensation and function approximation. Chapter 3 gives the research theory employed in this study and all the instruments used in this research. Chapter 4 is devoted to the presentation of methodology employed in the proposed thermocouple signal conditioning using neural networks. Chapter 5 presents experimental results and analysis of this study with a focus on the ANN performance in function approximation/linearization of thermocouple characteristics and the overall performance of the signal condition system. Chapter 6 concludes the thesis by giving the conclusions based on the performance of the designed ANN and the overall performance of the embedded controller for thermocouple signal conditioning, and the evaluation of the proposed method on accuracy enhancement in temperature measurement using thermocouples.

1.5 Conclusion

In conclusion, thermocouples have challenges with reference junction temperature variations, dc offset, and nonlinearity that give rise to measurement errors. The following chapters of this study will address the aforementioned challenge by designing and implementing a technique for reference junction compensation, dc offset correction, and thermocouple linearization using neural networks, using the literature review presented in chapter 2 of this thesis.

1.6 References

- [1] P. Foote, "Note on the cold-junction corrections for thermocouples", Bulletin of the Bureau of Standards, 1913., vol. 9, no. 4, p. 553
- [2] A. Mukherjee, D. Sarkar, A. Sen, D. Dey, S. Munshi, "An analog signal conditioning circuit for thermocouple temperature sensor employing thermistor for cold junction compensation", International Conference on Control, Automation, Robotics and Embedded System (CARE), 2013
- [3] J. Tang, Y. Zhang, X. Tang, J. Liu, "Nonlinearity correction of the thermocouple based on neural network", Global Congress on Intelligent Systems, 2009, pp. 28-32.
- [4] U. Sarma, P.K. Boruah, "Design and development of a high precision thermocouple based smart industrial thermometer with online linearization and data logging feature", Measurement 43, 2010, pp. 1589 – 1594.
- [5] R.P. Areny, J.G. Webster, Sensors and Signal Conditioning, second ed., Wiley, New York, 2001.
- [6] T. Goker. "Constraints on monitoring resin flow in transfer molding (RTM) process by using thermocouple sensors," Applied Science and Manufacturing, 2007, vol. 38, pp. 1363-1386
- [7] Y. Yuyan. "The design of intelligent temperature control system of thermocouples sensor". Proceedings of the international symposium on Test and Measurement, 2003, vol. 3, pp. 2269-2272
- [8] V. P. Preobrazhensky, "Measurements and Instrumentation in Heat Engineering", MIR Publishers, Moscow, 1980.
- [9] U. Tietze, and C. Schenk, "Electronic circuit design and applications", Narosa Publishing House, New Delhi, 1992.
- [10] T. R. Padmanabhan, "Industrial Instrumentation", Springer-Verlag, London, 2000.
- [11] U. Sinha, "Cold junction compensation of thermocouple by using semiconductor diode", Journal of the IETE, Vol. 17, No. 1&2,2000, pp. 101-105.
- [12] M. Engin, D. Engin, "Compensation of thermocouple nonlinearities with embedded system", 5th Mediterranean Conference on Embedded Computing (MECO), 2016, pp. 234 – 237.
- [13] M. Zlatanovic, M. Dukic, I. Popovic and Z. Zirojevic, "Compensation of thermocouple reference junction temperature variation by a silicon temperature sensor", 21st International conference on microelectronics, vol.2,1997, pp. 557-560.
- [14] S. Chakravarthy and J. Ghosh, "Function Emulation Using Radial Basis Function Networks", Neural Networks, vol. 10, no. 3, pp. 459-478, 1997.

- [15] S. Hannan, R. Manza and R. Ramteke, "Generalized Regression Neural Network and Radial Basis Function for Heart Disease Diagnosis", *International Journal of Computer Applications*, vol. 7, no. 13, pp. 7-13, 2010.
- [16] F. Caldwell, "Temperatures of thermocouple reference junctions in an ice bath", *Journal of Research of the National Bureau of Standards, Section C: Engineering and Instrumentation*, vol. 69, no. 2, p. 95, 1965.
- [17] H. Shaker, A. Saleh, A. Ali and M. Abd Elaziz, "Self-Calibrating Enabled Low Cost, Two Channel Type K Thermocouple Interface for Microcontrollers", *Arab Journal of Nuclear Sciences and Applications*, vol. 0, no. 0, pp. 1-9, 2018.
- [18] Y. WANG, Z. YAN and W. HE, "Thermocouple Cold End Compensation System with Programmable Function", *DEStech Transactions on Computer Science and Engineering*, no. -, 2017.
- [19] Z. Zainuddin, O. Pauline, "Function Approximation Using Artificial Neural Networks", *INTERNATIONAL JOURNAL OF SYSTEMS APPLICATIONS, ENGINEERING & DEVELOPMENT* Issue 4, Volume 1, 2007
- [20] L. Marquez, T. Hill, "Function Approximation Using Backpropagation and General Regression Neural Networks"
- [21] Massoud, May, et al. "The Path to Informed Policies: Environmental Health Indicators and the Challenges of Developing a Surveillance System in Lebanon." *Journal of Environmental Health*, vol. 79, no. 8, National Environmental Health Association, Apr. 2017, p. E1.
- [22] Ponce, "Greenhouse automation and control", *Greenhouse Design and Control*, 2014.

2. LITERATURE REVIEW

2.1 Introduction

A thermocouple is defined as a thermoelectric device that is used for measuring temperature, consisting of two wires of different metals connected at two points and a voltage being developed between the two junctions in proportion to the temperature difference [1]. This chapter seeks to present a review of the literature undertaken to clarify the research problem and the methodology used in solving the thermocouple conditioning problem. This chapter will discuss thermocouple drift errors, the nonlinearity of thermocouple(s), as well as variation in thermocouple junction temperature.

Thermocouples are used in many temperature-sensing applications, including the control of deposition process for thin films [1], measurement of a plant, and water potential [2] – [4]. Furthermore, thermocouples are used for monitoring temperature in gas turbines for jet engines [5] and measuring the temperature of power electronics components [7] – [9]. There are favorable factors that attribute to the extensive use of thermocouple temperature sensors in the industry, that includes the vast temperature range of operation of thermocouples, their fast response time, durability or resistance to corrosion, small dimensions, relatively cheap pricing, high accuracy, and stability [10] – [12].

A thermocouple consists of two dissimilar metals joined together by two junctions. The principle of operation of thermocouples is based on the thermoelectric effects between these two dissimilar metals [13]. Due to this effect, a thermoelectric EMF or voltage is generated at the connected ends (junctions) of the two metals when their junctions are kept at different temperatures. This thermoelectric is known to be related to the difference in temperature between the two junctions in a generally nonlinear manner [14]. The sensitivity and calibration of a thermocouple are determined by the thermo-elements (thermoelectric junction). The thermoelectric effect leads to a thermocouple voltage of the form:

$$V = a_0 + a_1(T_H - T_{ref}) + a_2(T_H^2 - T_{ref}^2) + \dots + a_n(T_H^n - T_{ref}^n) \quad (2.1)$$

Where: a_0, a_1, \dots, a_n ; are the thermocouple coefficients of type K, J, B, R, or S.

T_H is hot junction temperature and

T_{ref} the reference/cold junction temperature (junction temperatures measured in degree centigrade)

Typical thermocouple nonlinearities can be seen from the characteristics shown in Figure 2-1. The nonlinear relationship between the thermoelectric voltage and the junction temperatures leads to three challenges in the utilization of thermocouple devices as temperature sensors. These challenges are

nonlinearity [14] – [18], low drift voltages [19, 21], variation of the output voltage with changes in the reference junction temperature [20] – [26], and pressure dependence of the EMF of thermocouples [37] – [39].

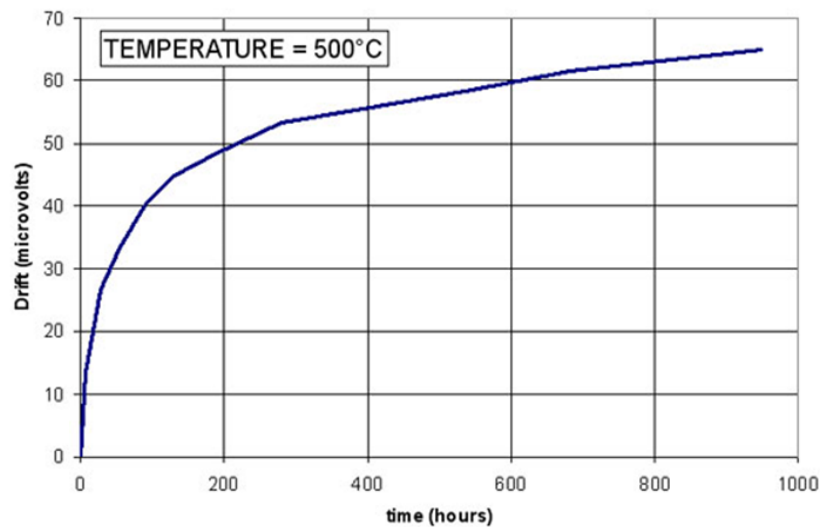


Figure 2-1 Type K Thermocouple drift with time [14]

2.2 Thermocouple drift errors

Thermocouples have a challenge of drift errors. In a method of minimizing temperature drift errors of conditioning circuits through the use of artificial neural networks, in the current study, an ANN is proposed to overcome the problem of temperature drift errors associated with temperature variation [19]. An AD595 temperature sensor is used to generate a voltage proportional to the temperature of the conditioning circuit, and a type K thermocouple is used to measure the temperature of the quantity of interest. The limitation of this method is that it does not account for drift errors at high temperatures, which may be a result of long-time in service. The present study is focusing only on thermocouple cold junction compensation and linearization, but the low drift is not considered [19]. Thermocouple stability when measuring temperatures above 1000 degrees' centigrade results in drift velocities that can impact the measurement accuracy of the measured temperature. Thermocouples are the most used sensors for temperature measurement in nuclear applications, and they are affected by the intense neutron fluxes due to interaction with neutrons. The thermo-elements of the thermocouples undergo composition resulting in a time-dependent drift of the thermocouple signals [20]. Metallurgical changes of the thermos-elements during the operation of the thermocouple at high-temperature causes drift (change in voltage from expected value), which results in an error in the measured thermocouple signal. Figure 2-

1 displays type K thermocouple exposed at 500 degrees centigrade and drift as a function of the exposure with time. Thermocouples used in high-temperature applications experience atomic displacements and transmutation. Atomic displacement is defined as the displacement of atoms from their mean position in the crystal structure, which may be the result of temperature-dependent atomic vibrations or static disorder in a crystal lattice [41]. In thermocouples, atomic displacement generates dislocation loops and voids into the irradiated thermo-elements, thus leading to very significant drift. In [20], Cambridge type N thermocouples are compared with conventional Inconel 600 sheathed type N thermocouples during an out-of-pile test undertaken at INL has proved that the Cambridge sheath can provide a significant drift reduction of about 60%. The Cambridge sheath allows for the removal of contaminants that reduce the change in the composition of the thermo-elements during operation, so thus minimizing drift. Contamination can be built-in, acquired in service, or originate from the thermocouple's alloy combination.

Hygiene is essential in the use of thermocouples, and the user must ensure that a thermocouple is not contaminated before or during the service. It is critical not to build in contamination such as metal swarf derived from end caps. Burning out ceramics and wiping wires with industrial methylated spirits are both essential practices to follow. The upper operating temperatures of Pt thermocouples are sufficiently high to destabilize lower grade ceramics, releasing metallic elements from their oxides. Thus, the preferred insulation for both twin-bore and outer sheaths is high purity recrystallized alumina. Another source of contamination is the furnace load; metallic vapour in vacuum brazing furnaces can condense on the thermocouple and cause damage. It is vital that the design of the installation protects the thermocouple with suitable physical barrier layers of metallic and ceramic closed-end tubes. However, while additional layers prolong the life of the couple, they do this to the detriment of the response rate and accuracy. Thick metal cladding, which conducts heat to the furnace wall, can act as a heat sink, attracting and condensing contamination.

In order to improve the accuracy of thermocouple measurement and prolong the usage of thermocouples, one should ensure that:

- The environment is clean.
- The thermocouples are not stressed.
- They are annealed before use.
- High-quality ceramics are used, and mechanical damage is avoided.

The disadvantage of thermocouples is their relatively low output signal in the millivolts range, therefore making thermocouple reading sensitive to corruption from electrical noise. Due to the low drift and low

output signal, it is essential that the thermocouple output signal is amplified using an amplifier with a low offset. Therefore, in this study, an instrumentation amplifier will be used for the amplification of a thermocouple signal as it has a low offset and low common rejection ratio.

2.3 Nonlinearity of thermocouple

There exist a number of temperature measuring devices such as pressure transducers, strain gauges, and resistance temperature devices (RTDs). Nonetheless, thermocouples are the most popular temperature sensors. Thermocouples operate under the principle of the Seebeck Effect (thermoelectric effect); their outputs are nonlinear to the measured temperature. Thermocouple types exhibit distinctive nonlinearity, moreover results in increased error over a wide temperature range. A solution of thermocouple nonlinearity correction using a neural network is presented in [18], whereby a Backpropagation (BP) neural network is employed. The thermoelectric potential of a K-type thermocouple is used as the neural network inputs and the equivalent temperature used as target (output) value; thereafter, the BP neural network is trained. The reduction in nonlinearity is seen by the deviation between the results of the training and the target values, with the suitable measurement error being small, nonlinear correction is finished [18]. The limitation with this proposed solution is that the network is trained with 0°C reference temperature, which in an industrial application, the reference temperature may vary, leading to error measurements. Moreover, it is expensive to maintain a reference temperature at 0°C in industrial applications where thermocouples are most used.

A multilayer neural network-based system for processing thermocouple signals and performing linearization of the sensor output exists [19]. The reference junction of the thermocouple is at ambient temperature, and it is allowed to vary in order to remove the contribution of reference junction to the measured voltage a thermocouple is used. The thermistor is placed in series with a known resistance; the voltage drop across the constant resistance is measured and as temperature increases [42]. The resistance of the thermistor decreases; therefore, the contribution of the ambient temperature block can be subtracted from the measured thermoelectric voltage. The effectiveness of this solution for linearization lies in the selection of the constant resistor. The infirmity of the proposed solution is that it can only work on a single thermocouple type, and if another thermocouple type is used, a new constant resistance must be selected since thermocouple types have different characteristics. Zhang and Dai [20] presented a nonlinear calibration of a thermocouple sensor using least squares support vector regression (LS-SVR). The proposed method of LS-SVR takes the output voltage of the thermocouple sensor as input and measured temperature output to eliminate the nonlinear errors in the detection process. The calibration process of a thermocouple sensor is based on system identification and the numerical algorithm.

Thermocouples require signal conditioning for linearization and error compensation to achieve better performance. Furthermore, the low voltage outputs of thermocouples must be compensated by amplification. Conversion and transmission of the sensor output process have an influence on the accuracy of measurement, so these processes must be taken into consideration when developing a signal conditioning system for thermocouples. This proposed thermocouple signal conditioning using the neural network will incorporate all the challenges nonlinearity exploited in this section through a neural network. All the limitations with thermocouple nonlinearity correction using the neural network will be addressed, and neural networks will be used due to their capability to approximate any nonlinear function.

2.4 Variation in thermocouple junction temperature

The most significant disadvantage of thermocouples is dependent on the variation of reference/cold junction thermoelectric that contribute to the measured temperature according to the polynomial equation given by:

$$V = a_0 + a_1(T_H - T_{ref}) + a_2(T_H^2 - T_{ref}^2) + \dots + a_n(T_H^n - T_{ref}^n) \quad (2.2)$$

Where: V = thermocouple EMF/thermoelectric voltage.

A thermocouple measurement accuracy is only determined by accurate measurement of the reference junction temperature. Therefore, in order to improve thermocouple accuracy, effort must be directed in solving the concern of reference junction variations. When thermocouples were first used in temperature measurement, reference junction was placed in an ice bath and kept constant at 0°C [22]. Temperature measurement was carried out since reference temperature is known, and from the polynomial equation, it can be solved. This method is not feasible for use as maintaining the ice bath is costly; therefore, the solution to this problem is a technique called cold (reference) Junction Compensation (CJC). A solution of cold junction compensation for a K-type thermocouple based on the AD8495 thermocouple amplifier was presented [22]. The AD8495 amplifier has a gain of 122 that is used to amplify the thermocouple signal, resulting in the system having a 5mV/°C output with a sensitivity of 200°C/V. However, challenges associated with this solution exist, and the challenges are that it is thermocouple type-specific (K-type). Therefore, it does not accommodate other thermocouple types. In [23], a proposed solution for thermocouple reference junction compensation using operational amplifiers is presented. Thermocouple linearization is through a method called polynomial linearization, where a thermocouple polynomial equation is used [23].

Li-Hui [24] presents a thermocouple signal conditioning the Radial Basics function (RBF) neural network to compensate for thermocouple nonlinearity and cold junction offset. Radial Basis Function

Neural Network (RBFNN) was selected due to that it has robust nonlinear parallel processing and fault-tolerant capability [51] – [53]. The RBFNN was designed for the compensation of an S-type thermocouple in the range of 0 to 1600 degrees centigrade; the error of the neural network was found to be 0.00013. The shortcomings in [24] the method of cold junction compensation is that the reference junction temperature was set to 0°C, which may result in the error of the measured temperature to increase if the reference junction temperature changes significantly. In [25], a study of thermocouple reference junction compensation and nonlinearity correcting is presented, where a microcontroller is used for its computation capabilities to compute the measured temperature with the use of a K-type thermocouple in the range zero up to 250 degrees Celsius with one °C resolution. Reference junction compensation is achieved by using a DS18B20 digital thermometer integrated circuit (IC) to measure the reference temperature on the cold junction formed when connecting K-type thermocouple to the Printed Circuit Board (PCB) connector (copper metals). The measured temperature (DS18B20) is converted into its equivalent K-type thermocouple EMF using the calculations in [26]. The challenge with this method with a resolution of 1-degree centigrade is that the system cannot perform temperature measurement above 50 degrees Celsius and that the method presented in that study uses a thermocouple look-up table.

In [27], a solution is proposed to overcome the problem of temperature drift errors using a two-sensor system. With the two sensors, the first is used to measure the temperature of the object of interest, and the other is used to measure temperature drift errors. The cold junction compensation sensor used is the AD595 which generates a voltage proportional to the temperature of the conditioning circuit. Moreover, the system uses a trained neural network to compensate for external disturbances affecting the thermocouple. Engin et al. [29] presented a compensation of thermocouple nonlinearities using an embedded system, in which a microcontroller is used for measuring the temperature of the isothermal block by the use of a thermistor or RTD sensor, moreover to measure the voltage of the thermocouple. The voltage from the isothermal temperature is subtracted from the measured voltage of the thermocouple, giving the hot junction thermocouple voltage. Using the standard thermocouple table [28], the temperature value corresponding to the obtained voltage can be read [29]. The challenge with this method of thermocouple compensation is that the resulting voltage may not be in the standard tables in such a case; the accuracy of the results will be compromised as either chooses the closest one to the results or perform the interpolation. A new scheme for cold junction compensation and linearization is presented in [30], Differential Evolution (DE) algorithm for neural network training. The circuit for cold junction compensation uses a low-cost thermistor with a negative temperature coefficient (NTC), and linearization is through an artificial neural network. The scheme has been simulated in MATLAB, and it showed excellent performance in linearization and compensation of the cold junction of the thermocouple [30].

Haruyama and Ryoza Yoshizaki [28] conducted a study of 0°C baths for the reference junctions of thermocouples using a solid-state heat pump, which is a system consisting of a thermoelectric heat pump module clamped between the copper block and an aluminum heat sink. This system uses an electronic system to regulate the temperature, and the pre-set temperature is compared with that of a thermistor (13k Ohms at 0°C) [31].

2.5 Summary and conclusion

There are many challenges with the current methods used, mainly on thermocouple cold junction compensation and linearization. The proposed study aims to address all the shortcomings discussed and produce a thermocouple signal condition unit that can cater to several thermocouple types without the need for new hardware. The signal conditioning system using the neural network will ensure high accuracy and cost-effectiveness in the measurement of temperature by using the capability of the neural network to approximate any nonlinear function. Linearization of thermocouples has presented a challenge in the past, but we believe that this proposed method will effectively solve the challenges with thermocouple linearization. Since thermocouples have a low drift, an amplifier will be designed with good linearity, low offset, high sensitivity, low drift, and high common-mode rejection ratio to address some of the challenges discussed.

2.6 References

- [1] R. Generosi, C. Barchesi, M. Luce, and A. Cricenti, "Personal Computer (PC)-based digital apparatus with temperature compensation for measurement of thin films during deposition", American Institute of Physics, 1993
- [2] B.D. Millar, "Improved thermocouple psychrometer for the measuring of plant and soil water potential", *Journal of Experimental Botany*, 1974, Vol. 25, no. 89, pp. 1070 -1084.
- [3] R. Farré, J.M. Montserrat, M. Rotger, E. Ballester and D. Navajas, "Accuracy of thermistors and thermocouples as flow-measuring devices for detecting hypopnoeas", *European Respiratory Journal*, 1997
- [4] J. M.J. Savage, A. Cass and J.M. de Jager, "An accurate temperature correction model for thermocouple hygrometers", *Plant Physiology*, 1982, Vol. 69, pp. 526-530.
- [5] M. Scervini, C. Rae, R. Page, M. Rudkin, S. O'Dell, D. Loveless, and G. Marchais, "The ALPHET Project: a new approach to improve the lifing methodology for thermocouple probes used in gas turbines"
- [6] E.T. Salem¹, D. Ibitayo and B.R. Geil, "A Technique for Die Surface Temperature Measurement of High-Voltage Power Electronic Components using Coated Thermocouple Probes", *Instrumentation and Measurement Technology Conference*, 2006, pp. 651-654.
- [7] R.P. Areny, J.G. Webster, *Sensors and Signal Conditioning*, second ed., Wiley, New York, 2001.
- [8] Tuncol, Goker. "Constraints on monitoring resin flow in transfer molding (RTM) process by using thermocouple sensors," *Applied Science and Manufacturing*, 2007, vol. 38, pp. 1363-1386
- [9] L. Ding, L. Xiaobin and Z. Lei. "Nonlinear calibration for N thermocouple sensor based on least squares support vector machine," *Chinese Journal of Scientific Instrument*. 2007, vol. 28, pp. 640-644
- [10] A. Mukherjee, D. Sarkar, A. Sen, D. Dey, S. Munshi, "An analog signal conditioning circuit for thermocouple temperature sensor employing thermistor for cold junction compensation", *International Conference on Control, Automation, Robotics and Embedded System (CARE)*, 2013
- [11] E. H. McLarain, E. G. Murdock, *The Pt/Au Thermocouple part I and part II*, NRCC/27703, National Research Council of Canada, Ottawa, 1987.
- [12]. G. W. Burns, G. F. Strause, B. M. Liu, and B. W. Mangum, in *Temperature: Its Measurements and Control in Science and Industry*, vol. 6 (Edited by J. F. Schooley), New York, American Institute of Physics, 1992, pp. 531-536.

- [13] D. Lampasi and L. Podesta "A Measurement System Exploiting Non-Linearity of Thermocouples for Cold Junction Compensation", Instrumentation and Measurement Technology Conference, 2004, pp.2170-2175.
- [14] OMEGA Temperature Measurement Handbook, Handbook, Omega Engineering Inc., Stamford, Connecticut, 1979.
- [15] D. Wen, L. Qing, and L. Qiang, "Calibration system for thermocouple application based on the technology of virtual instrument and neural network," 2007 8th International Conference on Electronic Measurement and Instruments, 2007, pp. 1268-1273
- [16] Liu Ding, Li Xiaobin, Zuo Lei. "Nonlinear calibration for N thermocouple sensor based on least squares support vector machine," Chinese Journal of Scientific Instrument. 2007, vol. 28, pp. 640-644
- [17] Dalkiran I., Danisman K, Linearizing E-Type Thermocouple Output Using artificial neural network and Adaptive Neuro-Fuzzy Inference Systems, IEEE 14th Signal Processing and Communications Applications, 2006, pp. 1-4.
- [18] J. Tang, Y. Zhang, X. Tang, J. Liu, "Nonlinearity correction of the thermocouple based on neural network", Global Congress on Intelligent Systems, 2009, pp. 28-32.
- [19] D. Dey and S. Munshi, "A new intelligent scheme for simultaneous cold junction compensation and linearization of thermocouples", Leonardo Electronic Journal of Practices and Technologies, issue 19, 2011, pp. 13 – 28
- [20] S. Zhang and Q. Dai, "Nonlinear calibration of thermocouple sensor based on least squares support vector regression", 5th International Conference on Computer Sciences and Automation Engineering, 2015, pp. 5 – 10
- [21] A.V. Vamsi, G.S. Mohan, and S.S. Skrikanth, "Simplified thermocouple Interface for hot only or cold only measurement with Linearization circuits", IJERA, 2012, Vol. 2, issue 5, pp.1663 – 1667
- [22] M. Duff and J. Towey, "Two ways to measure temperature using thermocouple feature simplicity, accuracy, and flexibility", Analog Dialogue, Vol. 44, 2010
- [23] A. Fang, X. Ye, A. Chen, X. Xu, and R Yu, "Using operational amplifiers to realize the compensation of thermocouples", ISECS International Colloquium on Computing, Communication, Control, and Management, 2008, pp.774 – 777
- [24] G. Li-Hui W. Wu, J. Xiao-bo, "Thermocouple Signal Conditioning with Genetic Optimizing RBF Neural Networks", 2011 IEEE 3rd International Conference on Communication Software and Networks, 2011

- [25] H.H. Shaker, A.A. Saleh, A.H. Ali, and M.A. Elaziz, "Self-Calibrating Enabled Low Cost, Two Channel Type K Thermocouple Interface for Microcontrollers", ICM, 2016, pp. 309-312
- [26] M. Duff and J. Towey," Two Ways to Measure Temperature Using Thermocouples Feature Simplicity, Accuracy, and Flexibility", Analog Devices. [online] Analog.com. Available at: <https://www.analog.com/en/analog-dialogue/articles/measuring-temp-using-thermocouples.html> [Accessed 2 May. 2017].
- [27] J.M.D. Pereira, O. Postolache, P. M. B. S. Girão, and M. Cretu, "Minimizing Temperature Drift Errors of Conditioning Circuits Using Artificial Neural Networks", IEEE TRANSACTIONS ON INSTRUMENTATION AND MEASUREMENT, 2000, Vol. 49, no. 5, pp.1122-1127
- [28] U.S. Secretary of Commerce. (1995). NIST ITS-90 thermocouple database. Available from <http://srdata.nist.gov/its90/main/>.
- [29] M. Engin and D. Engin," Compensation of Thermocouple Nonlinearities with Embedded System", 5th Mediterranean Conference on Embedded Computing (MECO), 2016, pp. 234-237.
- [30] F.R. Caldwell, "Temperatures of Thermocouple Reference Junctions in an Ice Bath", JOURNAL OF RESEARCH of the National Bureau of Standards-C. Engineering and Instrumentation, 1965, Vol. 69C, No. 2, pp. 95-101.
- [31] T. Haruyama, R. Yoshizaki, "A 0 O C bath for the reference junctions of thermocouples by using a solid-state heat pump", J. Phys. E: Sci. Instrum. 19 (1986).
- [32] U. Sarma, P.K. Boruah, "Design and development of a high precision thermocouple based smart industrial thermometer with online linearization and data logging feature", Measurement 43, 2010, pp. 1589 – 1594.
- [33] Y. Yuyan. "The design of intelligent temperature control system of thermocouples sensor". Proceedings of the international symposium on Test and Measurement, 2003, vol. 3, pp. 2269-2272
- [34] M. Zlatanovic, M. Dukic, I. Popovic and Z. Zirojevic, "Compensation of thermocouple reference junction temperature variation by a silicon temperature sensor", 21st International conference on microelectronics, 1998, vol. 2, pp. 557-560.
- [35] Y. WANG, Z. YAN and W. HE, "Thermocouple Cold End Compensation System with Programmable Function", DEStech Transactions on Computer Science and Engineering, 2017.
- [36] W.U. De-hui, "Study on nonlinearity compensation of temperature sensor based on LS-SVM, Transducer, and Microsystem Technologies",2007, pp.35-41.

- [37] D. Bloch and F. Chaissé, “Effect of Pressure on emf of Thermocouples”, American Institute of Physics,
- [38] F. P. Bundy, “Effect of Pressure on emf of Thermocouples”, Journal of Applied Physics, 1961, Vol. 32, no. 3, pp. 483-488
- [39] R. E. Hanneman and H. M. Strong, “Pressure Dependence of the emf of Thermocouples to 1300°C and 50 kbar”, Journal of Applied Physics, 1965, Vol. 36, no. 2, pp. 523-528
- [40] FINAL ANALYSIS | Johnson Matthey Technology Review.
<https://www.technology.matthey.com/article/48/3/145-145/>
- [41] Team:TU Dresden/Project/Results - 2015.igem.org.
http://2015.igem.org/Team:TU_Dresden/Project/Results
- [42] NTC Thermistor with Ring Lug - ProtoSupplies. <https://protosupplies.com/product/ntc-thermistor-with-solder-lug/>
- [43] National Institute of Standards and Technology Salary....
<https://www.federalpay.org/employees/natl-institute-of-standards-and-tech>
- [44] The Kelvin and temperature measurements. - Free Online Library.
<https://www.thefreelibrary.com/The+Kelvin+and+temperature+measurements.-a082777389>
- [45] Thermocouple measurement| data acquisition | cold junction.... <http://www.mosaic-industries.com/Products/WildCards/tcm/>
- [46] Chapter I - Analog Devices. <https://www.analog.com/media/en/training-seminars/design-handbooks/designers-guide-instrument-amps-chI.pdf>
- [47] Activation Functions in Neural Networks | Deep Learning.... <https://www.deeplearning-academy.com/p/ai-wiki-activation-functions>
- [48] Push Button | Definition of Push Button by Lexico.
https://www.lexico.com/en/definition/push_button
- [49] R. Rojas, Neural Networks, A Systematic Introduction. New York: Springer-Verlag, 1995.
- [50] E. M. Petriu, “neural network and fuzzy systems for modeling applications,” in IMTC’98, St. Paul, MN, May 1999, Session 4 Tutorial.
- [51] B. Kosco, Neural Networks for Signal Processing, ser. NJ. Englewood Cliffs: Prentice-Hall, 1992.

[52] A. Bernieri, "A neural network approach for identification and fault diagnosis on dynamic systems," *IEEE Trans. Instrum. Meas.*, vol. 43, pp.867–873, Dec. 1994.

[53] Thermocouple data available at: <http://www.omega.com>

3. THEORETICAL FRAMEWORK

3.1 Introduction

In the current chapter, we present a review of the theory on thermocouples, information on techniques that will be used to solve the problems identified in the literature review, and the methodology used in solving the thermocouple conditioning problem.

3.2 Thermocouple: Physics of thermoelectric energy conversion

In 1821, a German Physicist by the name of Thomas Seebeck discovered that when two dissimilar metal wires are joined at both ends to form a loop, a voltage is developed when the two junctions are kept at different temperatures. The so-called “Seebeck Effect” creates the theoretical basis for the operation of thermocouples. The Seebeck Effect itself is due to the conversion of thermal energy to electrical energy [30] – [34]. The open-circuit electrical potential difference in the circuit with two junctions maintained at temperatures T_{ref} / T_c and T_H ($>T_{ref}$) is given by

$$V = S_{AB}(T_H^n - T_{ref}^n) \quad (3.1)$$

Where the coefficient of proportionality (S_{AB}) is known as thermoelectric power or the Seebeck coefficient.

The Seebeck coefficient depends on factors such as work functions of the metals, electron densities of the two components, and scattering mechanism within each solid. [33,36,44]. Seebeck Effect is set upon the assumption that if two points in a conductor (or a semiconductor) are maintained at different temperatures, the charged carriers (electrons or holes) in the hotter region, being more energetic (having higher velocities), will diffuse towards the region of lower temperature [37,44]. The diffusion stops when the electric field is generated because of the movement of charges that has established a strong enough field to stop further movement of charges. For a metal carrier being negatively charged electrons, the colder end would become negative in order for the Seebeck coefficient to be negative. For a p-type semiconductor, on the other hand, holes diffuse towards the lower temperature resulting in a positive Seebeck coefficient [33, 36, and 37].

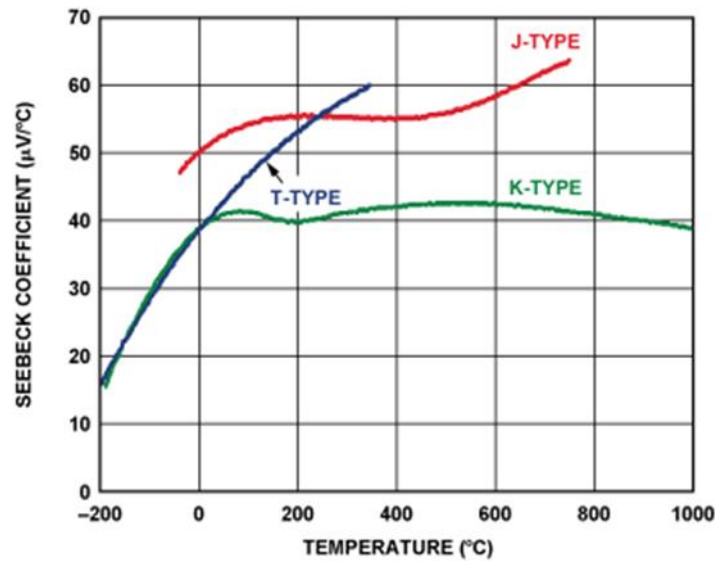


Figure 3-1 Thermocouple Seebeck Coefficient vs. temperature [40]

Mathematically expressed, the Seebeck coefficient or thermoelectric sensitivity is the change in EMF with respect to a change in temperature, and it is a nonlinear function of temperature. The nonlinearity of the Seebeck coefficients for typical thermocouple systems is shown in Figure 3-1. Seebeck coefficient (volts per unit of temperature) can be given by:

$$\sigma(T) = \lim_{\Delta T \rightarrow 0} \frac{\Delta E}{\Delta T} = \frac{dE}{dT} \quad (3.2)$$

Two other related thermo-electric effects in metals, the Peltier [42] and Thomson [43] effects, are current dependent and also could cause a voltage potential to exist in the circuit due to temperature when two dissimilar metals are joined together. According to the Peltier effect, when two dissimilar metals are connected, there will be an EMF developed in that circuit due to different temperatures in the junctions created. On the other hand, according to the Thomson effect, when two different metals are connected, making two junctions, a potential or voltage exists in the circuit due to the temperature gradient along the whole length of the thermocouple conductor. In general, the EMF due to Peltier and Thomson effects is very small and can be neglected [39].



Figure 3-2 Simple Thermocouple [13]

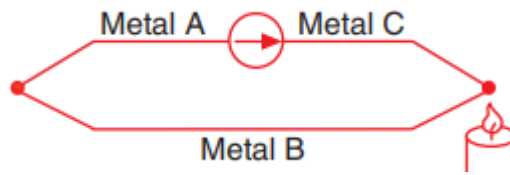


Figure 3-3 Thermocouple with hot and cold junction [13]

Thermoelectric voltage cannot be directly measured since a voltmeter must be used. Moreover, voltmeter leads also create a thermoelectric circuit. The most common combination of metals used in the design of thermocouples is Iron, Platinum, Rhodium, Rhenium, Tungsten, Copper, Alumel (composed of Nickel and Aluminium), Chromel (composed of Nickel and Chromium), and Constantan (composed of Copper and Nickel). Commonly used types of thermocouples are presented in chapter 1; each type has characteristics that can be matched with its industrial application [2, 3, 4, and 38].

$$V = S_{ab}(T_H - T_{ref}) \quad (3.3)$$

Where: S_{ab} , is the Seebeck coefficient, is the constant of proportionality

Thermocouple output voltages are highly nonlinear, resulting in the Seebeck coefficient varying by a factor of three or more over the operating temperature range of some thermocouples. For this reason, thermocouple voltages can be approximated using the thermocouple-versus-temperature curve using the look-up table or the polynomials. Thermocouple Seebeck voltage can also be expressed as a polynomial function of temperature as:

$$V = a_0 + a_1(T_H - T_{ref}) + a_2(T_H^2 - T_{ref}^2) + \dots + a_n(T_H^n - T_{ref}^n) \quad (3.4)$$

Where V is the thermocouple voltage in volts, a_0 to a_n ; are coefficients that are specific for each thermocouple type; these coefficients can be found on the NIST tables for thermocouple types.

3.3 Thermocouple linearization

Thermocouple voltage is a nonlinear function of temperature; therefore, they require some form of temperature reference to compensate for the contribution of the cold or reference junction in the measured voltage. The NIST standard tables for thermocouples were created using the practice of holding the reference junction at 0°C in an ice bath. Thermocouple cold junction is kept at 0°C or very close to zero due to the contribution that the cold junction has on the total EMF produced by the thermocouple when the two junctions are placed at different temperatures. From the Equation 3.3, when reference junction temperature is kept at zero degrees centigrade, Equation 3.3 is simply given as;

$$V = S_{\alpha b}(T_H) \quad (3.5)$$

Although thermocouple linearization using the ice bath technique is accurate, it is not always practical in application. A more practical approach is through the process called cold junction compensation by merely taking advantage of the thermocouple characteristics. Linearization with the process of cold junction compensation is by measuring the reference junction temperature or voltage and subtracting it from the measured temperature or voltage as thermocouple equation can be reduced to:

$$V_{meas} = V_H(T_H) - V_{ref}(T_{ref}) \quad (3.6)$$

Where: V_{meas} , is the voltage measured, $V_H(T_H)$ is hot junction voltage, and $V_{ref}(T_{ref})$ Cold junction voltage.

There are two theoretical methods for cold junction compensation, hardware compensation, and software compensation. With hardware compensation, a variable voltage source is inserted into the circuit to cancel the contribution of the reference junction in the measured voltage. This variable voltage source generates a compensation voltage according to the ambient temperature, thus adds the correct voltage to cancel the reference junction voltage. The resulting voltage measured at the output is used to compute thermocouple temperature using the ITS-90 tables. The major disadvantage of hardware compensation is that it is expensive as each thermocouple type must have a separate compensation circuit that can add correct compensation voltages, as each thermocouple type has different characteristics to the other.

Software cold compensation has better accuracy than hardware compensation. It requires a direct reading sensor to measure the reference junction temperature; thereafter, the software can add the correct compensation voltage to the measured voltage of the thermocouple. Software cold compensation generally follows the steps below:

1. Compute the reference junction temperature.
2. Convert this temperature into an equivalent voltage for the thermocouple type undergoing testing/ in use by either using the ITS-90 reference tables or polynomials.
3. Add this equivalent voltage to the measured voltage to obtain the open0circuit voltage that the thermocouple would produce at 0°C reference junction.

Software systems used for thermocouple compensation are widely available and the common one being the National Instrument SCXI product line which includes a variety of signal conditioning modules for various types of signals.

3.4 Artificial Neural networks

An artificial neural network is composed of a large number of interconnected units called neurons that have a certain natural tendency for learning information from the outside world. Neural networks are best at estimating functions that may depend on many variables [49], nonlinear function approximation. Thermocouples are nonlinear temperature measuring devices; therefore, neural networks will be used to linearize thermocouples in this cold junction compensation mechanism presented in this study. Thermocouple linearization is critical to the successful development of signal conditioning, the neural network trained to understand the relationship between the thermoelectric voltages produced by thermocouples with temperature. The theory of artificial neural network design is presented in this section, and the focus is on the Back propagation algorithm as it is the best algorithm for linearization and has excellent generalization.

3.4.1 Perceptron

Perception is the most straightforward neural “connectionist” network possible that consists of one or more inputs, a processor, and a single output. A perceptron is a feed-forward network, where there are no loops and the inputs sent into the neuron for processing and result in an output.

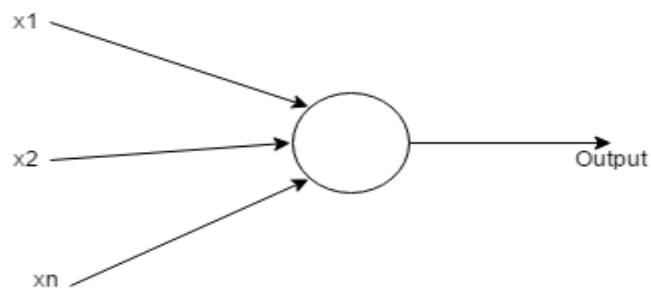


Figure 3-4 Perceptron

Inputs of a perceptron are each multiplied by weights (between -1 and 1) before being passed to the neuron. The weights of a perceptron are randomly assigned at the beginning of the training, and then the weighted inputs are summed and passed through the network activation function to generate the output of the perceptron. The perceptron algorithm can be summarized as follows:

- For every input, multiply it by its weight.
- Sum all the weighted inputs.
- Compute the output of the perceptron based on that sum passed through an activation function.

$$y = Q(\sum_{i=1}^n w_i x_i + b) = Q(W^T X + b) \quad (3.7)$$

Where W denotes the vector of weights, X is the vector of inputs, b is the bias, and Q is the activation function.

When a problem is complicated, then a complex network of perceptron can be used for complex decision-making. The complex network is called a neural network. Figure 3-5 below depicts a neural network structure.

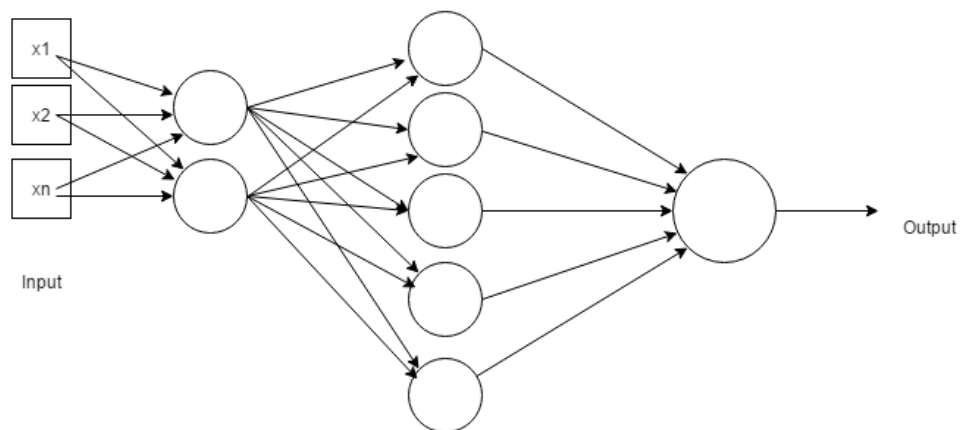


Figure 3-5 Neural Network Structure

The neural network creates a relation between its units (e.g., neurons) through a series of trials to learn the characteristics of the task to be performed, and once the network has learned the type of relations that are appropriate among its units, then it can learn another task like the ones it has already learned. The activation function of a neural network is the core of the network as they decide whether a neuron should be activated or not. They are essential in neural network learning and making sense of the given

information. Without activation function, weighted inputs and the bias would simply be passed to the next layer, which would simply be a linear transformation. The linear transformation would not solve complex problems; the activation function does nonlinear transformation making the neural network capable of learning and performing complex tasks. Back propagation is only possible with activation functions in the network since the gradients are supplied along with errors to update the weights and biases [49]. Neural networks are considered universal function approximations, meaning they can compute and learn any function that exists, thus the need for the network to perform the nonlinear transformation. Below are the plots of popular activation functions.

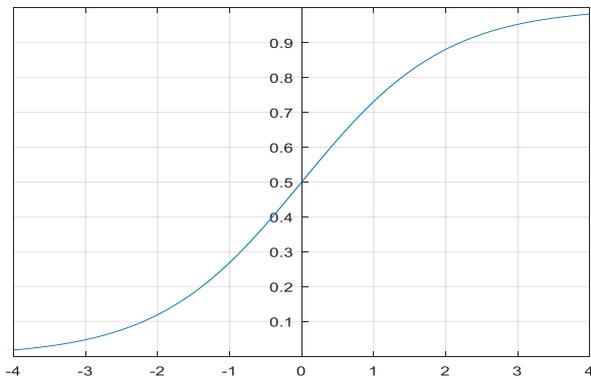


Figure 3-6 Sigmoid activation function

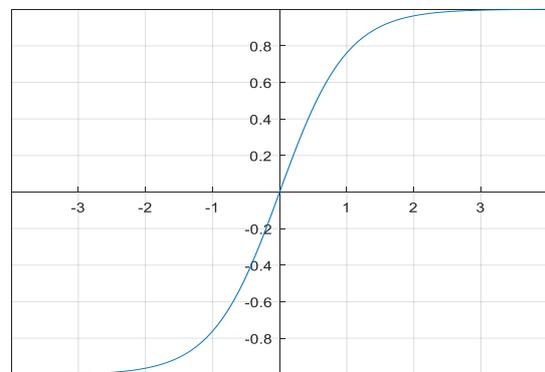


Figure 3-7 Hyperbolic tangent activation function

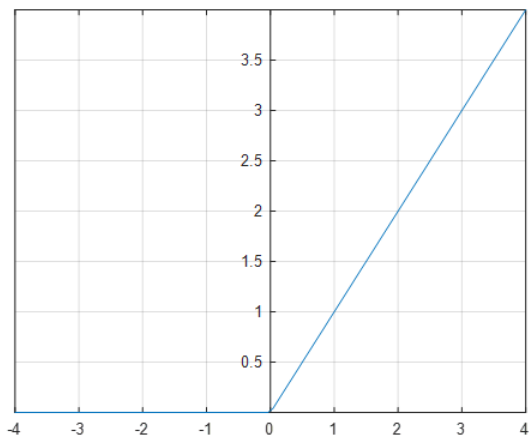


Figure 3-8 Rectified linear units (ReLU)

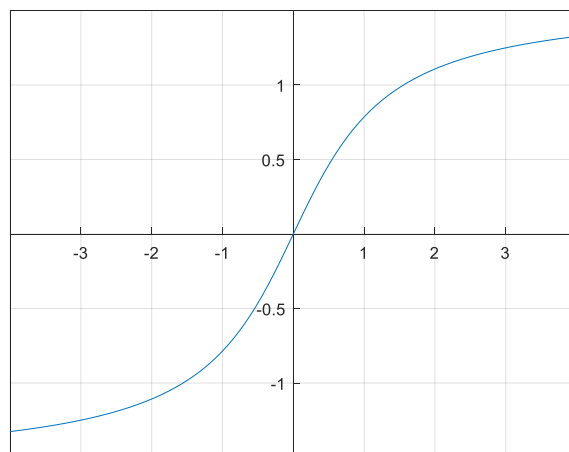


Figure 3-9 Inverse tangent function

The sigmoid activation function is widely used, and it is of the form:

$$f(net_i) = \frac{1}{1+e^{-net_i}} \quad (3.8)$$

This is a smooth function and is continuously differentiable, and it is bounded in the range (0, 1). The advantage of the activation function is its non-linearity, which allows the network with sigmoid activation to learn and perform complex tasks. As neural networks are regarded as universal function approximations, the sigmoid function can be used to approximate almost any function due to its non-linearity property.

3.4.2 Back propagation

Back propagation: An algorithm for supervised learning of artificial networks using gradient descent. This algorithm is currently the most widely used algorithm for connectionist learning, and this algorithm is used for learning in the feed-forward networks using mean squared error and gradient descent. The objective of this algorithm is to minimize the error between the output y computed by the network and the designed output (target). Back propagation makes it easy to find the network's weight gradient, $\nabla o(W)$. The updating of neural network weights by a small step to form new weights given by:

$$W^* = W - \rho \nabla o(W) \quad (3.9)$$

Where the parameter ρ controls the step size.

Given an artificial neural network and an error function, the algorithm calculates the gradient of the error function with respect to the neural network's weights. The "backward" part of the name comes from the fact that the calculation of the gradient proceeds backward through the network, with the gradient of the final layer of weights being calculated first and the gradient of the first layer of weights being calculated last. Partial computations of the gradient from one layer are reused in the computation of the gradient for the previous layer [48]. This backward flow of the error information allows for efficient computation of the gradient at each layer versus the naive approach of calculating the gradient of each layer separately.

To perform gradient descent, we need a differentiable error function; therefore, Back propagation accomplishes this by using mean squared error and by using continuous-valued cells with activations given by

$$E_{MSE} = E = \sum_{k=1} (d_k - a_k)^2 \quad (3.10)$$

$$net_i = \sum_{j=0}^J w_{i,j} y_j \quad (3.11)$$

$$a_i = f(net_i) = \frac{1}{1+e^{-net_i}} \quad (3.12)$$

The sigmoid function f is sometimes called a squashing function because it monotonically maps its inputs into $[0, 1]$. The aim of the Back propagation algorithm is to find weights and biases for the network that will minimize the mean squared error. The derivative of the activation function can be

$$\begin{aligned} \text{evaluated as follows } f'(net_i) &= \frac{d}{dnet_i} (1 + e^{-net_i})^{-1} & (3.13) \\ &= -(1 + e^{-net_i})^{-2} e^{-net_i} (-) \\ &= \frac{1}{1 + e^{-net_i}} \left(1 - \frac{1}{1 + e^{-net_i}} \right) \end{aligned}$$

Therefore, the result of the derivation of the activation function leads to

$$f'(net_i) = a_i(1 - a_i) \quad (3.14)$$

In order to break symmetry so that various intermediate cells take on different roles, the algorithm begins by randomly assigning small initial weights in the range $[-0.1, 0.1]$. Computing the gradient involves a forward pass over the network to compute cell activations, followed by a backward pass that computes gradients. Once we know the gradient, we can take a small step to update the weights. This process continues until changes become sufficiently small, i.e., the algorithm converges.

When computing the gradient, it is necessary to compute δ_i defined by:

$$\delta_i = -\frac{\partial E}{\partial net_i} \quad (3.15)$$

Then the weights can be updated as follows

$$w_{i,j}^* = w_{i,j} + \alpha \delta_i u_j \quad (3.16)$$

Artificial neural network forms a more significant part of the proposed solution to thermocouple nonlinearity correction; a feed-forward neural network using Back propagation with a sigmoid activation function will be utilized to realize the linearization of thermocouples.

3.5 Instrumentation amplifiers

Thermocouples produce a thermoelectric voltage in the millivolts range and are affected by drift voltages. Based on the voltage produced and drift voltages, it is necessary to amplifier the signal

produced by thermocouples before the signal can be sent to the neural network for processing. An instrumentation amplifier is a closed-loop gain block that has a differential input and output that may be differential or single-ended with respect to a reference terminal. An in-amp differs from an operational amplifier as the in-amp uses an internal feedback resistor network that is isolated from its signal input terminals. The primary reason for choosing an instrumentation amplifier to amplify the difference between two input signals is that a single operational amplifier (op-amp) has a lower rejection (CMRR) and the impedances of the inverting and non-inverting inputs are relatively low and unequal. The common-mode rejection ratio (CMRR) is the property of the in-amp in canceling out any signals that are common (the same potential on both inputs). The instrumentation amplifier consists of several operational amplifiers (op-amps) with a high CMRR.

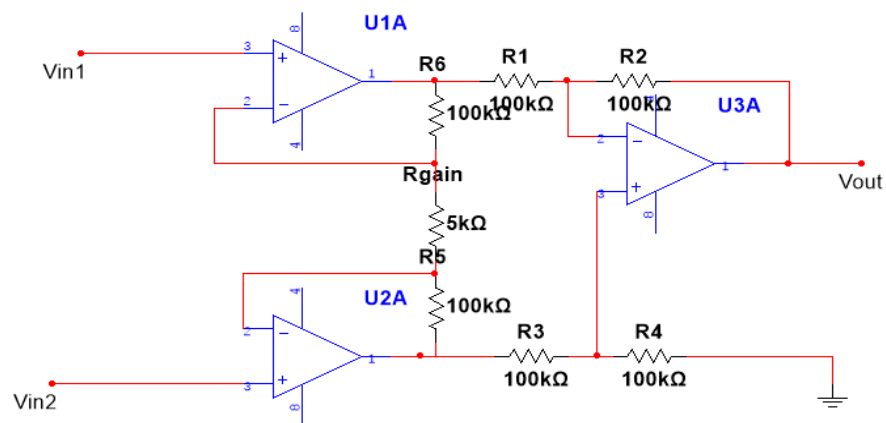


Figure 3-10 Instrumentation amplifier

The most common in-amps usually consist of three operational amplifiers in a two-stage configuration, namely buffering and a differential stage, with the two op-amps serving as a buffer for the two input circuits and the third as a differential operational amplifier. The input signals are applied to each non-inverting terminal of the op-amps in the buffering stage for the device to see a large resistance and reduce current drawn. In the configuration in Figure 3-10, a single gain resistor (R_{gain}) is connected between the summing junctions of the two input buffers. The full differential input voltage will appear across R_{gain} since the voltage at the summing junction of each amplifier is equal to the voltage applied to its positive input. The amplifier input voltage at the output (at the U1A, U2A) appears differentially across the three resistors, R_5 , R_6 , R_{gain} , the differential gain can be varied by just changing R_{gain} . If the resistors are matched as $R_5 = R_6$, $R_1 = R_3$, and $R_2 = R_4$ then there is no further resistor matching required as the gain of the in-amp will be controlled by varying R_{gain} , then the output voltage of the in-amp is as follows:

$$V_{out} = (V_{in2} - V_{in1}) \left(1 + \frac{2R_5}{R_{gain}}\right) \left(\frac{R_2}{R_1}\right) \quad (3.17)$$

Then the gain of the instrumentation amplifier is represented by:

$$A = \frac{V_{out}}{(V_{in2} - V_{in1})} = \left(1 + \frac{2R_5}{R_{gain}}\right) \left(\frac{R_2}{R_1}\right) \quad (3.18)$$

Common-mode rejection (CMR) is the property of an operational amplifier that quantifies the ability of the device to reject or canceling out signals that are common (same potential and in-phase on both inputs). CMRR is simply the ratio of the differential gain to the common-mode gain; this property is essential as it indicates how much of the common-mode signal will appear in the measurements. The mathematical representation of CMRR is as follows:

$$CMRR = A_D \left(\frac{V_{CM}}{V_{OUT}}\right) \quad (3.19)$$

Where:

A_D is the differential gain of the amplifier;

V_{CM} is the common-mode voltage present at the amplifier inputs;

V_{OUT} is the output voltage present when a common-mode input signal is applied to the amplifier.

3.5.1 Merits of using instrumentation amplifiers in signal conditioning

Thermocouples have thermoelectric signals that are very low in ranges of millivolts; therefore, signal amplification is required to measure the voltage by a processing instrument (microcontroller). Instrumentation amplifiers are ideal for amplification of low signals as they have low drift errors and they have a high CMRR. For best resolution and noise performance, instrumentation amplifiers produce great results compare with other amplifiers. Therefore, an instrumentation amplifier will be used in this proposed solution for the amplification of thermocouple signals.

3.6 Microcontroller

Thermocouples are analog devices, it is necessary for the system to have a processor that will run the neural network, and such a processor must be capable of processing the voltage of the thermocouple and reference junction sensor. A microcontroller is a small computer on a single integrated circuit

containing a processor core, memory, and programmable input/output peripherals, and it can be used as an embedded system. Microcontrollers are designed for embedded applications, in contrast to microprocessors used in personal computers or other general-purpose applications processors. Microcontrollers are embedded in our everyday consumer products, including phones, automobiles, and computer systems. The microcontroller has input/output devices for interfacing sensors, Liquid Crystal Display (LCD), and other devices. The biggest advantage of microcontrollers is the design and hardware costs, and it is cheap to replace. The typical architecture of a microcontroller may include the following:

- CPU, ranging from simple 4-bit to complex 64-bit processors.
- Peripherals such as timers and watchdogs.
- RAM (Volatile memory) for data storage.
- ROM, EPROM, or flash memory for program and operating parameter storage.
- Serial input/output such as serial ports.
- A clock generator for the resonator, quartz timing crystal, or Resistor-Capacitor (RC) circuit.
- Analog to digital converters.
- Serial Ports.
- Database to carry information.



Figure 3-11 Atmega32 microcontroller [36]

A button that is pushed to operate an electrical device, such a signal can be low or high. In this project, pushbuttons may be used to implement a mouse selection of thermocouple types; when a push button is clicked, an electrical signal can be sent to the microcontroller for computation.



Figure 3-12 Pushbutton [38]

3.6.1 Merits of microcontrollers

A microcontroller is needed in this study as the system needs a controller for processing data from the thermocouple, cold junction compensation sensor, and selection push buttons. Moreover, for the system to be complete, it is recommended that the artificial neural network be programmed in a chip so that the system does not depend on many peripherals such as PC. Microcontrollers have the capability of measuring data from sensors, this functionality will be used in this proposed method of thermocouple signal conditioning using the neural network, and the microcontroller is capable of running the ANN program.

3.7 Conclusion

The artificial neural network has been identified as the best approach in solving this problem; thus, an introduction to back propagation is presented in this study as it is an algorithm chosen to implement the neural network.

3.8 References

- [1] W. Long, S. Naimi, M. Criscitello, "Development of a knowledge base for diagnostic reasoning in cardiology", *Computers in Biomedical Research*, 25, 292–311, 1992
- [2] F. Azuaje, W. Dubitzky, P. Lopes, N. Black, K. Adamson, "Predicting coronary disease risk based on short-term RR interval measurements: A neural network approach", *Artificial Intelligence in Medicine*, 15, 275–297, 1999
- [3] P. Foote, "Note on the cold-junction corrections for thermocouples", *Bulletin of the Bureau of Standards*, vol. 9, no. 4, p. 553, 1913.
- [4] S. Chakravarthy and J. Ghosh, "Function Emulation Using Radial Basis Function Networks", *Neural Networks*, vol. 10, no. 3, pp. 459-478, 1997.
- [5] S. Hannan, R. Manza and R. Ramteke, "Generalized Regression Neural Network and Radial Basis Function for Heart Disease Diagnosis", *International Journal of Computer Applications*, vol. 7, no. 13, pp. 7-13, 2010.
- [6] F. Caldwell, "Temperatures of thermocouple reference junctions in an ice bath", *Journal of Research of the National Bureau of Standards, Section C: Engineering and Instrumentation*, vol. 69, no. 2, p. 95, 1965.
- [7] H. Shaker, A. Saleh, A. Ali and M. Abd Elaziz, "Self-Calibrating Enabled Low Cost, Two Channel Type K Thermocouple Interface for Microcontrollers", *Arab Journal of Nuclear Sciences and Applications*, vol. 0, no. 0, pp. 1-9, 2018.
- [8] U. Sinha, "Cold-Junction Compensation of Thermocouple by using Semiconductor Diode", *IETE Technical Review*, vol. 17, no. 1-2, pp. 71-72, 2000.
- [9] Y. WANG, Z. YAN and W. HE, "Thermocouple Cold End Compensation System with Programmable Function", *DEStech Transactions on Computer Science and Engineering*, no. -, 2017.
- [10] M. Gardner, S. Dorling, "Artificial Neural Networks (Multilayer Perceptron) –A Review of applications in the atmospheric sciences, *Atmospheric Environment* Vol. 32, No. 14/15, pp. 2627–2636, 1998
- [11] C. Medeiros, G. Barreto, "Pruning the Multilayer Perceptron Through the Correlation of Backpropagated Errors", *Seventh International Conference on Intelligent Systems Design and Applications*,

- [12] G. Wei, X. Wang, J. Sun, "Signal processing method with cold junction compensation for thermocouple", I2MTC 2009 - International Instrumentation and Measurement Technology Conference Singapore, 5-7 May 2009
- [13] D. Lampasi, L. Podesta "A Measurement System Exploiting Non-Linearity of Thermocouples for Cold Junction Compensation", Instrumentation and Measurement Technology Conference Como, Italy. May 18-20, 2004
- [14] J. Agee, S. Masupe, D. Setlhaolo, "Feedforward Neural-Network Conditioning of Type-B Thermocouple with Variable Reference-Junction Temperature", 2nd International Conference on Adaptive Science & Technology, pp. 296 – 300, 2009
- [15] M. Engin, D. Engin, "Compensation of Thermocouple Nonlinearities with Embedded System", 5th Mediterranean Conference on Embedded Computing (MECO), 2016, pp. 234 – 237.
- [16] M. Garcia, C. Sánchez, M. López, D. Hornero, R. Hornero, "Automatic Detection of Red Lesions in Retinal Images Using a Multilayer Perceptron neural network", 30th Annual International IEEE EMBS Conference Vancouver, British Columbia, Canada, August 20-24, 2008
- [17] T. Haruyama, R. Yoshizaki, "A 0 °C bath for the reference junctions of thermocouples by using a solid-state heat pump", J. Phys. E: Sci. Instrum. 19 (1986).
- [18] A. Mubalike (Mubarck), E. Adah, "Multilayer Perceptron neural network Technique for Fraud Detection", 2nd International Conference on Computer Science and Engineering, pp. 383 – 387, 2017
- [19] A. Mukherjee, D. Sarkar, A. Sen, D. Dey, S. Munshi, "An Analog Signal Conditioning Circuit for Thermocouple Temperature Sensor employing Thermistor for Cold Junction Compensation", International Conference on Control, Automation, Robotics and Embedded Systems (CARE), 2013
- [20] D. Specht, "A General Regression neural network", IEEE TRANSACTIONS ON NEURAL NETWORKS, VOL. 2. NO. 6. NOVEMBER 1991
- [21] S. Nandakumar, A. Abraham, P. Panicker, C. Hari, M. Priya, "THERMOD- Signal Conditioning Module with Cold Junction Compensation in Thermocouple", International Journal of Scientific & Engineering Research Volume 8, Issue 8, August-2017
- [22] Z. Zainuddin, O. Pauline, "Function Approximation Using Artificial Neural Networks", INTERNATIONAL JOURNAL OF SYSTEMS APPLICATIONS, ENGINEERING & DEVELOPMENT Issue 4, Volume 1, 2007
- [23] L. Marquez, T. Hill, "Function Approximation Using Backpropagation and General Regression Neural Networks",

- [24] M. Attari, F. Boudema, M. Heniche, “AN ARTIFICIAL NEURAL NETWORK TO LINEARIZE A G (TUNGSTEN VS. RANGE OF ZERO TO 2000°C TUNGSTEN 26% RHENIUM) THERMOCOUPLE CHARACTERISTIC IN THE RANGE OF ZERO TO 2000°C”,
- [25] J. Dias Pereira, O. Postolache, P. Silva Girão, M. Cretu, “MINIMISING TEMPERATURE DRIFT ERRORS OF CONDITIONING CIRCUITS USING ARTIFICIAL NEURAL NETWORKS”, IEEE Instrumentation and Measurement Technology Conference, vol. 49, no. 5, October 2000
- [26] D. DEY and S. MUNSHI, “A New Intelligent Scheme for Simultaneous Cold Junction Compensation and Linearization of Thermocouples”, Leonardo Electronic Journal of Practices and Technologies, Issue 19, p. 13-28, July-December 2011,
- [27] J. Tang, Y. Zhang, X. Tang, J. Liu, “Nonlinearity correction of the thermocouple based on neural network”, Global Congress on Intelligent Systems, pp. 28 – 32, 2009
- [28] “ITS-90 Thermocouple Database, Web Version 2.0”, Srdata.nist.gov, 2017. Available: <https://srdata.nist.gov/its90/main/>. [Accessed: 20 May 2017]
- [29] G. W. Burns and M. G. Scroger, “The Calibration of Thermocouples and Thermocouple Materials”, NIST Measurement Services, June 12, 1989
- [30] OMEGA Temperature Measurement Handbook, Omega Instruments, Inc.
- [31] Pyromation.com, [online] Available at: https://www.pyromation.com/Downloads/Doc/Training_TC_Theory.pdf [Accessed 2 Nov. 2018].
- [32] K. Binoy, K. Santhosh, “An Intelligent Temperature Measurement Technique Using J Type Thermocouple with an Optimal neural network”, Sensors and Transducers, Vol.147, issue 12, pp. 6 - 14, 2012
- [33] Krzysztof Konopka, “Thermocouple Dynamic Errors Correction for Instantaneous Temperature Measurements in Induction Heating”, 19th IMEKO TC 4 Symposium and 17th IWADC Workshop Advances in Instrumentation and Sensors Interoperability, July 18-19, 2013, Barcelona, Spain
- [34] Walt Kester, Editor, System Applications Guide, Section 1, 6, Analog Devices, Inc., 1993.
- [35] Dan Sheingold, Nonlinear Circuits Handbook, Analog Devices, Inc.
- [36] James Wong, Temperature Measurements Gain from Advances in High-precision Op-Amps, Electronic Design, 15 May 1986.
- [37] G. Recktenwald, Conversion of Thermocouple Voltage to Temperature, July 14, 2010

- [38] Duff, M. and Towey, J. (2017). Two Ways to Measure Temperature Using Thermocouples Feature Simplicity, Accuracy, and Flexibility | Analog Devices. [online] Analog.com. Available at: <https://www.analog.com/en/analog-dialogue/articles/measuring-temp-using-thermocouples.html> [Accessed 2 May. 2017].
- [39] Web.mst.edu. (2017). [online] Available at: <https://web.mst.edu/~cottrell/ME240/Resources/Temperature/Temperature.pdf> [Accessed 15 Aug. 2017].
- [40] M. Buscema, “Back Propagation Neural Networks”, Substance Use & Misuse, February 1998
- [41] M. Nielsen, Neural Networks and Deep Learning. [online] [Neuralnetworksanddeeplearning.com](http://neuralnetworksanddeeplearning.com). Available at: <http://neuralnetworksanddeeplearning.com/chap1.html> [Accessed 6 March. 2018].
- [42] X. Wang, “An Improved LSSVR-based nonlinear calibration for thermocouple”, First International Conference on Intelligent Networks and Intelligent Systems, 2008, pg. no 421 – 424
- [43] Z. Song, C. Liu, and X. Song, “Mathematical Model of Thermocouple Characteristics based on neural network”, Proceedings of the Second International Conference on Machine Learning and Cybernetics, 2003, pg. 1404 – 1407
- [44] Module 4: THERMOELECTRICITY Lecture 21: Seebeck Effect. <https://nptel.ac.in/content/storage2/courses/122101002/downloads/lec-21.pdf>
- [45] thermocouple measurement| data acquisition | cold junction.... <http://www.mosaic-industries.com/Products/WildCards/tcm/>
- [46] Chapter I - Analog Devices. <https://www.analog.com/media/en/training-seminars/design-handbooks/designers-guide-instrument-amps-chI.pdf>
- [47] Activation Functions in Neural Networks | Deep Learning.... <https://www.deeplearning-academy.com/p/ai-wiki-activation-functions>
- [48] Push Button | Definition of Push Button by Lexico. https://www.lexico.com/en/definition/push_button

4. METHODOLOGY

4.1 Introduction

The theoretical basis for the project implementation has been presented in chapter three of the thesis. The methodology chapter focuses on the translation of the theoretical concepts of chapter three through MATLAB simulations, neural network training, implementation, testing of the instrumentation amplifier, and the deployment of the final system on an ARDUINO UNO. An augmented thermocouple table for a given neural network, in the context of the current study, is a polynomial function implementation of the nonlinear millivolt or micro-volt output produced by the thermocouple polynomial equation using a combination of non-standard values of the hot junction and reference junction temperatures of the thermocouple. The nonlinear polynomial equations for the J, T, E, and R are found in existing literature [1] – [3] and have been discussed earlier in the current study. The most significant contribution of this study is the training of a form of a ‘look-up’ neural network that makes use of the reference temperature measurement and the thermocouple output voltage to look up the value of an unknown hot junction temperature from the augmented thermocouple table. Section three of this chapter presents the training of the look-up neural networks for each of the thermocouples studied in the current work. Figure 4-1 summarizes the implementations of the activities in both sections two and three. The actual implementation of the instrumentation amplifier for amplifying thermocouple output voltages and the test results obtained from the performance of the amplifier. In section four, the neural network design, training, and selection of neural networks for the proposed thermocouple signal conditioning are presented.

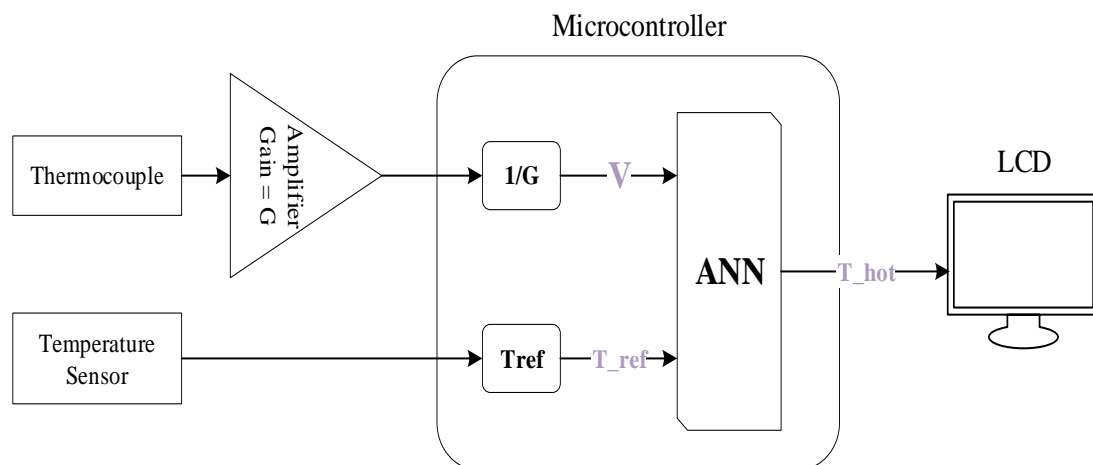


Figure 4-1 Block diagram of the proposed thermocouple signal conditioning system

In Figure 4-1 above is the overall thermocouple signal conditioning system block diagram, which consists of a microcontroller that is performing the computation for the system. The microcontroller is interfaced with an instrumentation amplifier with voltage gain G to amplify the thermocouple thermoelectric voltage readings produced. Furthermore, the measured reference temperature using a temperature measuring device (LM35) is read off by the microcontroller. The microcontroller will be running neural network(s) designed for conditioning of thermocouple signal. The output of the neural network is the measured thermocouple temperature ($^{\circ}\text{C}$) and will be displayed on an LCD/PC.

4.2 Thermocouple ITS-90 table augmentation

Data available from the National Institute of Standards and Technology (NIST) thermocouple ITS-90 tables is limited by the fact that the International Temperature Scale of 1990 (ITS-90) tables were calibrated only for reference junction temperature of 0°C . For the approach used in this research, where the thermocouple reference junction temperature is assumed variable beyond the 0°C value, augmented ITS-90 thermocouple tables are required. In this thesis, these augmented tables are required for the J, T, E, and R thermocouples used in the experimental validation of the signal conditioning approach used in this thesis. The approach of this thesis was to start with the thermocouple polynomial equation (with the polynomial coefficients for each of the studied thermocouples), then using MATLAB, evaluate several values of the thermocouple output voltage V , using randomly generated values of T_H and T_{ref} (within pre-defined ranges) to form new, expanded thermocouple tables with varying reference junction temperatures can be generated. This expanded thermocouple table is referred to as an augmented table for the given thermocouple. A neural network is then trained using the set of V, T_H, T_{ref} Entries from the expanded table so that it is able to accurately generate the millivolt or micro-volt output of the thermocouple beyond the data available in the ITS-90 table. A typical thermocouple polynomial equation is shown in equation 4.1;

$$V = a_0 + a_1(T_H - T_{ref}) + a_2(T_H^2 - T_{ref}^2) + \dots + a_n(T_H^n - T_{ref}^n) \quad (4.1)$$

Where V is the thermocouple voltage in volts, a_0 to a_n be coefficients that are specific for each thermocouple type; these coefficients can be found on the NIST website for thermocouple types.

Since the reference temperature of the thermocouple cannot be at the extreme, to train the artificial neural network (ANN), the reference temperature was set to vary between -10°C and 30°C in the generated table using the equation above. Appendix C contains tables for J, T, E, and R thermocouples, generated using the MATLAB script in Appendix B using the polynomial equation of the thermocouple.

In the study [2], a J-type and T-type thermocouple were used in calculating thermoelectric voltage using the thermocouple coefficient in the thermocouple equation. Therefore, the thermocouple equation has been used in this study to generate a thermocouple table at the varying reference temperature, and the accuracy of the results has been verified by the findings in [2] and thermocouple standard tables [3] at a reference temperature of 0°C. The ITS-90 standard tables were generated with reference junction kept at 0°C, to verify the accuracy of the new tables generated using the MATLAB program, a random sample of hot junction temperature are generated at zero reference junction temperature, and the resulting thermoelectric voltages are compared with that from the ITS-90 tables.

4.2.1 Thermocouple polynomial function

ITS-90 thermocouple tables are generated at 0°C reference junction temperature; in this study, we explore a technique for measuring the hot junction temperature without maintaining the reference temperature at 0°C as such, it is required that the ITS-90 table be augmented to include thermoelectric voltage as a function of measured (hot junction) temperature (°C) with varying reference junction temperature. Therefore, to achieve this, an augmented ITS-90 table is generated using a thermocouples polynomial equation. Below is the MATLAB code for generating the augmented table for type J thermocouple. Each thermocouple type and range has different thermocouple functional coefficients, which can be found in [3] represented by array C in the program below. MATLAB “randi” function was used to generate random values for reference junction temperature and measured or hot junction temperature for each specific range of thermocouple coefficients. The reference junction temperature was varied between -10 to 30°C, due to average room/open-space temperature and application-specific temperature. Thereafter, MATLAB “polyval” function was used to calculate the thermoelectric voltage of the thermocouple pair of hot and cold junction temperatures (°C). Then the pair of thermoelectric voltage (mV), reference (cold) junction, and measured (hot) junction temperature (°C) is stored in “Dataset”, thereafter stored in the augmented ITS-90 table. This process is repeated for all the sample thermocouple types (J, T, E, and R) used in this study to generate a thermocouple augmented ITS-90 table with varying reference junction temperature.

```
%-----Type J Thermocouples Coefficients in mV-----
%----- Type J -210 to 760
C= [0.15631725697E-22 -0.12538395336E-18 0.20948090697E-15 -0.17052958337E-
12...
0.13228195295E-9 -0.8568106572E-7 0.3047583693E-4 0.50381187815E-1 0];
% %-----Type J 760 to 1200-----
%C= [-0.306913690560E-12 0.157208190040E-8 -0.318476867010E-5...
% 0.317871039240E-2 -0.149761277860E1 0.296456256810E3];
```

```

Th=randi ([-210 760], [1 1500]);
Tc=randi ([-10 30], [1 1500]);
% Th=randi ([760 1200], [1 500]);
% Tc=randi ([-10 30], [1 500]);

Vm= polyval(C,Th)- polyval(C,Tc);
C_Set=C';
Dataset= [Vm', Tc', Th'];

```

4.2.2 Testing of thermocouple augmented ITS-90 table

The augmented ITS-90 table generated in section 4.2.1 using MATLAB for thermocouple type (J, T, E, R) is tested in this section to verify the accuracy of reproducing the standard ITS-90 tables for 0°C reference junction temperature. Appendix C shows an augmented ITS-90 table of thermoelectric voltage as a function of temperature (°C) with varying reference junctions, and Appendix C was filtered for 0°C reference junction temperature to produce the table of thermoelectric voltage as a function of temperature (°C) with reference junctions at 0 °C that can be found in Appendix D. To verify the accuracy of the augmented ITS-90 tables, thermoelectric voltage from the standard ITS-90 tables corresponding to the hot junction temperature in Appendix D was collected for each thermocouple type to produce table in Appendix E. Figures 4-2 to 4-5 below shows the thermocouple thermoelectric voltage sample comparisons between the standard ITS-90 table and the augmented ITS-90 table at 0°C reference junction temperature.

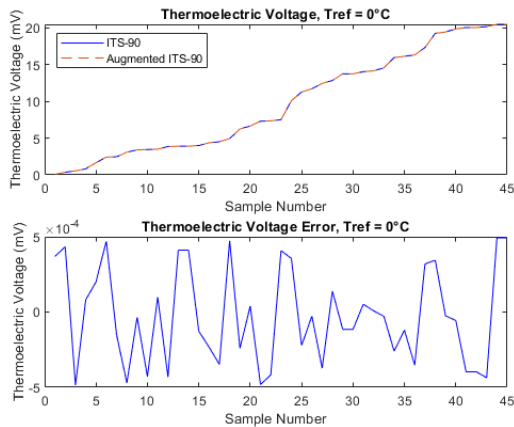


Figure 4-2 Type T Thermoelectric voltage at 0°C reference temperature

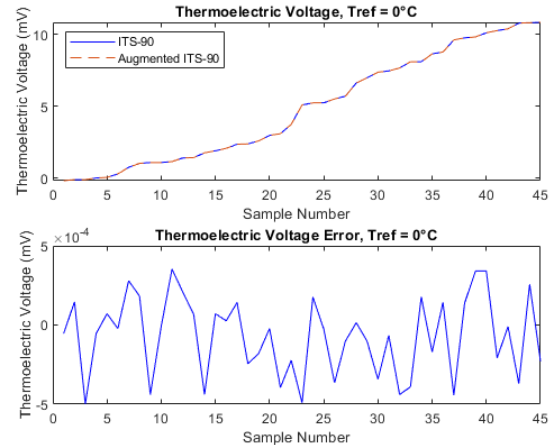


Figure 4-3 Type R Thermoelectric voltage at 0°C reference temperature

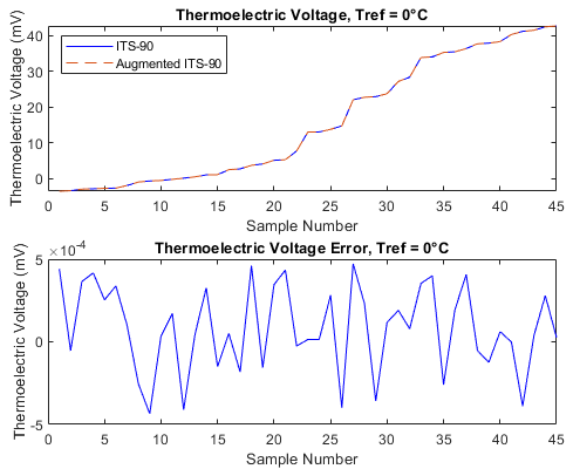


Figure 4-4 Type J Thermoelectric voltage at 0°C reference temperature

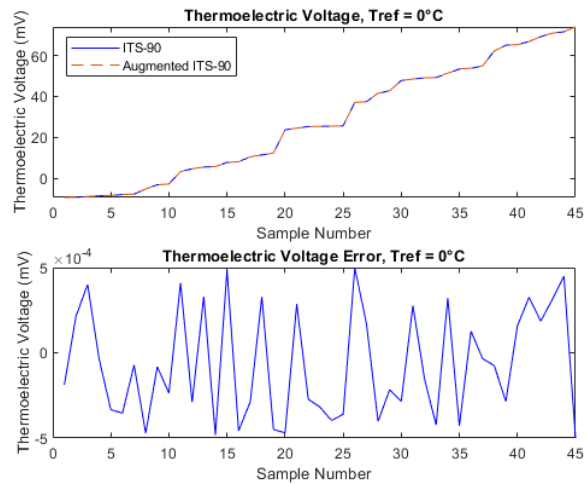


Figure 4-5 Type E Thermoelectric voltage at 0°C reference temperature

The results are shown in the graphs above support the hypothesis that the ITS-90 tables can be reproduced by using the polynomial equation of thermocouple with the functional coefficients for each thermocouple type per temperature range. Therefore, it can be concluded that the augmented ITS-90 tables (Appendix C) produced in this study are accurate and sufficient for the proposed study of thermocouple signal conditioning using a neural network.

4.3 Implementation of the instrumentation amplifier circuit

The instrumentation conditioning circuit amplifies the low output voltage of the thermocouple to enhance thermocouple sensitivity. The complete implementation of the instrumentation amplifier is shown in Figure 4-6.

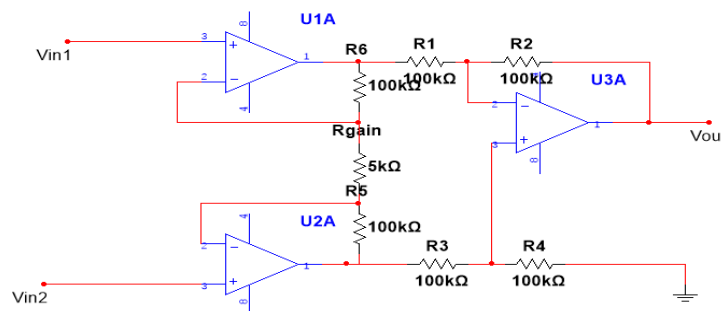


Figure 4-6 Instrumentation amplifier

Based on the equation below, as discussed in chapter 3.6, the gain of the instrumentation amplifier can be computed using the formulae:

$$A = \frac{V_{out}}{(V_{in2} - V_{in1})} = \left(1 + \frac{2 R_5}{R_{gain}}\right) \left(\frac{R_2}{R_1}\right) \quad (4.2)$$

Where V_{in1} , represent the positive end/leg of thermocouple, and V_{in2} , represent the negative end of the thermocouple. Therefore, minimum instrumentation amplifier gain with thermocouple outputs in millivolts:

$$A = \frac{V_{out}}{(V_{in2} - V_{in1})} = \left(1 + \frac{2 R_5}{R_{gain}}\right) \left(\frac{R_2}{R_1}\right) \quad (4.3)$$

$$A = \left(1 + \frac{2 * 100k}{5k}\right) \left(\frac{100k}{100k}\right) = 41$$

Maximum instrumentation amplifier gain with thermocouple outputs in microvolts;

$$R_6 = R_5 = R_4 = R_3 = R_2 = R_1 = 10M\Omega$$

$$A = \frac{V_{out}}{(V_{in2} - V_{in1})} = \left(1 + \frac{2 R_5}{R_{gain}}\right) \left(\frac{R_2}{R_1}\right)$$

$$A = \left(1 + \frac{2 * 10M}{5k}\right) \left(\frac{100k}{100k}\right) = 4001$$

The overall voltage gain of the instrumentation amplifier is 41. It was concluded upon based on the minimum and maximum thermoelectric voltage produced by the thermocouples used in the study. The maximum thermoelectric voltage produced by a thermocouple at high temperatures can go up to 100mV and 10 μ V for low temperatures when the reference junction is variable based on the tables generated in chapter 4.2 for J, T, R, and E using the polynomial equation of thermocouples.

The amplified voltage measurements of the thermocouple can be interpreted by the microcontroller through Analog to Digital Conversion (ADC), and the maximum output of the amplifier of 4.1V will not saturate the microcontroller as it operates at V_{CC} equals to 5V.

4.3.1 Performance of the instrumentation amplifier.

The performance of the design instrumentation amplifier is presented below. Thermocouple signals are amplified by the instrumentation amplifier with a voltage gain of 41.

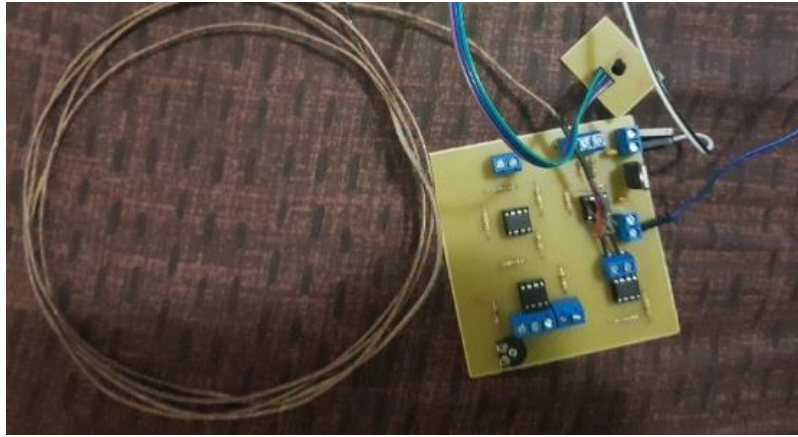


Figure 4-7 Instrumentation amplifier with Gain =41

Table 4-1 Instrumentation Amplifier Measurements Gain= 41

Measured on a Fluke 179 DMM multimeter on In- Amp input	Measured on a Fluke 179 DMM multimeter on In-Amp Output
1,84	75,716135
1,84	75,69666
2,92	119,782812
5,69	233,532638
5,74	235,538645
5,91	242,442963
6,79	277,910013
9,01	369,134193
9,62	394,483878
9,74	399,343157
14,66	601,36053
17,12	702,05653
18,04	739,73553
18,81	771,31127
19,14	785,99542

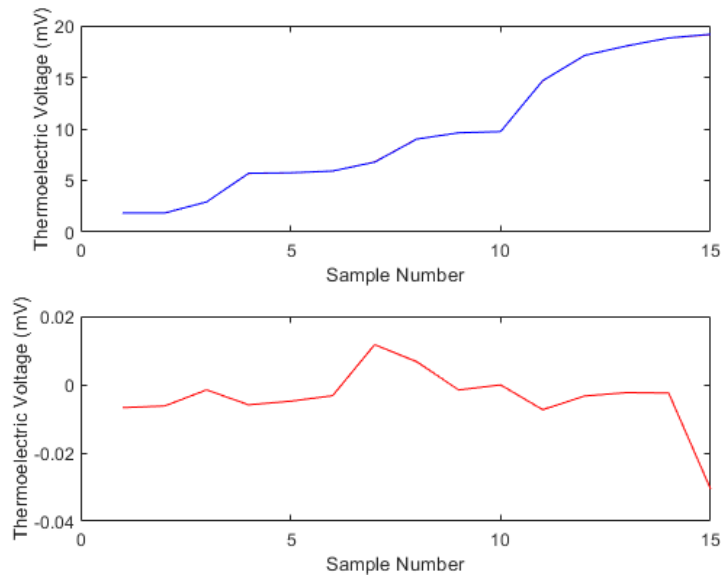


Figure 4-8 In-Amp performance with Gain of 41

In Figure 4-8 and Table 4-1, it can be seen that the resulting graph has a slope or gradient of 41, which is the desired gain of the instrumentation amplifier for high-temperature measurements. This gain is sufficient for temperature measurement for J, T, R, and E thermocouples that are used in this study to test the proposed thermocouple signal conditioning system.

4.4 Neural Network design: thermocouple linearization and compensation using a neural network

The proposed study of thermocouple signal conditioning using neural networks involves the design and training of neural networks for each of the studied thermocouples using the MATLAB neural network toolbox. The selection of the particular neural network structure for use in linearization and compensation for the J, T, R, and E-type thermocouples were decided after comparing the generalization capability of three different neural types or structures when trained to compensate and linearize the J, T, R and E-type thermocouple. Accordingly, subsection 4.4.1 presents results from the MATLAB training, and generalization tests carried out during the linearization of the J, T, R, and E-type thermocouple using the radial basis function neural network (RBFNN), the Multilayer Perceptron (MLP), and the generalized regression neural network (GRNN). The MLP was found to have superior accuracy in the generalization of the augmented ITS-90 table of thermocouple types. Consequently, subsection 4.4.2 presents results on the MLP augmentation of the J, T, R, and E thermocouple table;

and the subsequent pruning of the resulting MLP into a more straightforward neural network configuration that retains the initial generalization accuracy.

A neural network model for thermocouple nonlinear calibration or correction was designed, and this section of the report is based on the performance of the trained MLP neural network. To test the neural network performance and generalization capability, the network must be tested with unknown input vector(s), data that was not used to train the network in order to check the network capability to approximate network output based on a given input vector. The neural networks are based on the sigmoid symmetric activation function expressed as:

$$a = \frac{2}{(1 + \exp(-2 * n)) - 1} \quad (4.4)$$

The subsections below will show the resulting performance of the trained neural networks for different thermocouple types. The ability of the neural network to predict the unknown data given input data will be explored. It is to be noted that all the neural networks RBFN, GRNN, and MLP in this study will use be using the sigmoid symmetric activation function.

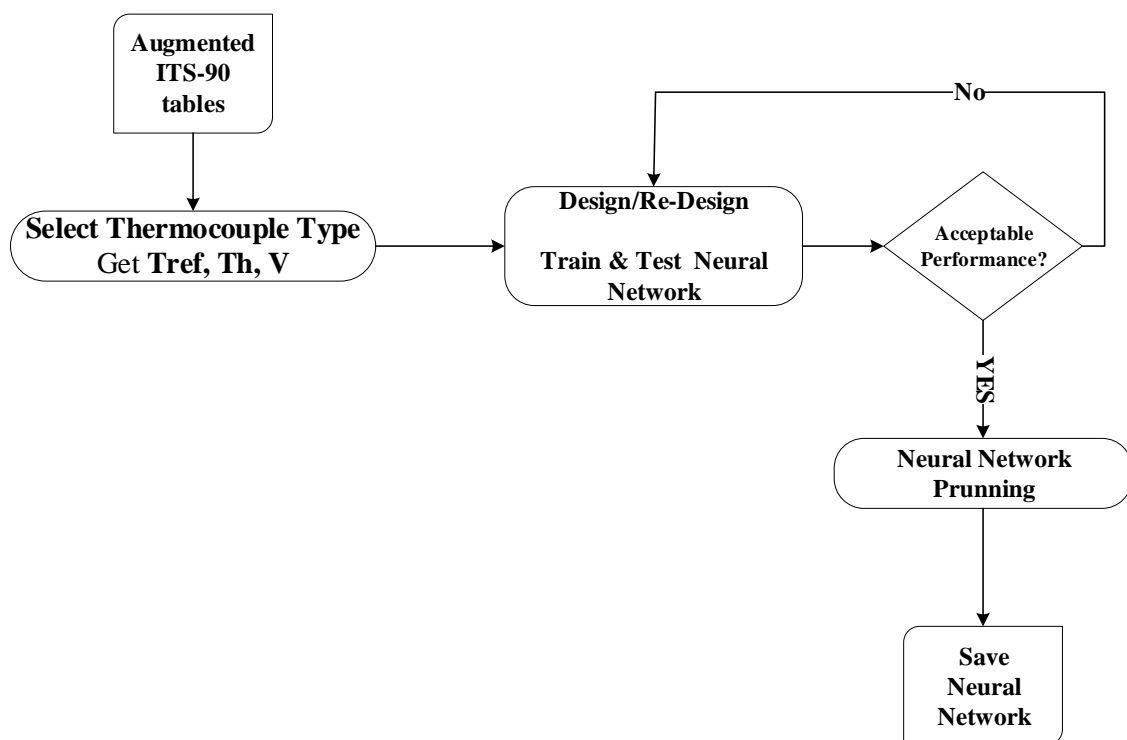


Figure 4-9 Block diagram of ANN design, train, and testing process

Figure 4-9 is the block diagram for the ANN design process. AN augmented ITS-90 table is used to get neural network training data (inputs and targets). The proposed method of thermocouple signal conditioning using a neural network is such that reference junction temperature T_{ref} and thermoelectric voltage V of thermocouple are used as inputs to the neural network. The neural network will therefore approximate the measured junction temperature of the thermocouple. The neural network is given vector of input pair: T_{ref}, V and corresponding output (targets) vector as training data, when the resulted performance of the network does not meet the minimum required generalization capability, the neural network is redesigned by changing its structure until the desired performance is meet. The neural networks are tested for generalization by using a new input pair and output vector that was not used during training. Once the performance is met, the network is pruned to optimize the structure but keeping the desired generalization and approximation capability of the network. Thereafter the network is saved for that particular thermocouple type, and the process is repeated for the next thermocouple type.

4.4.1 Neural network design and training

A neural network with sufficient nodes can approximate any function, either linear or nonlinear. Therefore, due to this property, neural networks are favorites in a variety of applications such as pattern recognition, classification, forecasting, process control, and image compression [4]. There are varieties of artificial neural network models that are used in function approximation, but the widely used method is the MLP [5]. The investigation for the best neural network for thermocouples function approximation was conducted with a variety of ANN models. ANN models (MLP, Radial Basis Function Network (RBFN), and GRNN) were tested as they all have advantages different from the other; moreover, they are all capable of approximating nonlinear functions. All the ANN models as stated above were used in this study to get the neural network model suitable for this proposed thermocouple signal conditioning system in terms of performance, generalization capability with minimal structure. The neural network training on J, T, E, and K-type thermocouple using augmented ITS-90 table showed that both RBFN and GRNN have excellent performance but poor generalization (performance on unknown inputs). MLP has shown great performance and generalization, and this was consistent with similar conclusions reached in reference [6], where it was indicated out that a Multilayer Perceptron is the best in approximating nonlinear function relationship between input and output and requires no prior knowledge of the nature of the relationship. Therefore, below is the resulting MLP neural network structures and their performance for all the sampled thermocouple types in this study. Note the neural network structure for thermocouple types J, R, and K is the same, but the performance was acceptable.

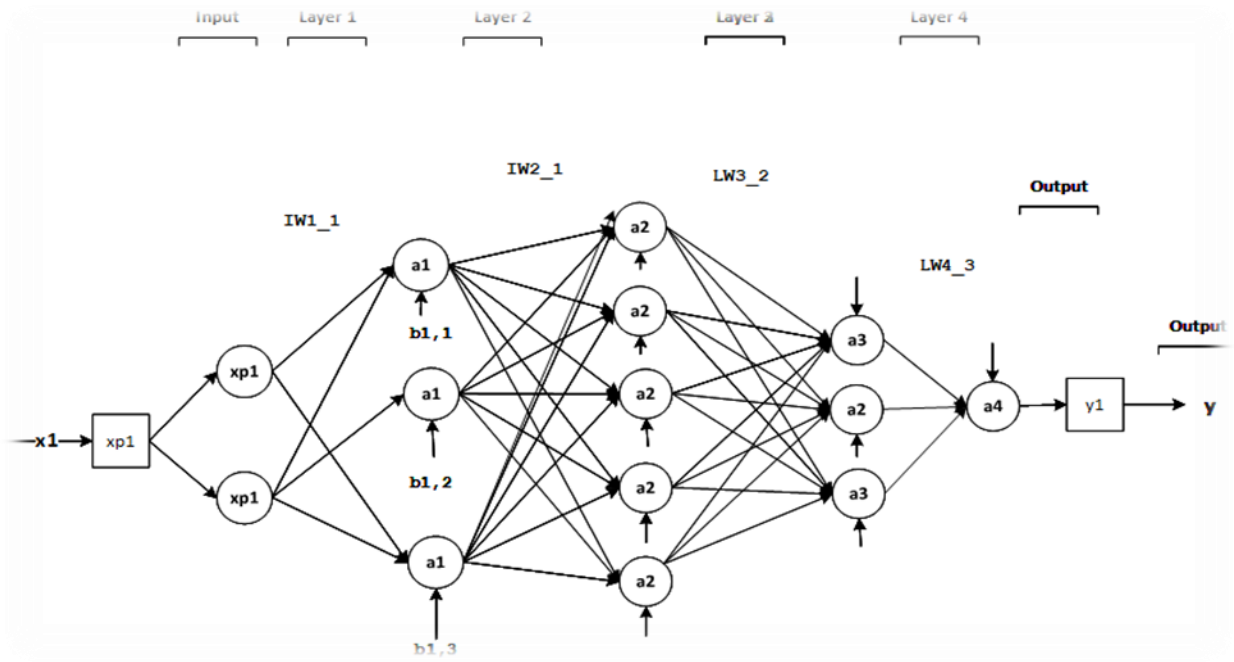


Figure 4-10 Type E Thermocouple Neural Network structure

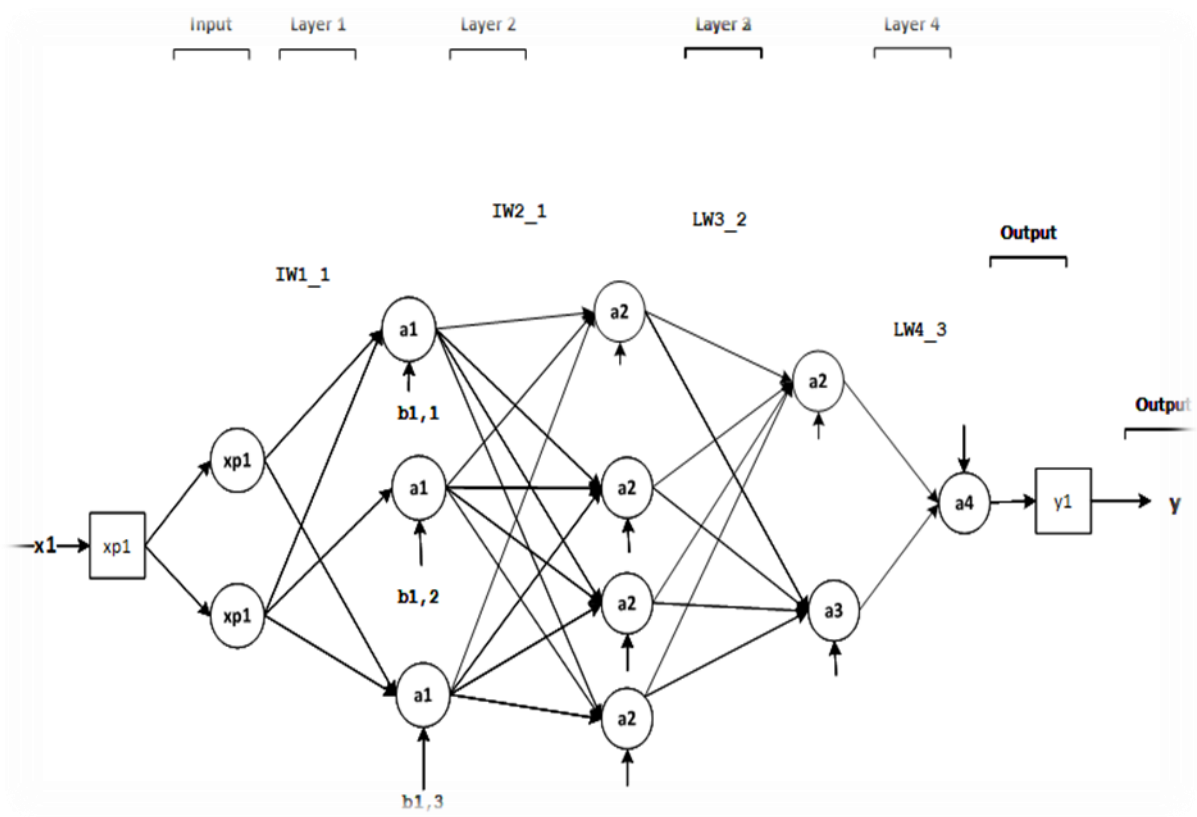


Figure 4-11 Type J, R, T Thermocouple Neural Network structure

The training error of the MLP was significantly better when compared with the other models, and the structure of the neural network was less complex in terms of the weights, biases, and hidden layers. After trying different parameters of the neural network structure, the above structures were selected based on their capability to approximate nonlinear thermocouple behavior. The functions represented by xp1, a1, a2, a3, a4, y1, can be found in Appendix G. All the activation functions of the hidden layer neurons are using the sigmoid function as discussed in the literature. Figures 4-12 to 4-15 show the MLP neural network performance validation.

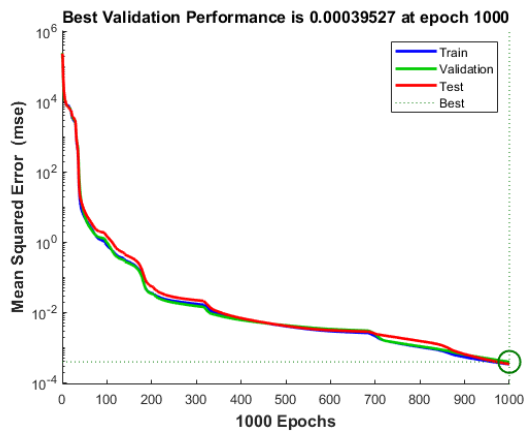


Figure 4-12 Type J: NN training error

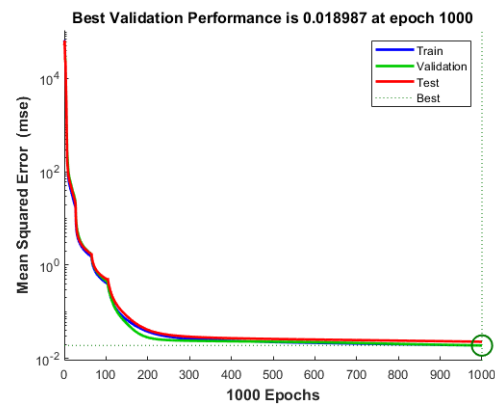


Figure 4-13 Type R: NN training error

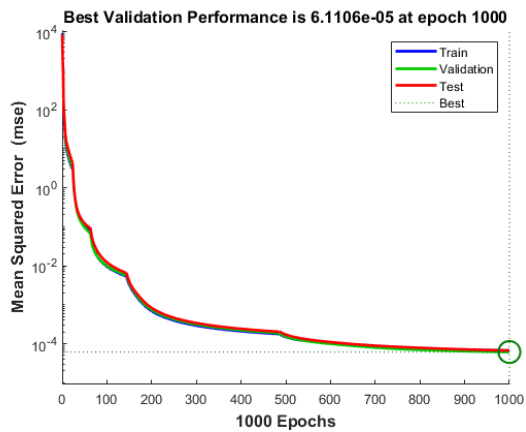


Figure 4-14 Type E: NN training error

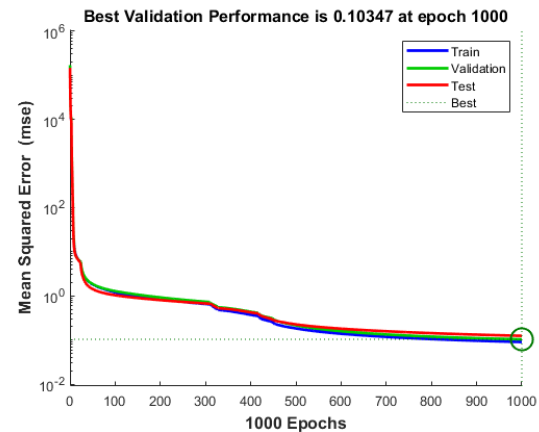


Figure 4-15 Type T: NN training error

4.4.2 MLP neural network pruning

The results from the comparison showed that the MLP neural network is better than the other models. The selection of an MLP was based on its ability to predict future variables given an input vector containing earlier observations [6]. The next step involved finding the smallest MLP architecture that had sufficient generalization capability without a significant loss of accuracy of generalization. Such pruning of the MLP neural network is required to reduce the requisite computational efforts during the microcontroller implementation of the conditioning system. The architecture of the MLP can be assessed by changing the ANN parameters (weights and biases) by using the pruning methods presented in [7]. Through pruning the size of the neural network, a neural network with excellent generalization capability was found. Below is the final neural network structure designed for approximating thermocouples characteristics. After a few try-and-error-based adjustments to the structure of the original MLP, the resulting MLP is shown below. It is to be noted that the pruned MLP has one less hidden layer and fewer neurons compared to the previous structure. The four neural networks designed and trained for each of the sampled thermocouple types are shown below, and the neural network code can be found in Appendix F.1 – F.4.

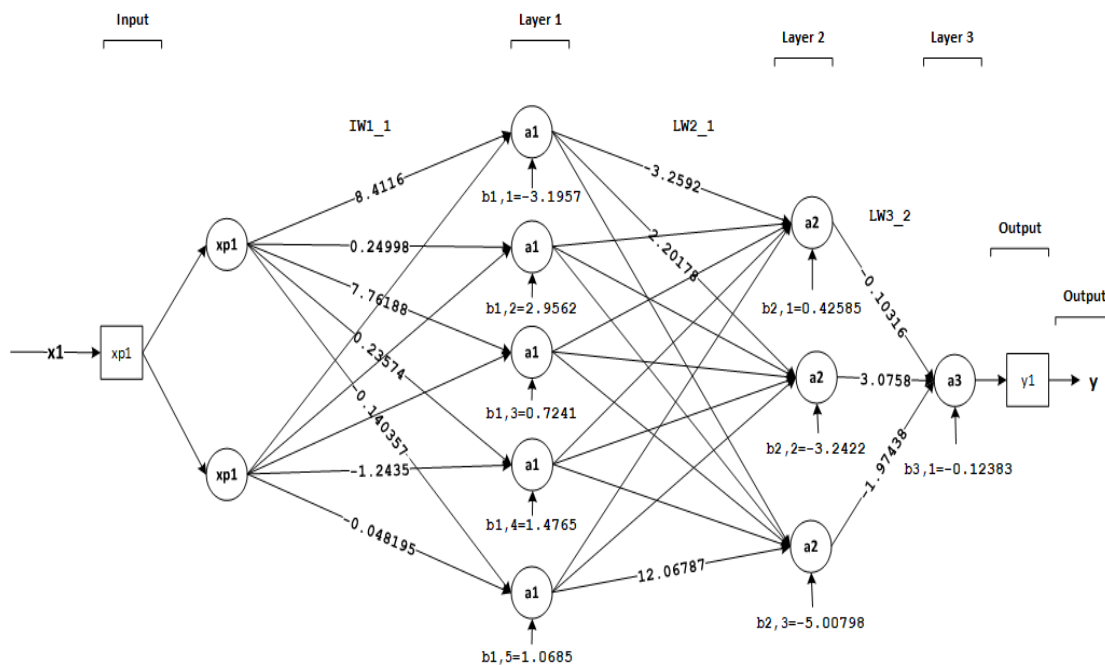


Figure 4-16 Type J Thermocouple neural network Structure with weights and biases

Table 4-2 Type J Thermocouple weights and biases

Neural Network structure		Weights & bias J-type thermocouple
Layer 1	IW1_1	[8.4116059433555943 0.24998504166793462;7.7618821407004583 0.23574223459283775;-0.14035704796217244 - 0.0054324299249743366;0.82730426660487533 0.032056168605518416;-1.2435151945493277 - 0.048195510008488311];
	b1	[-3.1957204495991407;- 2.9561682397139184;0.72406991335542414;1.4764589964920209;- 1.0684648875328424];
Layer 2	IW2_1	[-3.2592248341409715 2.2017835885621695 -2.5112480782549529 -0.67782740082033965 4.235815603877473;- 0.0044378596620069837 0.0052114000124296733 - 1.8138312924548463 4.8301396746704075 0.86805536390299598;1.1797553923805919 -6.2642707212977484 -6.3061012104616241 0.71269149372791518 12.067872446705174];
	b2	[0.42584797930671148;-3.2422037231362473;- 5.0079814593219369];
Layer 3	IW3_2	[-0.10316553920758917 3.0758300748226701 - 1.9743852642515622];
	b3	-0.12383316880726142;

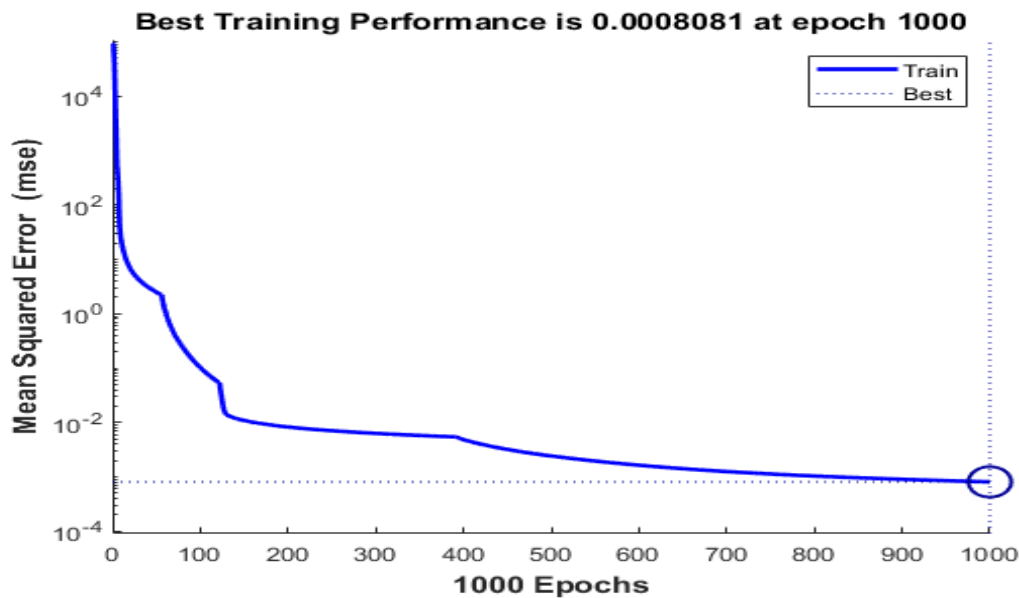


Figure 4-17 Type J Thermocouple: Neural Network training error with two hidden neurons

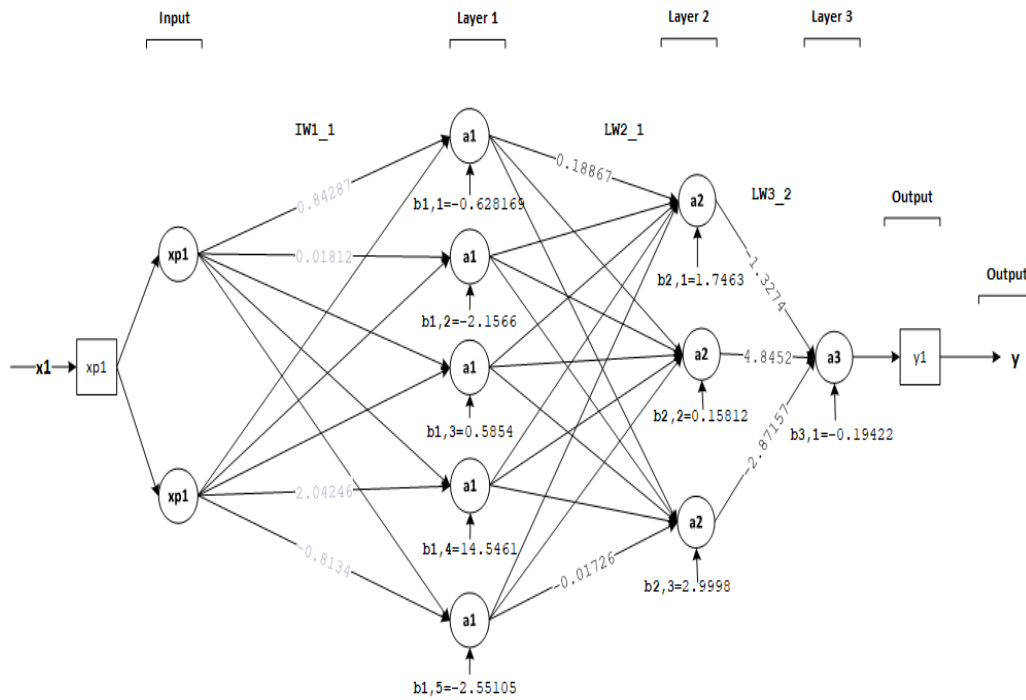


Figure 4-18 Type R Thermocouple neural network Structure with weights and biases

Table 4-3 Type R Thermocouple weights and biases

Neural Network structure		Weights & bias R-type thermocouple
Layer 1	IW1_1	[0.84287323136030500859 0.018122242071165511196; -1.5415819211474286465 -0.036442845611267996042; 0.51893150481563621312 0.55958547186916840488; 12.097791892917229006 0.24256080078522010424; -2.0424636603055312811 -0.81343565318491573013];
	b1	[-0.62816907211633221664; -2.1566234336574550134; 0.5854215255023416109; 14.546105422277856078; -2.5510536779032659815];
Layer 2	IW2_1	[0.18866786531833457108 -2.6137795170890916197 -0.6818915461680221668 0.19300126142076115543 -1.3860379609952582225; 1.0028383660661703836 -0.52310283060785423004 -0.0031308887678929671686 1.3331204748236777924 0.0016872909765237359327; -0.60297543489860916388 4.6106816087297932683 0.0073486507975941443502 2.7213707630366901213 -0.017263229932570837988];
	b2	[1.7463276861943701768; 0.15812302407012029937; 2.9997703091497651684];
Layer 3	IW3_2	[-1.3274451226999677278 4.8451543390231632813 -2.871573546832763224];
	b3	[-0.19421675529770310309];

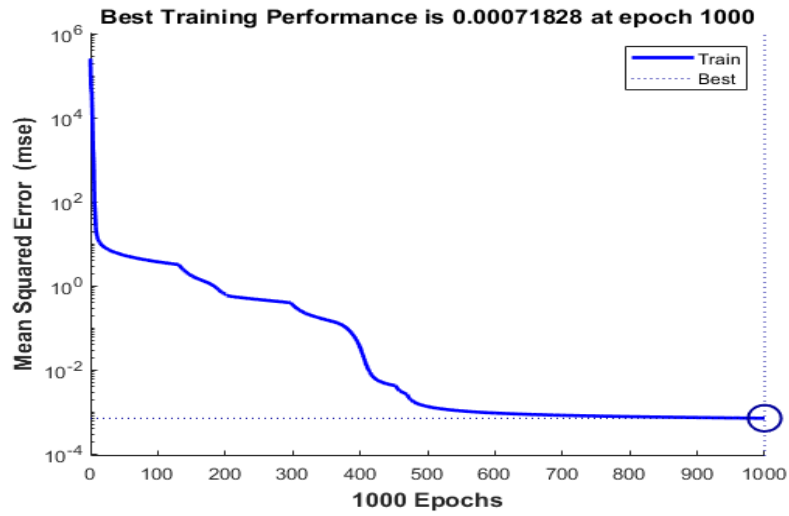


Figure 4-19 Type R Thermocouple: Neural Network training error with two hidden neurons

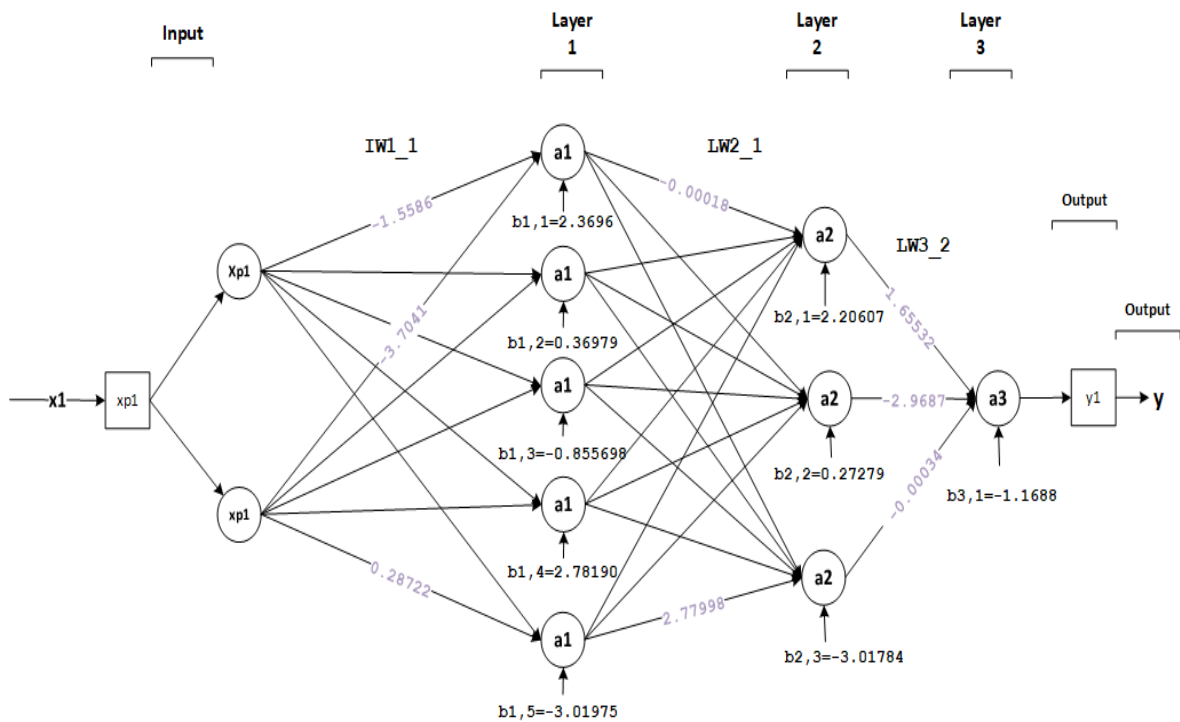


Figure 4-20 Type T Thermocouple neural network Structure with weights and biases

Table 4-4 Type T Thermocouple weights and biases

Neural Network structure		Weights & bias T-Type thermocouple
Layer 1	IW1_1	[-1.5586173768715507748 -3.7040889002138772668;- 0.3750257030376670242 - 0.024954342663195065721;2.5849882613984238589 2.5003595047438778032;0.97733814772277016747 0.065662195869926803793;-0.18957122958990110795 0.28721656119632360538];
	b1	[2.3695910760103582327;0.36978754244053091416;- 0.85569827983045865238;2.7819030466314016437;- 3.0197540598338892259];
Layer 2	IW2_1	[-0.00017855947179871590872 -1.1502730738210269479 - 2.7086743883620576406e-05 -1.2287381804824089038 1.3239839141695035618;-0.00030133687465747565444 1.6449737756686595436 -0.00016034916663146178131 - 2.2243481202138939423 -0.30197205981002112063;- 2.7975767060876730596 -1.4293430186634754619 2.3294233919455429316 0.16572495894353161949 2.7799778295614858692];
	b2	[2.2060719753030353374;0.27278875960066123474;- 3.0178356737378679853];
Layer 3	IW3_2	[1.6553222656154626957 -2.9687339126940814893 - 0.00033993104445808800364];
	b3	-1.1688218164800976417;

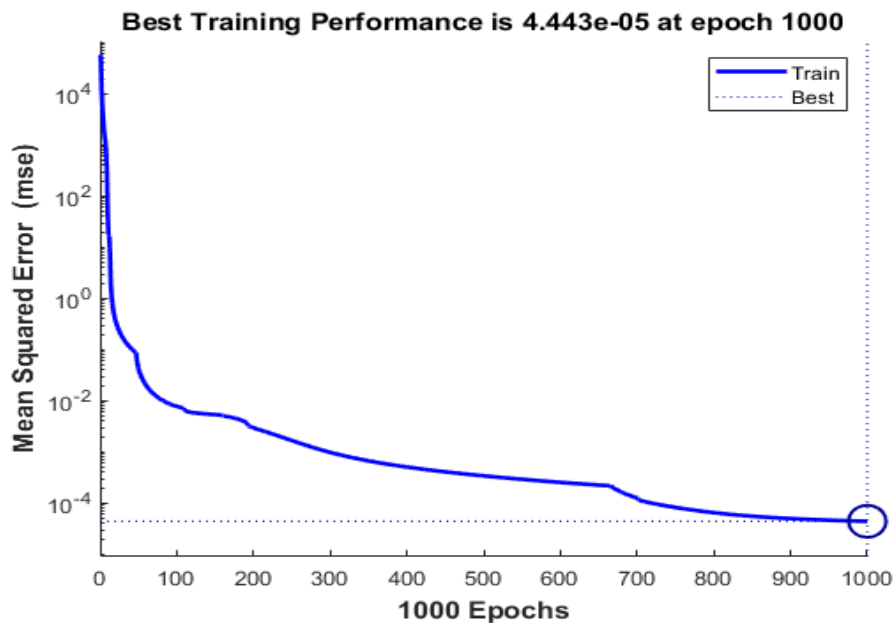


Figure 4-21 Type T Thermocouple: Neural Network training error with two hidden neurons

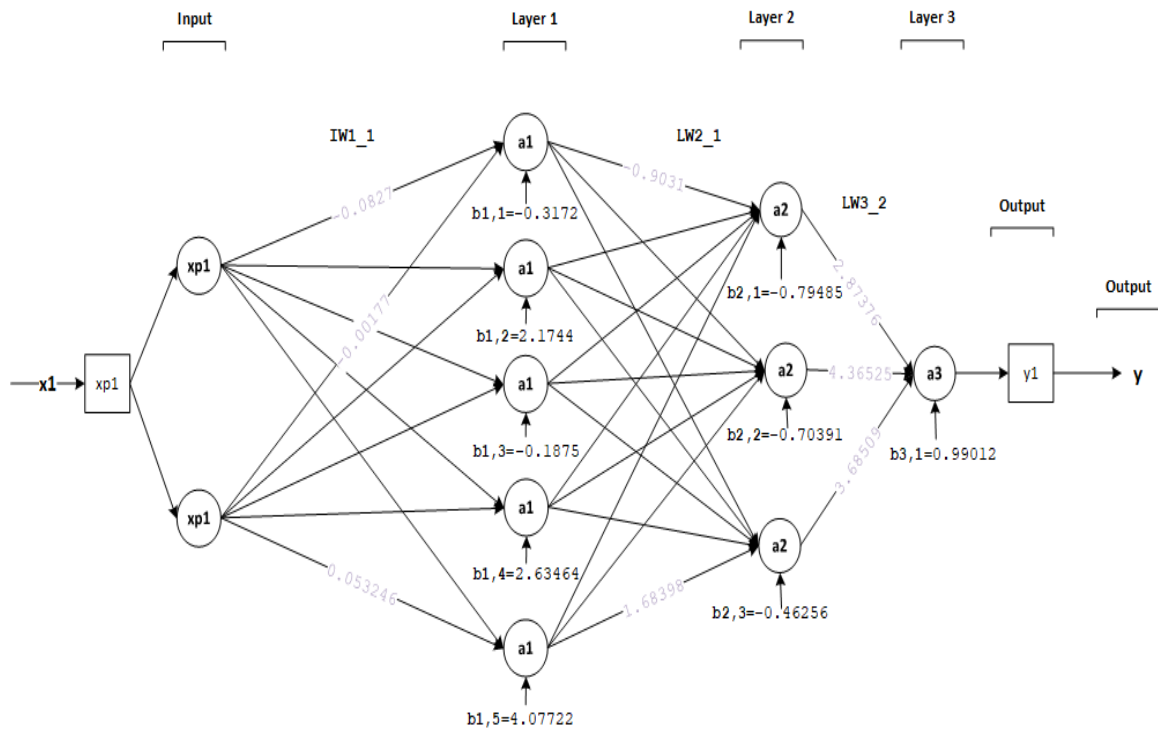


Figure 4-22 Type E Thermocouple neural network Structure with weights and biases

Table 4-5 Type E Thermocouple weights and biases

Neural Network structure		Weights & bias E -Type thermocouple
Layer 1	IW1_1	[-0.082718985387574398005 -0.0017797274698325242764; 0.20307244842051216938 - 0.68564276033515336728; 0.11342447437015074074 0.0042783761702323858805; 0.44844206616140036559 - 0.62857019254671364639; 2.1093442743122237104 0.053246869763761577043];
	b1	[-0.31720603283965898012; 2.1743939450111993139; - 0.18750284754824272926; 2.6346429925536472005; 4.07722354248546459 13];
Layer 2	IW2_1	[-0.90309850188499263268 -0.16546676903881518683 1.3156174168202814379 0.36692737126083313504 - 0.44380467096548142925; -1.5397599934107104591 0.087035532084973707412 0.64518315821542837618 -0.28230905642625969687 - 0.056434885334206902341; -5.223420270828670553 0.54886124833387295308 2.9166625646602191146 - 0.69794018270488922262 1.6839783587996524084];
	b2	[-0.79485331974848705272; -0.70391048004113487835; - 0.46256252123350632965];
Layer 3	IW3_2	[2.8737621175139338447 4.3652518920400620317 3.6850914744647327304];
	b3	0.99012204847402307539;

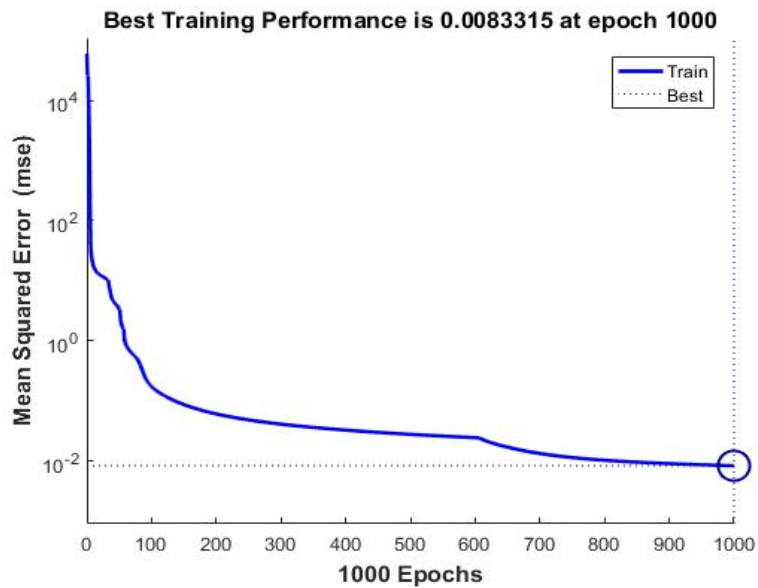


Figure 4-23 Type E Thermocouple: Neural Network training error with two hidden neurons

4.4.3 Generalization of neural networks testing

The designed neural networks in section 4.4.2 above showed great performance with very low training errors with the least error of 0.0083315 for type E thermocouple neural network. In this section, we look at the performance of the neural networks given unknown data. The performance indicates the accuracy of the neural networks to produce the measured temperature when the error-free reference temperature and thermoelectric voltage of the thermocouple is feed as input pair to the network. Data from the augmented ITS-90 table that was not used during the training of these neural networks are used to test the performance of the neural networks; Appendix H shows the table extracted from the augmented ITS-90 and the resulting measured temperature produced by the neural networks.

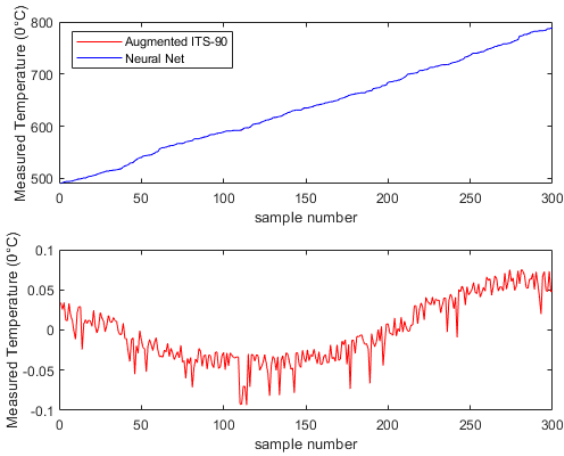


Figure 4-24 Type E: NN generalization error

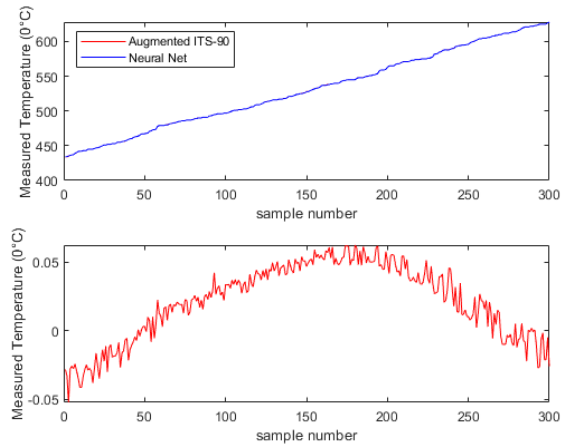


Figure 4-25 Type J: NN generalization error

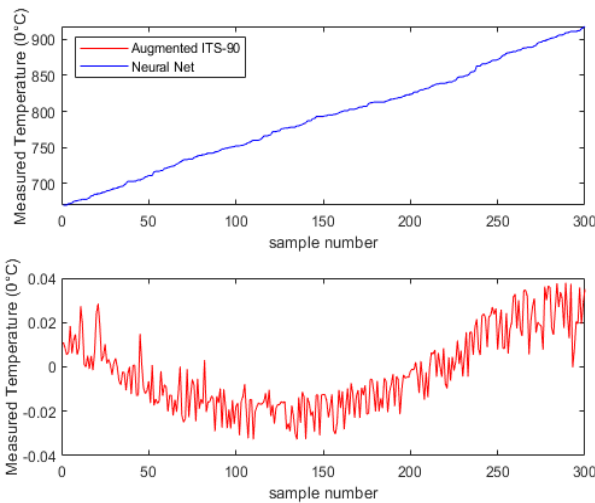


Figure 4-26 Type R: NN generalization error

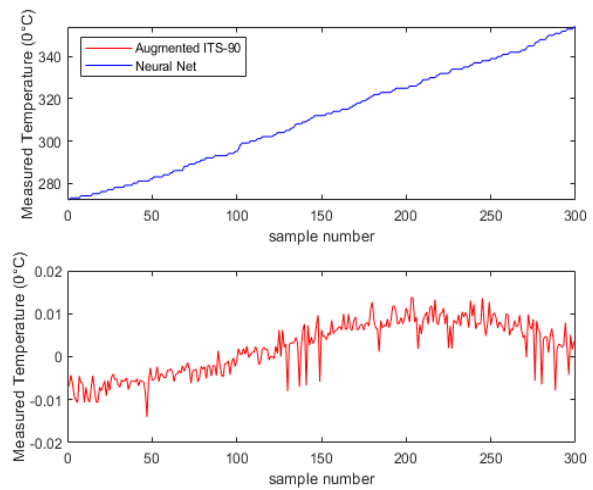


Figure 4-27 Type T: NN generalization error

Figures 4-24 to 4-27 show the performance of the designed neural networks for each thermocouple type sampled for this study, namely, J, T, R, and E. The neural networks were tested for their generalization capabilities using data from the augmented ITS-90 tables not used during the training of the neural networks. Each thermocouple type (J, E, T, and R) has one neural network that evaluates thermocouple temperature given reference junction temperature from the LM 35 temperature reading and thermoelectric voltage of the thermocouple as the neural network input vector. The validation for the augmented ITS-90 thermocouple tables showed that the E, T, R, and J thermocouples could all reproduce the hot junction temperature within 0.01% of the results found on the ITS-90 tables. The E-

type thermocouple neural network has a worst-case error within 0.2% in reproducing the hot junction temperature, while the neural network for the type J thermocouple produced a worse case measurement error within 0.1% in reproducing the measured junction temperature of the thermocouple. Neural networks for type T and R thermocouple showed worse case error within 0.04% in reproducing the hot or measured junction temperature, as can be seen from Figures 4-26 and 4-27.

4.5 References

- [1] J. Tang, Y. Zhang, X. Tang, J. Liu, “Nonlinearity correction of the thermocouple based on neural network”, Global Congress on Intelligent Systems, pp. 28 – 32, 2009
- [2] D. Lampasi, L. Podesta “A Measurement System Exploiting Non-Linearity of Thermocouples for Cold Junction Compensation”, Instrumentation and Measurement Technology Conference Como, Italy. May 18-0.2004
- [3] “ITS-90 Thermocouple Database, Web Version 2.0”, Srdata.nist.gov, 2017. Available: <https://srdata.nist.gov/its90/main/>. [Accessed: 20 May 2017]
- [4] F. Caldwell, "Temperatures of thermocouple reference junctions in an ice bath", Journal of Research of the National Bureau of Standards, Section C: Engineering and Instrumentation, vol. 69, no. 2, p. 95, 1965.
- [5] L. Marquez, T. Hill, “Function Approximation Using Backpropagation and General Regression Neural Networks”,
- [6] M. Gardner, S. Dorling, “Artificial Neural Networks (MLP) –A Review of applications in the atmospheric sciences, Atmospheric Environment Vol. 32, No. 14/15, pp. 2627-2636, 1998
- [7] C. Medeiros, G. Barreto, “Pruning the MLP Through the Correlation of Backpropagated Errors”, Seventh International Conference on Intelligent Systems Design and Applications,
- [8] Liu Ding, Li Xiaobin, Zuo Lei. “Nonlinear calibration for N thermocouple sensor based on least squares support vector machine,” Chinese Journal of Scientific Instrument. 2007, vol. 28, pp. 640-644
- [9] Dalkiran I., Danisman K, Linearizing E-Type Thermocouple Output Using ANN and Adaptive Neuro-Fuzzy Inference Systems, IEEE 14th Signal Processing and Communications Applications, 2006, pp. 1-4.
- [10] J. Tang, Y. Zhang, X. Tang, J. Liu, “Nonlinearity correction of the thermocouple based on neural network”, Global Congress on Intelligent Systems, 2009, pp. 28-32.
- [11] D. Dey and S. Munshi, “A new intelligent scheme for simultaneous cold junction compensation and linearization of thermocouples”, Leonardo Electronic Journal of Practices and Technologies, issue 19, 2011, pp. 13 – 28
- [12] S. Zhang and Q. Dai, “Nonlinear calibration of thermocouple sensor based on least squares support vector regression”, 5th International Conference on Computer Sciences and Automation Engineering, 2015, pp. 5 – 10

- [13] A.V. Vamsi, G.S. Mohan, and S.S. Skrikanth, "Simplified thermocouple Interface for hot only or cold only measurement with Linearization circuits", *IJERA*, 2012, Vol. 2, issue 5, pp.1663 – 1667
- [14] M. Duff and J. Towey, "Two ways to measure temperature using thermocouple feature simplicity, accuracy, and flexibility", *Analog Dialogue*, Vol. 44, 2010
- [15] A. Fang, X. Ye, A. Chen, X. Xu, and R Yu, "Using operational amplifiers to realize the compensation of thermocouples", *ISECS International Colloquium on Computing, Communication, Control, and Management*, 2008, pp.774 – 777
- [16] G. Li-Hui W. Wu, J. Xiao-bo, "Thermocouple Signal Conditioning with Genetic Optimizing RBF Neural Networks", 2011 IEEE 3rd International Conference on Communication Software and Networks, 2011
- [17] H.H. Shaker, A.A. Saleh, A.H. Ali, and M.A. Elaziz, "Self-Calibrating Enabled Low Cost, Two Channel Type K Thermocouple Interface for Microcontrollers", *ICM*, 2016, pp. 309-312
- [18] M. Duff and J. Towey," Two Ways to Measure Temperature Using Thermocouples Feature Simplicity, Accuracy, and Flexibility", *Analog Devices*. [online] *Analog.com*. Available at: <https://www.analog.com/en/analog-dialogue/articles/measuring-temp-using-thermocouples.html> [Accessed 2 May. 2017].
- [19] J.M.D. Pereira, O. Postolache, P. M. B. S. Girão, and M. Cretu, "Minimizing Temperature Drift Errors of Conditioning Circuits Using Artificial Neural Networks", *IEEE TRANSACTIONS ON INSTRUMENTATION AND MEASUREMENT*, 2000, Vol. 49, no. 5, pp.1122-1127
- [20] U.S. Secretary of Commerce. (1995). NIST ITS-90 thermocouple database. Available from <http://srdata.nist.gov/its90/main/>.
- [21] M. Engin and D. Engin," Compensation of Thermocouple Nonlinearities with Embedded System", 5th Mediterranean Conference on Embedded Computing (MECO), 2016, pp. 234-237.
- [22] F.R. Caldwell, "Temperatures of Thermocouple Reference Junctions in an Ice Bath", *JOURNAL OF RESEARCH of the National Bureau of Standards-C. Engineering and Instrumentation*, 1965, Vol. 69C, No. 2, pp. 95-101

5. EXPERIMENTAL WORK, RESULTS AND DISCUSSIONS

5.1 Introduction

In this Chapter, all the experimental results from the experiments conducted at the Department of Chemical Engineering at the University of Kwa-Zulu Natal using temperature controller or Oven TTM-004 are presented and examined in detail.

5.2 Circuit implementation

In this system, an Atmega32/Arduino Uno microcontroller receives two analog inputs, namely the reference temperature and the hot junction temperatures. The amplification of thermocouple voltage(s) is achieved through the use of an instrumentation amplifier due to the characteristics of the amplifier such as low drift, low DC offset, low noise, very high open-loop gain, etc., as discussed in the amplifier section. The microcontroller is programmed with an MLP ANN for thermocouple function approximation designed in section 4.4.3 of this study. The code is written in the C programming language. The microcontroller program running the MLP neural network computes measured temperature given an input vector (reference temperature ($^{\circ}\text{C}$) and thermocouple voltage (millivolts)), the measured temperature is displayed on an LCD or viewed on a PC monitor.

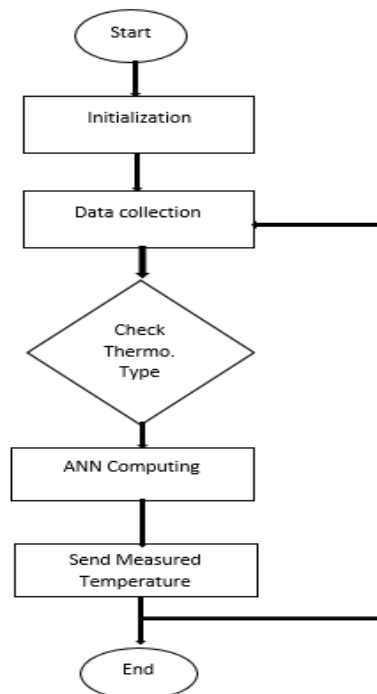
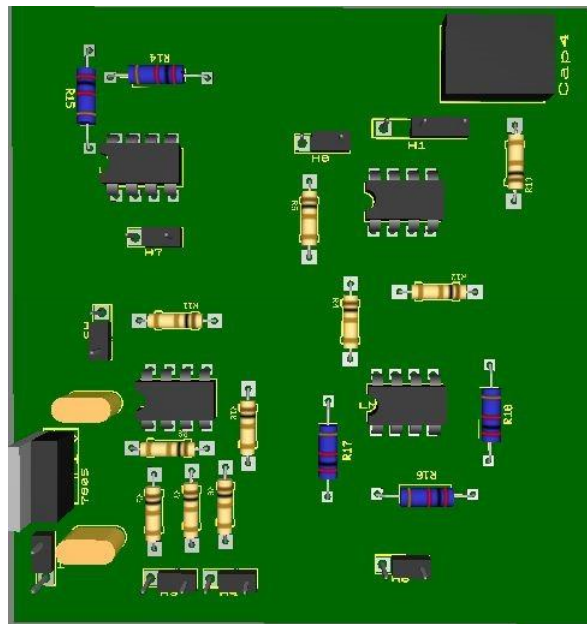


Figure 5-1 Flow Chart of the Proposed Software Design

Figure 5-1 is the flow chart of the complete software design for computing temperature using a thermocouple through artificial intelligence. The system collects data, namely thermocouple reference temperature and voltage, check the type of neural network selected through a “select push button “as the system has ANN (weights and bias) for each thermocouple type (J, R, E, and T) and runs the correct neural network. The controller of the application has an inbuilt ADC that is used to measure reference temperature, thermocouple EMF. In the microcontroller, Digital to analog conversion is done to compute reference temperature ($^{\circ}\text{C}$) and get thermoelectric voltage (millivolts), send the input vector to the neural network for processing.



5.3 Experimental results

In this section of the report, experimental results for type T, J, and E thermocouples are presented. This experiment was conducted at the University of KwaZulu-Natal Chemical Engineering Laboratory to evaluate the theoretical findings/results of this study. In the Chemical Engineering laboratory, there is Temperature controller TTM-004 that was used for temperature set points in the measurement. A thermocouple is placed inside and through the small opening on the TTM-004 oven/controller, and the other ends of the thermocouple are put on the input stage of the instrumentation amplifier for amplification of the signal. The output of the instrumentation amplifier is sent to the Arduino Uno. An LM35 temperature sensor measures the reference temperature of the thermocouple or surrounding area, and for verification purposes, a Fluke infrared thermometer (Infrared Thermometer (IR)-561) was used to measure the reference junction temperature and the measured thermocouple temperature inside the TTM-004. Fluke IR thermometer was used to compare the result of the signal condition system with a well-recognized temperature measuring device which is available in the market. To quantify the performance of the designed signal conditioning system, a Fluke IR thermometer is used for data collection to formulate facts and uncover patterns in the analysis of the designed system. Figure 5-3 below shows the experimental setup of the overall system testing.

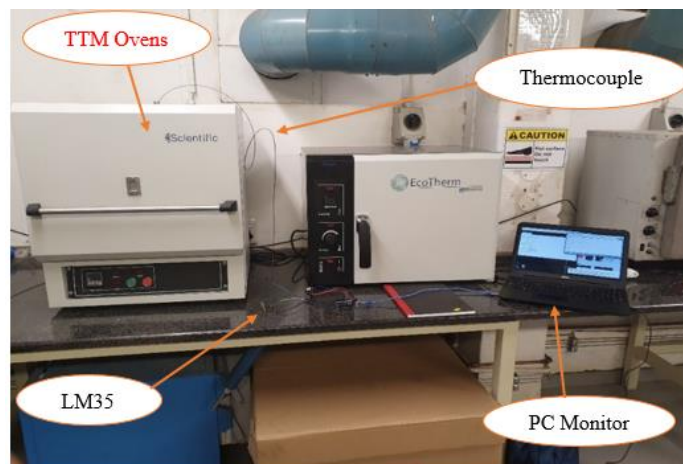


Figure 5-3 Experimental setups at Chemical Engineering Laboratory

In this setup, a PC was used to display reference temperature measured by the LM35 and the measured thermocouple voltage inside the TTM oven. First, the temperature of the oven is set; once the temperature of the TTM oven has reached the set-point, the reference temperature displayed on the PC is captured and verified by using Fluke 561 IR thermometer. The measured thermocouple temperature is captured from the PC, and simultaneously TTM oven temperature is measured using the IR thermometer. The temperature of the TTM-004 controller/oven is varied from 100°C to 350°C for both heating and cooling conditions of the controller or oven. After every thermocouple type testing has been

conducted, the thermocouple is changed to the next thermocouple type, and the neural network changes to the neural network of that thermocouple type.

5.3.1 Type T thermocouple experimental results and analysis

The data in Table 5-1 shows temperature measurement evaluated by the signal conditioning system when the experiment was conducted. The temperature of the oven was adjusted between 100°C to 300°C, and the signal conditioning neural network was selected or set for a T-type thermocouple. In Table 5-1, the LM 35 reference junction temperature is the temperature reading evaluated by the microcontroller subroutine used together with thermocouple thermoelectric voltage readings as input vector for the neural network subroutine.

Table 5-1 Experimental results for TTM-004 temperature (°C) measurement using type T thermocouple

TTM – 004	Signal Conditioning: Neural Network		Infrared (IR) Thermometer		TTM-004 and NN	TTM-004 and IR-561
	LM35 reference temperature	Temperature evaluated by neural network	Reference temperature	Measured temperature		
Set temperature	LM35 reference temperature	Temperature evaluated by neural network	Reference temperature	Measured temperature	Percentage error	Percentage error
100	23.587	100.755	23.2	99	0,75%	1,00%
125	24.206	125.627	23.6	122	0,50%	2,40%
150	24.375	150.168	23.8	145	0,11%	3,33%
175	24.15	176.994	23.9	168	1,14%	4,00%
200	24.506	202.23	24.1	192	1,11%	4,00%
225	24.806	223.343	24.2	236	0,74%	4,89%
250	24.694	250.438	24.6	252.7	0,18%	1,08%
275	24.994	277.323	24.9	260	0,84%	5,45%
300	24.9	297.049	25.1	314	0,98%	4,67%
275	24.812	276.045	25	266	0,38%	3,27%
250	24.711	255.084	24.8	251	2,03%	0,40%
200	24.543	201.044	24.4	199	0,52%	0,50%
140	24.075	139.934	23.5	141	0,05%	0,71%
162	24.113	162.38	23.9	155	0,23%	4,32%

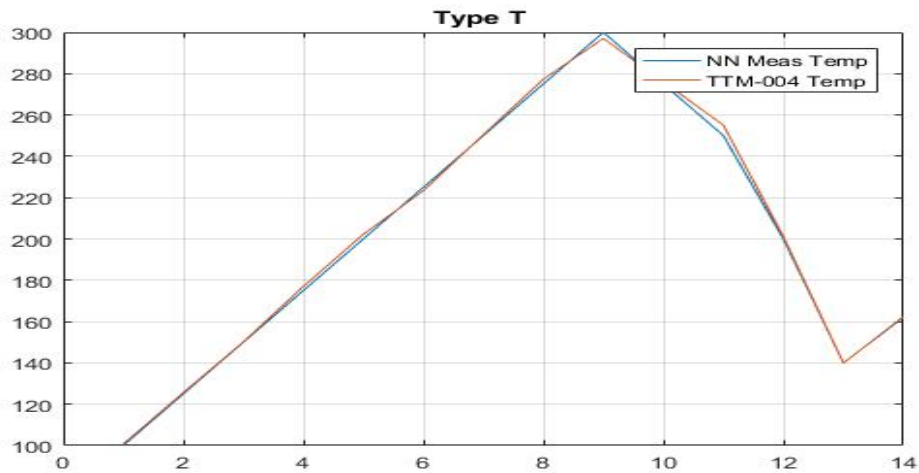


Figure 5-4 Type T: Temperature evaluated by neural network and TTM-004 Oven

Figure 5-4 shows the plot of temperature evaluated by signal conditioning system neural network subroutine and temperature of the TTM-004 temperature controller. As can be seen in Table 5-1, the designed thermocouple signal condition system using a neural network accurately evaluates the temperature of the TTM-004 controller within 2% of the temperature of the TTM-004. Temperature measurement using Fluke IR thermometer shows an error within 5% of the readings recorded by the TTM-004 controller. It appears that the measurement of TTM-004 controller temperature using the designed neural network has high-quality results as compared to the commercial Fluke 561 IR thermometer.

5.3.2 Type J thermocouple experimental results and analysis

In this section, the experimental results obtained during the evaluation of the thermocouple-designed signal conditioning system using neural networks for type J thermocouples are presented and discussed. The temperature of the oven or TTM-004 controller was adjusted from 150°C to 300°C, and the neural network for type J thermocouple was selected.

Table 5-2 Experimental results for TTM-004 temperature (°C) measurement using type J thermocouple

TTM – 004	Signal Conditioning: Neural Network (NN)		Infrared (IR) Thermometer		TTM-004 and NN	TTM-004 and IR-561
	LM35 reference temperature	Temperature evaluated by neural network	Reference temperature	Measured temperature		
Set temperature					Percentage error	Percentage error
150	22.701	151.823	22.7	149	1,22%	0,67%
175	22.83	172.078	23	164.5	1,67%	6,00%
200	23.06	192.789	22.9	187	3,61%	6,50%
225	23.006	219.801	23.3	230	2,31%	2,22%
250	23	246.845	23.3	262	1,26%	4,80%
275	20.925	273.183	20.4	280	0,66%	1,82%
300	21.337	295.852	20.6	323	1,38%	7,67%
275	21.769	282.864	21	279	2,86%	1,45%
250	22.106	256.12	21.3	253	2,45%	1,20%
225	22.086	226.7	22.2	229	0,76%	1,78%
200	22.612	195.806	22.4	202	2,10%	1,00%
175	21.113	174.242	21.8	162	0,43%	7,43%
150	21.433	152.369	22.9	151	1,58%	0,67%

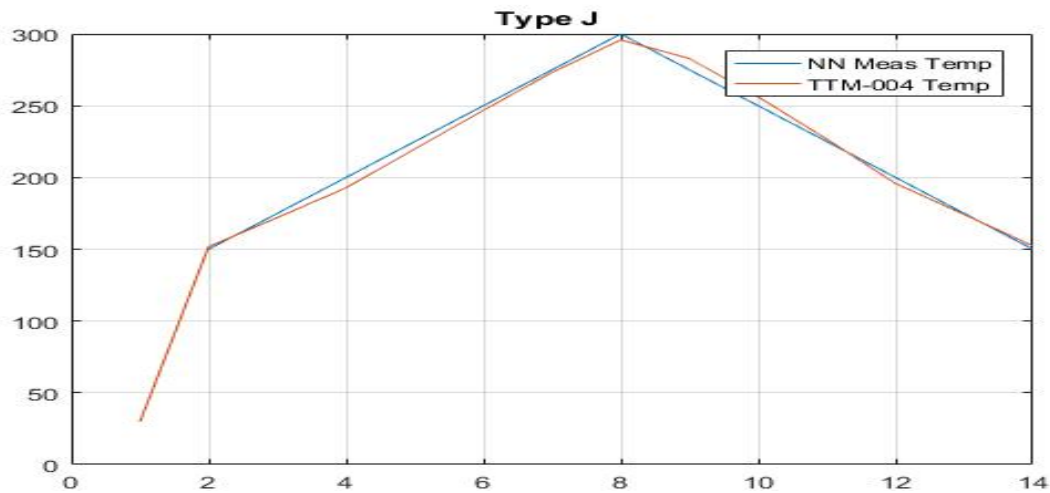


Figure 5-5 Type J: Temperature evaluated by neural network and TTM-004 Oven

Table 5-2 shows data recorded during the experimental test of the type J thermocouple signal conditioning using a neural network. The data shown in the table is the temperature measurement of the TTM-004 controller using the designed signal conditioning neural network for type J thermocouple and Fluke IR 561 thermometer. A plot of temperature evaluated by the designed type J neural network and TTM-004 temperature controller is shown in Figure 5-5. Moreover, Table 5-2 shows the percentage error of the temperature evaluated by TTM-004 and neural network and the error between TTM-004 and IR thermometer. From Table 5-2, it can be seen that temperature measurements evaluated by the signal conditioning system for type J thermocouple are within 4% of the readings from the TTM-004 oven. While the measurements evaluated using the Fluke IR thermometer are within 8% of the TTM-004 controller. The results above indicate that the designed signal conditioning system using a neural network has improved accuracy as compared to the Fluke 561 IR.

5.3.3 Type E thermocouple experimental results and analysis

Experimental work was undertaken using standard ovens at the Department of Chemical Engineering of the University of Kwa-Zulu Natal to validate the theoretical results for the E-type thermocouple signal conditioning system using neural networks.

Table 5-3 Experimental results for TTM-004 temperature (°C) measurement using type E thermocouple

TTM – 004	Signal Conditioning: Neural Network (NN)		Infrared (IR) Thermometer		TTM-004 and NN	TTM-004 and IR-561
	LM35 reference temperature	Temperature evaluated by neural network	Reference temperature	Measured temperature		
Set temperature					Percentage error	Percentage error
150	22.316	148.779	22.4	158	0,81%	5,33%
175	23.309	176.877	22.9	181	1,07%	3,43%
200	23.212	200.317	23.1	199.5	0,16%	0,25%
225	23.88	223.309	23.9	215	0,75%	4,44%
250	23.719	247.761	23.4	238	0,90%	4,80%
275	24.056	271.328	23.7	262	1,34%	4,73%
300	24.15	291.061	23.8	282	2,98%	6,00%
350	24.169	347.22	23.6	335	0,79%	4,29%
275	24.023	277.309	24.1	286	0,84%	4,00%
250	23.911	252.744	24.3	243	1,10%	2,80%
200	23.946	201.123	24.1	208	0,56%	4,00%
175	24.104	174.485	24.3	169	0,29%	3,43%
150	23.122	151.286	23.4	144	0,86%	4,00%

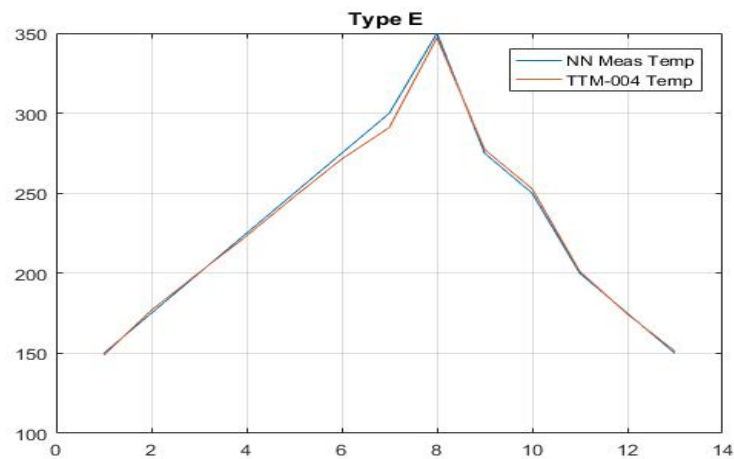


Figure 5-6 Type E: Temperature evaluated by neural network and TTM-004 Oven

Figure 5-6 shows the plot of the temperature of the TTM-004 evaluated by the signal conditioning neural network for the type E thermocouple. Table 5-3 shows temperature measurement results obtained during the experimental test conducted to test the study of enhancing measurement accuracy of thermocouples using neural networks. The TTM-004 temperature controller was varied from 150°C to 350°C, and the table shows the recorded data during the experiment. From Table 5-3, it can be seen that the TTM-004 controller temperature was evaluated to be within 3% by the neural network for the E-type thermocouple. The measurement of the TTM-004 oven temperature was evaluated to be within 6% by the Fluke IR 561. Therefore, it is evident that the neural network for the type T thermocouple produced high measurement accuracy compared to the Fluke 561 IR thermometer.

5.4 Results analysis and conclusion

The use of the neural network in thermocouple temperature measurement accuracy enhancement was explored by designing and testing a microcontroller-based thermocouple signal conditioning system using neural networks. The results of the experimental study indicated that neural networks could be used in thermocouple measurement accuracy enhancement with the thermocouple subjected to both random variations in the reference junction temperature and nonlinearities. From the experimental results, the neural networks for each thermocouple type (T, J, and E) all had better performance compared to a commercially available infrared thermometer (Fluke 561 IR) with 2%, 4%, and 3%, respectively. Therefore, it is evident from the results that the designed thermocouple signal conditioning system is capable of enhancing temperature measurement accuracy.

6. CONCLUSION AND RECOMMENDATIONS

6.1 Introduction

The closing comments on the study are presented in this chapter, providing an overview and conclusion of the research. The study is examined in terms of both its contribution to the field and its limitations. Recommendations are made with regard to aspects that could be explored in future research, especially within the context of thermocouple cold junction compensation in enhancing temperature measurement using thermocouples.

6.2 Conclusion

The purpose of this research was to study the enhancement of the accuracy of thermocouple temperature measurement subjected to both random variations in the reference junction temperature and nonlinearities. Based on the analysis conveyed, it can be concluded that a neural network-based signal conditioning system is capable of enhancing the accuracy of thermocouple temperature measurement subjected to variations in the reference junction of the thermocouple. The microcontroller-based thermocouple signal conditioning system using a neural network showed high-quality measurement accuracy compared to a commercially available Fluke 561 thermometer for the three thermocouples sampled for this study. The temperature adjustments for the oven often took several hours to reach their steady-state values. Steady-state oven, hence thermocouple hot junction temperatures, were simultaneously monitored using the existing oven temperature sensor, one commercially available infrared thermometer, and the thermoelectric output voltage of the thermocouple. The settings on the external switch provided the information used by the microcontroller to select the neural network subroutine for the thermocouple being tested. By calling the appropriate subroutine with thermoelectric voltage produced by the corresponding thermocouple, together with the LM 35 cold junction readings, the microcontroller returns the hot junction temperature reading corresponding to the measured thermoelectric voltage. The experimental results showed that the temperature of the TTM-004 controller or oven was evaluated to within 2% by type T neural network and within 5% of the readings recorded using Fluke IR 561. Similarly, the experimental results for the J-type thermocouple neural network showed that the temperature readings for the evaluated temperature of the TTM-004 oven were within 4%, and the readings by the Fluke IR 561 were within 8% of the TTM-004 controller temperature. Lastly, the experimental results showed that, for the E-type thermocouple neural network, temperature readings of TTM-004 temperature were evaluated by the designed neural network to within 3% and within 6% of the readings recorded by the Fluke 561 IR thermometer.

6.3 Recommendations for further study

Further studies and investigations can be conducted in the following areas:

- Development of high accuracy instrumentation amplifier to improve the accuracy of thermocouple thermoelectric voltage readings by the microcontroller.
- Selection of cold or reference junction voltage to temperature sensor used for reading the reference junction temperature of the thermocouple.

7. BIBLIOGRAPHY

- [1] W. Long, S. Naimi, M. Criscitello, "Development of a knowledge base for diagnostic reasoning in cardiology", *Computers in Biomedical Research*, 25, 292–311, 1992
- [2] F. Azuaje, W. Dubitzky, P. Lopes, N. Black, K. Adamson, "Predicting coronary disease risk based on short-term RR interval measurements: A neural network approach", *Artificial Intelligence in Medicine*, 15, 275–297, 1999
- [3] P. Foote, "Note on the cold-junction corrections for thermocouples", *Bulletin of the Bureau of Standards*, vol. 9, no. 4, p. 553, 1913.
- [4] S. Chakravarthy and J. Ghosh, "Function Emulation Using Radial Basis Function Networks", *Neural Networks*, vol. 10, no. 3, pp. 459-478, 1997.
- [5] S. Hannan, R. Manza and R. Ramteke, "Generalized Regression Neural Network and Radial Basis Function for Heart Disease Diagnosis", *International Journal of Computer Applications*, vol. 7, no. 13, pp. 7-13, 2010.
- [6] F. Caldwell, "Temperatures of thermocouple reference junctions in an ice bath", *Journal of Research of the National Bureau of Standards, Section C: Engineering and Instrumentation*, vol. 69, no. 2, p. 95, 1965.
- [7] H. Shaker, A. Saleh, A. Ali and M. Abd Elaziz, "Self-Calibrating Enabled Low Cost, Two Channel Type K Thermocouple Interface for Microcontrollers", *Arab Journal of Nuclear Sciences and Applications*, vol. 0, no. 0, pp. 1-9, 2018.
- [8] U. Sinha, "Cold-Junction Compensation of Thermocouple by using Semiconductor Diode", *IETE Technical Review*, vol. 17, no. 1-2, pp. 71-72, 2000.
- [9] Y. WANG, Z. YAN and W. HE, "Thermocouple Cold End Compensation System with Programmable Function", *DEStech Transactions on Computer Science and Engineering*, no. -, 2017.
- [10] M. Gardner, S. Dorling, "Artificial Neural Networks (Multilayer Perceptron) –A Review of applications in the atmospheric sciences, *Atmospheric Environment* Vol. 32, No. 14/15, pp. 2627–2636, 1998
- [11] C. Medeiros, G. Barreto, "Pruning the Multilayer Perceptron Through the Correlation of Backpropagated Errors", *Seventh International Conference on Intelligent Systems Design and Applications*,

- [12] G. Wei, X. Wang, J. Sun, "Signal processing method with cold junction compensation for thermocouple", I2MTC 2009 - International Instrumentation and Measurement Technology Conference Singapore, 5-7 May 2009
- [13] D. Lampasi, L. Podesta "A Measurement System Exploiting Non-Linearity of Thermocouples for Cold Junction Compensation", Instrumentation and Measurement Technology Conference Como, Italy. May 18-20, 2004
- [14] J. Agee, S. Masupe, D. Setlhaolo, "Feedforward Neural-Network Conditioning of Type-B Thermocouple with Variable Reference-Junction Temperature", 2nd International Conference on Adaptive Science & Technology, pp. 296 – 300, 2009
- [15] M. Engin, D. Engin, "Compensation of Thermocouple Nonlinearities with Embedded System", 5th Mediterranean Conference on Embedded Computing (MECO), 2016, pp. 234 – 237.
- [16] M. Garcia, C. Sánchez, M. López, D. Hornero, R. Hornero, "Automatic Detection of Red Lesions in Retinal Images Using a Multilayer Perceptron Neural Network", 30th Annual International IEEE EMBS Conference Vancouver, British Columbia, Canada, August 20-24, 2008
- [17] T. Haruyama, R. Yoshizaki, "A 0 °C bath for the reference junctions of thermocouples by using a solid-state heat pump", J. Phys. E: Sci. Instrum. 19 (1986).
- [18] A. Mubalike (Mubarck), E. Adah, "Multilayer Perceptron Neural Network Technique for Fraud Detection", 2nd International Conference on Computer Science and Engineering, pp. 383 – 387, 2017
- [19] Anish Mukherjee, Debarghya Sarkar, Arijit Sen, Debangshu Dey, Sugata Munshi. "An analog signal conditioning circuit for thermocouple temperature sensor employing thermistor for cold junction compensation", 2013 International Conference on Control, Automation, Robotics and Embedded Systems (CARE), 2013
- [20] D. Specht, "A General Regression neural network", IEEE TRANSACTIONS ON NEURAL NETWORKS, VOL. 2. NO. 6. NOVEMBER 1991
- [21] S. Nandakumar, A. Abraham, P. Panicker, C. Hari, M. Priya, "THERMOD- Signal Conditioning Module with Cold Junction Compensation in Thermocouple", International Journal of Scientific & Engineering Research Volume 8, Issue 8, August-2017
- [22] Z. Zainuddin, O. Pauline, "Function Approximation Using Artificial Neural Networks", INTERNATIONAL JOURNAL OF SYSTEMS APPLICATIONS, ENGINEERING & DEVELOPMENT Issue 4, Volume 1, 2007

- [23] L. Marquez, T. Hill, “Function Approximation Using Backpropagation and General Regression Neural Networks”,
- [24] M. Attari, F. Boudema, M. Heniche, “AN ARTIFICIAL NEURAL NETWORK TO LINEARIZE A G (TUNGSTEN VS. RANGE OF ZERO TO 2000°C TUNGSTEN 26% RHENIUM) THERMOCOUPLE CHARACTERISTIC IN THE RANGE OF ZERO TO 2000°C”,
- [25] J. Dias Pereira, O. Postolache, P. Silva Girão, M. Cretu, “MINIMISING TEMPERATURE DRIFT ERRORS OF CONDITIONING CIRCUITS USING ARTIFICIAL NEURAL NETWORKS”, IEEE Instrumentation and Measurement Technology Conference, vol. 49, no. 5, October 2000
- [26] D. DEY and S. MUNSHI, “A New Intelligent Scheme for Simultaneous Cold Junction Compensation and Linearization of Thermocouples”, Leonardo Electronic Journal of Practices and Technologies, Issue 19, p. 13-28, July-December 2011,
- [27] J. Tang, Y. Zhang, X. Tang, J. Liu, “Nonlinearity correction of the thermocouple based on neural network”, Global Congress on Intelligent Systems, pp. 28 – 32, 2009
- [28] “ITS-90 Thermocouple Database, Web Version 2.0”, Srdata.nist.gov, 2017. Available: <https://srdata.nist.gov/its90/main/>. [Accessed: 20 May 2017]
- [29] G. W. Burns and M. G. Scroger, “The Calibration of Thermocouples and Thermocouple Materials”, NIST Measurement Services, June 12, 1989
- [30] OMEGA Temperature Measurement Handbook, Omega Instruments, Inc.
- [31] Pyromation.com, [online] Available at: https://www.pyromation.com/Downloads/Doc/Training_TC_Theory.pdf [Accessed 2 Nov. 2018].
- [32] K. Binoy, K. Santhosh, “An Intelligent Temperature Measurement Technique Using J Type Thermocouple with an Optimal Neural Network”, Sensors and Transducers, Vol.147, issue 12, pp. 6 - 14, 2012
- [33] Krzysztof Konopka¹, “Thermocouple Dynamic Errors Correction for Instantaneous Temperature Measurements in Induction Heating”, 19th IMEKO TC 4 Symposium and 17th IWADC Workshop Advances in Instrumentation and Sensors Interoperability, July 18-19, 2013, Barcelona, Spain
- [34] Walt Kester, Editor, System Applications Guide, Section 1, 6, Analog Devices, Inc., 1993.
- [35] Dan Sheingold, Nonlinear Circuits Handbook, Analog Devices, Inc.
- [36] James Wong, Temperature Measurements Gain from Advances in High-precision Op-Amps, Electronic Design, 15 May 1986.

- [37] G. Recktenwald, Conversion of Thermocouple Voltage to Temperature, July 14, 2010
- [38] Duff, M. and Towey, J. (2017). Two Ways to Measure Temperature Using Thermocouples Feature Simplicity, Accuracy, and Flexibility | Analog Devices. [online] Analog.com. Available at: <https://www.analog.com/en/analog-dialogue/articles/measuring-temp-using-thermocouples.html> [Accessed 2 May. 2017].
- [39] Web.mst.edu. (2017). [online] Available at: <https://web.mst.edu/~cottrell/ME240/Resources/Temperature/Temperature.pdf> [Accessed 15 Aug. 2017].
- [40] M. Buscema, “Back Propagation Neural Networks”, Substance Use & Misuse, February 1998
- [41] M. Nielsen, Neural Networks and Deep Learning. [online] Neuralnetworksanddeeplearning.com. Available at: <http://neuralnetworksanddeeplearning.com/chap1.html> [Accessed 6 March. 2018].
- [42] X. Wang, “An Improved LSSVR-based nonlinear calibration for thermocouple”, First International Conference on Intelligent Networks and Intelligent Systems, 2008, pg. no 421 – 424
- [43] Z. Song, C. Liu, and X. Song, “Mathematical Model of Thermocouple Characteristics based on neural network”, Proceedings of the Second International Conference on Machine Learning and Cybernetics, 2003, pg. 1404 – 1407
- [44] Module 4 : THERMOELECTRICITY Lecture 21 : Seebeck Effect. <https://nptel.ac.in/content/storage2/courses/122101002/downloads/lec-21.pdf>
- [45] thermocouple measurement| data acquisition | cold junction.... <http://www.mosaic-industries.com/Products/WildCards/tcm/>
- [46] Chapter I - Analog Devices. <https://www.analog.com/media/en/training-seminars/design-handbooks/designers-guide-instrument-amps-chI.pdf>
- [47] Activation Functions in Neural Networks | Deep Learning.... <https://www.deeplearning-academy.com/p/ai-wiki-activation-functions>
- [48] Push Button | Definition of Push Button by Lexico. https://www.lexico.com/en/definition/push_button
- [49] R. Rojas, Neural Networks, A Systematic Introduction. New York: Springer-Verlag, 1995.
- [50] E. M. Petriu, “neural network and fuzzy systems for modeling applications,” in IMTC’98, St. Paul, MN, May 1999, Session 4 Tutorial.
- [51] B. Kosco, Neural Networks for Signal Processing, ser. NJ. Englewood Cliffs: Prentice-Hall, 1992.

- [52] A. Bernieri, "A neural network approach for identification and fault diagnosis on dynamic systems," *IEEE Trans. Instrum. Meas.*, vol. 43, pp.867–873, Dec. 1994.
- [53] Thermocouple data available at: <http://www.omega.com>
- [54] M. K. Lenzi, F. M. Silva, E.L. Lim and J.C. Pinto, "Low cost thermocouple signal conditioning module", *Journal of Chemical Engineering*, vol. 52, no. 1, 2005. On <http://www.JCE.DivCHED.org>
- [55] G. W. Burns, G. F. Strouse, B. W. Magnum, M. C. Croarkin, W.F. Guthrie, and M. Chattle, *New Reference Functions for Platinum-13% Rhodium Versus Platinum -6% (type B) Thermocouple Based on the ITS-90*.
- [56] G. Burns, G. f. Strouse, B. W. Magnum, P. Marcarino, M. Battuello, H. K. Lee, J. c. Kim, K. S. Gam, C. Rhee, M. Chattle, M. Arai, H. Sakurai, A. I. Pokhodun, N. P. Moiseera, S. A. Perevalova, M. J. de Groot, J. Zhang, k. Fan and S. Wu, *New Reference Function for Platinum-10% Rhodium versus Platinum (type S) Thermocouple Based on the ITS-90. Part I: Experimental Procedure*.
- [57] G. Burns, G. f. Strouse, B. W. Magnum, P. Marcarino, M. Battuello, H. K. Lee, J. c. Kim, K. S. Gam, C. Rhee, M. Chattle, M. Arai, H. Sakurai, A. I. Pokhodun, N. P. Moiseera, S. A. Perevalova, M. J. de Groot, J. Zhang, k. Fan and S. Wu, *New Reference Function for Platinum-10% Rhodium versus Platinum (type S) Thermocouple Based on the ITS-90. Part I: Results and Discussions*.
- [58] Hornik, K., M. Stinchcombe & H. White, *Multilayer Feedforward Networks are Universal Approximator*, *Neural Networks*, Vol. 2, 1989,pg 359-3661.
- [59] M.H. Ahmad Fadzil & Zarita Zainuddin, *Optimization of Learning Methods for Face Recognition using MLP*, *Proceedings of the 3rd IASTED Int. Conf. On Signal and Image Processing*, Honolulu, Hawaii, USA, Aug 13-16 2001.
- [60] Zarita Zainuddin & Evans, D.J., "Human Face Recognition using Accelerated Multilayer Perceptrons", *International Journal of Computer Mathematics*, Vol. 80, No.5, pg 535-558
- [61] V. P. Preobrazhensky, "Measurements and Instrumentation in Heat Engineering", MIR Publishers, Moscow, 1980.
- [62] U. Tietze, and Ch. Schenk, "Electronic circuit design and applications", Narosa Publishing House, New Delhi, 1992.
- [63] T. R. Padmanabhan, "Industrial Instrumentation", Springer-Verlag, London, 2000.
- [64] U. Sinha, "Cold junction compensation of thermocouple by using semiconductor diode", *Journal of the IETE*, Vol. 17, No. 1&2,2000, pp.101-105.

- [65] B. L. Lu, Y. Bai, H. Kita, and Y. Nishikawa, "An efficient multilayer quadratic perceptron for pattern classification and function approximation," in Proc. Int. Joint Conf. Neural Networks, Nagoya, Japan, Oct. 25–29, 1993, pp. 1385–1388.
- [66] B. L. Lu, H. Kita, and Y. Nishikawa, "Inversion of feedforward neural networks by a separable programming," in Proc. World Congr. Neural Networks, Portland, OR, July 11–15, 1993, pp. IV415–IV420.
- [67] J. Webster, Measurement, instrumentation, and sensors handbook, CRCnetBase 1999, <http://www.crcnetbase.com/isbn/9780415876179>.
- [68] Yao Jun Yu. "Nonlinear Calibration of Thermocouple Sensor Using Least Squares Support Vector Regression", Advanced Materials Research, 2012
- [69] Z. Zirojevic. "Compensation of thermocouple reference junction temperature variation by a silicon temperature sensor", 1997 21st International Conference on Microelectronics Proceedings IC MEL-97, 1997
- [70] C.A. Jensen, R.D. Reed, R.J. Marks, M.A. El- Sharkawi, Jae-Byung Jung, R.T. Miyamoto, G.M. Anderson, C.J. Eggen. "Inversion of feedforward neural networks: algorithms and applications", Proceedings of the IEEE, 1999
- [71] Oscar May, Luis J. Ricalde, Bassam Ali, Eduardo Ordoñez López, Eduardo Venegas- Reyes, Oscar A. Jaramillo. "Chapter 15 Neural Network Inverse Modeling for Optimization", IntechOpen, 2016
- [72] Thomas E. Salem, Dimeji Ibitayo, Bruce R. Geil. "A Technique for Die Surface Temperature Measurement of High-Voltage Power Electronic Components using Coated Thermocouple Probes", 2006 IEEE Instrumentation and Measurement Technology Conference Proceedings, 2006
- [73] M.W Gardner, S.R Dorling. "Artificial neural networks (the multilayer perceptron)—a review of applications in the atmospheric sciences", Atmospheric Environment, 1998
- [74] Liang Jin, P.N. Nikiforuk, M.M. Gupta. "Fast neural learning and control of discrete-time nonlinear systems", IEEE Transactions on Systems, Man, and Cybernetics, 1995
- [75] Zhuang, Zhemin, Weiyi Huang, and Shunqing Xu. "", International Conference on Sensor Technology (ISTC 2001), 2001.
- [76] Abdelaziz, Y.A.. "Stability and calibration of platinum/palladium thermocouples following heat treatment", Measurement, 200406
- [77] "Thermoelectricity abstracts", Advanced Energy Conversion, 1961

- [78] Orest Kochan, Roman Kochan, Volodymyr Kochan, Jun Su. "Thermocouple with adjustable error", 2017 9th IEEE International Conference on Intelligent Data Acquisition and Advanced Computing Systems: Technology and Applications (IDAACS), 2017
- [79] J.M.D. Pereira, O. Postolache, P.M.B.S. Girao, M. Cretu. "Minimizing temperature drift errors of conditioning circuits using artificial neural networks", IEEE Transactions on Instrumentation and Measurement, 2000
- [80] D.A. Lampasi, L. Podesta. "A measurement system exploiting non-linearity of thermocouples for cold junction compensation", Proceedings of the 21st IEEE Instrumentation and Measurement Technology Conference (IEEE Cat. No.04CH37510), 2004
- [81] Aditva Mukherjee, Tamojit Saha. "Precision Thermocouple Amplifier for Substrate Temperature Monitoring in an ECR-PE Nano- Film Deposition System", 2018 2nd International Conference on Electronics, Materials Engineering & Nano-Technology (IEMENTech), 2018
- [82] Rong Yu. "Using Operational Amplifiers to Realize the Compensation of Thermocouples", 2008 ISECS International Colloquium on Computing Communication Control and Management, 08/2008
- [83] G. Li-Hui W. Wu, J. Xiao-bo, "Thermocouple Signal Conditioning with Genetic Optimizing RBF Neural Networks", 2011 IEEE 3rd International Conference on Communication Software and Networks, 2011
- [84] Debarpan Bhattacharya, Pranabendra Prasad Chandra, Biswajit Bhattacharyya, Sugata Munshi. "Optimized Thermocouple Temperature Sensor using 555 Timer and ANN Based Linearization", 2020 IEEE Calcutta Conference (CALCON), 2020
- [85] P. Cappa. "AN EXPERIMENTAL ANALYSIS OF THE METROLOGICAL PERFORMANCES OF AN AUTOMATIC THERMOCOUPLE INSTRUMENTATION SYSTEM CONDUCTED BY A SIMPLE CALIBRATION SETUP", Experimental Techniques, 01/28/2008

Appendix A

Thermocouple functional Coefficients - reference function on ITS-90							
Type R		Type T		Type E		Type J	
Range	coefficients	Range	coefficients	Range	coefficients	Range	coefficients
-50 to 1064	-2.81038625251000e-27	0 to 400	-2.75129016730000e-20	-270 to 0	-3.46578420130000e-29	-210 to 760	1.56317256970000e-23
	1.57716482367000e-23		4.54791352900000e-17		-5.58273287210000e-26		-1.25383953360000e-19
	-3.73105886191000e-20		-3.08157587720000e-14		-3.96736195160000e-23		2.09480906970000e-16
	5.00777441034000e-17		1.09968809280000e-11		-1.64147763550000e-20		-1.70529583370000e-13
	-4.62347666298000e-14		-2.18822568460000e-09		-4.39794973910000e-18		1.32281952950000e-10
	3.56916001063000e-11		2.06182434040000e-07		-8.03701236210000e-16		-8.56810657200000e-08
	-2.38855693017000e-08		3.32922278800000e-05		-1.02876055340000e-13		3.04758369300000e-05
	1.39166589782000e-05		0.0387481063640000		-9.32140586670000e-12		0.0503811878150000
	0.00528961729765000		0		-5.94525830570000e-10		0
	0		7.97951539270000e-31		-2.58001608430000e-08		-3.06913690560000e-13
1064.18 to 1664.5	-2.93359668173000e-16	-270 to 0	1.39450270620000e-27	0 to 1000	-7.79980486860000e-07	760 to 1200	1.57208190040000e-09
	2.05305291024000e-12		1.07955392700000e-24		4.54109771240000e-05		-3.18476867010000e-06
	-7.64085947576000e-09		4.87686622860000e-22		0.0586655087080000		0.00317871039240000
	1.59564501865000e-05		1.42515947790000e-19		0		-1.49761277860000
	-0.00252061251332000		2.82135219250000e-17		3.59608994810000e-28		296.456256810000
	2.95157925316000		3.84939398830000e-15		-1.43880417820000e-24		
			3.60711542050000e-13		2.14892175690000e-21		
			2.26511565930000e-11		-1.25366004970000e-18		
	9.01380195590000e-10	-1.91974955040000e-16					
	2.00329735540000e-08	6.50244032700000e-13					
	1.18443231050000e-07	-3.30568966520000e-10					
	4.41944343470000e-05	2.89084072120000e-08					
	0.0387481063640000	4.50322755820000e-05					
	0	0.0586655087100000					
		0					

Appendix B

```

%=====-Type K Thermocouples Coefficients in mV-----
% % %----- Type K -270 to 0-----
% C=[-0.163226974860E-22 -0.198892668780E-19 -0.104516093650E-16 -0.310888728940E-14
-0.574103274280E-12 -0.675090591730E-10...
%   -0.499048287770E-8   -0.328589067840E-6   0.236223735980E-4   0.394501280250E-1
0.000000000000E0];
% Th=randi([-270 0],[1 500]);
% Tc=randi([-10 20],[1 500]);
% %----- Type K 0 to 1372-----
% C=[-0.121047212750E-25 0.971511471520E-22 -0.320207200030E-18...
% 0.560750590590E-15 -0.560728448890E-12 0.318409457190E-9...
% -0.994575928740E-7 0.185587700320E-4 0.389212049750E-1 -0.176004136860E-1];
% Th=randi([0 1372],[1 2000]);
% Tc=randi([-10 30],[1 2000]);
%
% a0 = 0.118597600000E+00; a1= -0.118343200000E-03; a2=0.126968600000E+03;
%End=====Type K Thermocouples Coefficients in mV-----
%-----Type J Thermocouples Coefficients in mV-----
%----- Type J -210 to 760
% C=[ 0.15631725697E-22 -0.12538395336E-18 0.20948090697E-15 -0.17052958337E-12...
% 0.13228195295E-9 -0.8568106572E-7 0.3047583693E-4 0.50381187815E-1 0 ];
% Th=randi([-210 760],[1 1500]);
% Tc=randi([-10 20],[1 1500]);
% %-----Type J 760 to 1200-----
% C=[-0.306913690560E-12 0.157208190040E-8 -0.318476867010E-5...
% 0.317871039240E-2 -0.149761277860E1 0.296456256810E3];
% Th=randi([760 1200],[1 500]);
% Tc=randi([-10 20],[1 500]);
%End=====Type J Thermocouples Coefficients in mV-----
%-----Type T Thermocouples Coefficients in mV-----
% %----- Type T 0.00 to 400-----
% C=[-0.275129016730E-19 0.454791352900E-16 -0.308157587720E-13 0.109968809280E-10 -
0.218822568460E-08...
% 0.206182434040E-06 0.332922278800E-04 0.387481063640E-01 0.000000000000E+00];
% Th=randi([0 400],[1 2000]);
% Tc=randi([-10 30],[1 2000]);
%-----Type T -270 to 0 -----
% C=[ 0.797951539270E-30 0.139450270620E-26 0.107955392700E-23 0.487686622860E-21...
% 0.142515947790E-18 0.282135219250E-16 0.384939398830E-14 0.360711542050E-12...
% 0.226511565930E-10 0.901380195590E-9 0.200329735540E-7 0.118443231050E-6...
% 0.441944343470E-4 0.387481063640E-1 0.000000000000E0];
% Th=randi([-270 0],[1 500]);
% Tc=randi([-10 20],[1 500]);
%End=====Type T Thermocouples Coefficients in mV-----
%-----Type B Thermocouples Coefficients in mV-----
% %----- Type B 0 to 630-----
% C=[0.629903470940E-18 -0.169445292400E-14 0.156682919010E-11 -0.132579316360E-08
0.590404211710E-05...
% -0.246508183460E-03 0.000000000000E+00];
% Th=randi([0 630],[1 2000]);
% Tc=randi([-10 30],[1 2000]);
%-----Type B 630 to 1820-----
% C=[-0.937913302890E-24 0.989756408210E-20 -0.445154310330E-16 0.111097940130E-
12...
% -0.168353448640E-09 0.157852801640E-06 -0.848851047850E-04 0.285717474700E-01 -
0.389381686210E+01];
% Th=randi([630 1820],[1 500]);
% Tc=randi([-10 20],[1 500]);
%End-----Type B Thermocouples Coefficients in mV-----
%-----Type R Thermocouples Coefficients in mV-----
% %----- Type R -50 to 1064-----

```

```

% C=[-0.281038625251E-26 0.157716482367E-22 -0.373105886191E-19 0.500777441034E-
16...
% -0.462347666298E-13 0.356916001063E-10 -0.238855693017E-07 0.139166589782E-04
0.528961729765E-02 0];
% Th=randi([-50 1063],[1 2000]);
% Tc=randi([-10 30],[1 2000]);
% ----- Type R 1064 to 1664-----
% C=[-0.293359668173E-15 0.205305291024E-11 -0.764085947576E-08 0.159564501865E-
04...
% -0.252061251332E-02 0.295157925316E+01];
% Th=randi([1063 1664],[1 250]);
% Tc=randi([-10 20],[1 250]);
% ----- Type R 1664.5 to 1768-----
% C=[ -0.934633971046E-14 -0.345895706453E-07 0.171280280471E-03...
% -0.268819888545E+00 0.152232118209E+03];
% Th=randi([1665 1768],[1 250]);
% Tc=randi([-10 20],[1 250]);
%End-----Type R Thermocouples Coefficients in mV-----
% Th=randi([0 300],[1 10]);
% Tc=[0,0,0,0,0,0,0,0,0,0];

%
%-----Type E Thermocouples Coefficients in mV-----
%-----Type E -270 to 0 -----
% C =[-0.346578420130E-28 -0.558273287210E-25 -0.396736195160E-22 -0.164147763550E-
19 -0.439794973910E-17...
% -0.803701236210E-15 -0.102876055340E-12 -0.932140586670E-11 -0.594525830570E-09 -
0.258001608430E-07...
% -0.779980486860E-06 0.454109771240E-04 0.586655087080E-01 0.000000000000E+00];
% Th=randi([-270 0],[1 500]);
% Tc=randi([-10 30],[1 500]);
%-----Type E 0 to 1000 -----
C=[ 0.359608994810E-27 -0.143880417820E-23 0.214892175690E-20 -0.125366004970E-17 -
0.191974955040E-15 0.650244032700E-12...
-0.330568966520E-09 0.289084072120E-07 0.450322755820E-04 0.586655087100E-01
0.000000000000E+00];
Th=randi([0 1000],[1 1500]);
Tc=randi([-10 30],[1 1500]);
%Data=xlsread('TC_Data','R');
%Th=Data(:,1);
%Tc=zeros(33,1);
%Vm = c1*((Th).^1 - (Tc).^1) + c2*((Th).^2 - (Tc).^2) + c3*((Th).^3 -
(Tc).^3)+c4*((Th).^4 - (Tc).^4)+c5*((Th).^5 - (Tc).^5)+c6*((Th).^6 -
(Tc).^6)+c7*((Th).^7 - (Tc).^7)+c8*((Th).^8 - (Tc).^8)+c9*((Th).^9 -
(Tc).^9)+c10*((Th).^10 - (Tc).^10)+c11*((Th).^11 -
(Tc).^11)+c12*((Th).^12 - (Tc).^12)+c13*((Th).^13 -
(Tc).^13)+c14*((Th).^14 - (Tc).^14);

%Th=Th';
%Tc=Tc';
Vm= polyval(C,Th)- polyval(C,Tc);
C_Set=C';
Data_set=[Vm',Tc',Th'];

```

Appendix C

Thermocouple Measurement with varying cold junction temperature											
Type R			Type T			Type E			Type J		
EMF (mV)	T _{ref}	T _{hot}	EMF (mV)	T _{ref}	T _{hot}	EMF (mV)	T _{ref}	T _{hot}	EMF (mV)	T _{ref}	T _{hot}
6,8347	-4	706	13,6620	10	286	-10,2771	17	-220	30,4656	12	565
4,1981	29	490	1,3361	6	39	-1,1561	2	-18	25,0432	-2	456
-0,2020	25	-12	18,5916	5	366	-4,5785	-5	-92	-7,9445	-3	-210
0,4258	10	77	14,6466	26	314	-6,0805	29	-82	15,3597	-5	278
0,1690	6	35	1,7188	19	60	-3,7120	13	-53	41,6846	8	747
5,9179	-5	627	6,7871	21	168	-7,7815	-2	-168	-8,4316	9	-204
1,4050	27	210	19,3723	10	382	-8,8988	0	-203	-8,0680	18	-171
0,7592	-10	108	2,8986	6	75	-7,8950	-7	-181	-6,0043	19	-110
4,9262	-3	540	3,7105	25	109	-1,2954	17	-5	19,7584	14	375
10,3052	3	986	0,8299	0	21	-10,5518	28	-204	-7,4097	8	-166
6,0483	-8	637	2,8089	-10	59	-7,5329	-4	-164	9,8584	17	199
6,9825	-5	718	1,5485	-7	32	-10,8159	17	-263	6,8802	6	135
1,4611	19	211	13,0847	23	285	-4,6001	22	-60	25,3509	4	467
1,2452	9	180	-0,0820	30	28	-8,7989	26	-150	7,7197	-3	142
-0,0625	3	-9	9,4314	10	210	-10,1807	10	-239	4,8811	13	105
6,6064	-1	688	15,2891	7	312	-0,2943	5	0	24,0390	8	447
4,5919	8	515	0,4052	18	28	-5,7675	20	-86	19,9222	-10	356
4,3892	-3	491	12,9332	-2	265	-7,7872	8	-151	0,6671	10	23
9,3041	3	909	8,1954	-7	174	-10,2059	13	-229	7,2078	19	153
10,8381	0	1025	6,7951	8	158	-8,6251	3	-186	-0,8527	5	-12
7,7660	24	796	11,3740	5	242	-6,4136	1	-126	1,7064	8	41
1,5843	18	224	20,8489	-1	399	-8,5430	19	-154	33,1979	12	612
6,7622	3	703	1,2487	21	51	-1,0727	-10	-29	11,4517	-9	204
7,8173	13	795	2,1571	29	79	-10,3829	16	-229	23,5892	-5	427
5,6122	1	603	18,3896	-7	355	-6,5185	-2	-133	15,7391	17	305
8,7729	0	866	0,1214	21	24	-4,9539	16	-74	38,3586	14	699
10,2685	0	982	1,4361	-3	33	-4,0187	1	-73	5,0098	19	113
6,1795	17	660	11,5114	-10	234	-4,3560	25	-52	7,5090	-1	140
-0,2009	11	-29	0,3556	6	15	-4,7996	6	-83	27,3646	16	514

1,1187	-7	155	1,8467	-5	41	-7,3934	19	-124	33,9913	15	628
-0,0633	-8	-21	6,7783	11	160	-9,5924	1	-235	-8,3967	15	-189
10,3871	0	991	9,6216	12	215	-7,6328	6	-150	33,7732	3	614
4,3086	8	489	2,9215	18	86	-6,8507	1	-137	31,2890	6	574
8,3784	1	835	5,9132	25	154	-5,1177	13	-81	16,3514	18	317
3,9245	17	458	19,1706	-10	366	-6,7304	5	-128	10,9845	8	211
4,3127	28	500	5,7448	18	145	-8,7481	-5	-209	20,9150	-10	374
3,5412	21	424	9,0033	30	217	-6,7115	-4	-141	6,1874	-2	115
9,6708	16	943	1,8463	30	73	-10,9108	19	-259	30,2325	-6	545
9,3890	20	923	5,6959	8	136	-2,7872	0	-50	-5,8689	11	-117
6,1040	20	655	17,1233	4	341	-10,6006	24	-216	12,7845	-9	228
2,0827	14	275	18,8125	30	386	-6,2424	-4	-129	28,8724	3	529
2,0329	21	274	9,7401	9	215	-4,9634	17	-73	21,1248	11	397
1,6425	6	223	18,0423	2	355	-9,7035	-1	-255	-8,4303	7	-209
7,0710	14	734	14,6673	5	300	-8,4377	16	-156	-7,5035	-5	-194
8,0979	0	812	2,6786	-10	56	-9,8849	3	-249	13,0123	-8	233
8,7676	1	866	-0,3522	10	1	-7,0280	8	-131	0,5038	-5	5
8,5978	-10	848	16,0485	-5	317	-7,0430	18	-117	7,9595	1	150
1,7355	4	232	9,5304	2	206	-8,8237	4	-191	10,8619	18	218
8,4848	-5	841	3,9066	0	92	-2,1012	2	-35	-7,1234	11	-152
6,1365	6	651	14,2078	-10	282	-5,0395	20	-71	7,8751	-5	143
1,5517	-4	207	11,7439	21	260	-6,1179	22	-91	7,6260	13	155
3,0111	23	374	17,0292	17	348	-1,2308	11	-10	4,1935	2	82
3,8645	20	454	5,9225	6	139	-1,5923	-2	-30	37,3998	11	681
4,5788	-6	507	5,4206	10	132	-1,3895	5	-19	13,7217	0	253
4,9150	23	552	4,4949	15	117	-4,9830	14	-77	-2,0763	7	-35
2,7410	-1	334	0,3875	-5	5	-11,0493	23	-248	3,0598	20	78
2,1812	-6	274	4,8063	1	112	-8,4661	-7	-202	32,3036	10	595
7,0419	17	733	16,4472	24	343	-9,3883	21	-176	20,4317	17	390
10,2093	29	990	1,4762	25	60	-3,0628	25	-28	23,6745	1	434
5,5799	23	611	10,7245	-8	221	-5,5151	24	-76	21,0349	3	388
5,6149	15	610	0,5603	10	24	-10,3991	27	-200	1,6075	12	43
7,5910	3	772	16,2080	24	339	-9,9018	6	-236	34,2711	20	637
3,0428	1	365	18,9354	27	386	-5,0801	26	-65	-8,1984	4	-205
3,9380	7	454	4,3581	22	120	-3,4230	9	-52	7,6790	0	144

4,6356	4	517	2,7564	30	93	-8,2754	-9	-199	19,4579	8	364
10,1542	25	984	18,7639	13	374	-4,6787	29	-54	37,7287	13	688
4,0059	-10	452	17,3480	-8	337	-8,1311	12	-154	12,6164	1	234
6,1737	18	660	15,8317	-7	312	-1,7682	1	-30	11,0353	-4	201
4,0344	3	461	8,2514	30	203	-3,6596	6	-60	23,1772	1	425
5,1894	2	566	10,7598	8	233	-8,9757	3	-199	29,5946	-8	532
-0,1142	16	-5	10,1493	26	235	-10,4445	22	-214	8,3003	3	158
8,3312	27	843	6,5435	27	168	-7,3496	-10	-169	11,8869	11	230
6,5725	26	698	15,7059	29	334	-4,1749	20	-54	22,4229	5	415
1,0633	30	173	1,7257	21	62	-9,7737	14	-205	26,9519	12	503
-0,1214	-8	-34	0,6237	28	43	-4,2583	17	-59	22,1742	-1	405
7,9759	-5	800	9,0995	17	209	-10,1035	24	-195	29,6583	11	550
5,2092	30	582	9,6671	19	221	-6,1082	-7	-130	-8,2372	18	-177
6,5199	-7	678	2,8804	-5	65	-9,8613	18	-199	-5,7129	11	-113
6,1388	18	657	2,6942	-7	59	-5,6073	4	-103	-6,8217	-6	-170
7,3998	28	768	1,1827	-6	24	-8,7412	20	-158	-3,1700	10	-55
9,7201	-5	938	7,6795	5	173	-8,0991	-5	-184	33,0520	1	600
6,4899	26	691	7,9206	29	196	-9,6535	19	-189	17,8992	5	333
0,5814	-10	84	-0,0779	4	2	-6,5719	-9	-145	-2,2036	2	-43

Appendix D

Thermocouple Measurement with reference junctions at 0 °C											
Type R			Type T			Type E			Type J		
EMF (mV)	T_ref	T_hot	EMF (mV)	T_ref	T_hot	EMF (mV)	T_ref	T_hot	EMF (mV)	T_ref	T_hot
10,8381	0	1025	0,8299	0	21	-8,8988	0	-203	13,7217	0	253
8,7729	0	866	3,9066	0	92	-2,7872	0	-50	7,6790	0	144
10,2685	0	982	3,4484	0	82	-9,3314	0	-223	-2,9384	0	-61
10,3871	0	991	20,1934	0	389	-3,1520	0	-57	5,0517	0	96
8,0979	0	812	7,5146	0	166	-7,8987	0	-168	34,0426	0	616
1,0410	0	150	3,9066	0	92	-7,6996	0	-162	-1,0437	0	-21
1,4157	0	194	14,1680	0	288	-5,1919	0	-99	35,2903	0	637
2,3908	0	299	0,3516	0	9	-9,2135	0	-217	5,2146	0	99
-0,0906	0	-18	14,0529	0	286	-8,5609	0	-190	-0,7486	0	-15
1,0990	0	157	11,2922	0	237	-8,3328	0	-182	41,5180	0	738
2,6066	0	321	3,8604	0	91	73,8886	0	967	14,7204	0	271
0,0268	0	5	20,0704	0	387	53,3513	0	703	22,7308	0	416
7,6679	0	777	13,7661	0	281	8,1007	0	126	-2,8013	0	-58
0,0654	0	12	0,5495	0	14	5,7145	0	91	22,0135	0	403
8,0979	0	812	0,0776	0	2	69,1705	0	905	36,3726	0	655
10,1110	0	970	20,0704	0	387	49,0355	0	649	2,4269	0	47
5,2449	0	570	20,5015	0	394	51,3573	0	678	-0,3012	0	-6
1,7752	0	234	16,1501	0	322	25,4397	0	356	-3,4779	0	-73
0,7692	0	116	10,0916	0	215	4,6565	0	75	-2,0081	0	-41
3,0990	0	370	19,4570	0	377	5,5145	0	88	1,0191	0	20
5,5154	0	594	4,5133	0	105	23,7007	0	334	-3,0294	0	-63
6,9922	0	721	2,4682	0	60	25,5983	0	358	0,0504	0	1
7,3765	0	753	3,4939	0	83	41,5383	0	556	22,8964	0	419
9,8238	0	948	14,5720	0	295	71,5394	0	936	41,2014	0	733
0,3030	0	51	20,5015	0	394	62,1924	0	815	28,3469	0	517
2,0834	0	267	3,9991	0	94	64,9995	0	851	23,7249	0	434
1,9141	0	249	3,4030	0	81	24,4898	0	344	37,8961	0	680

3,7530	0	433	4,3722	0	102	25,3604	0	355	38,3269	0	687
1,4421	0	197	19,8861	0	384	53,7492	0	708	13,0000	0	240
9,6163	0	932	6,2552	0	141	37,0863	0	501	13,0000	0	240
1,1661	0	165	15,9733	0	319	70,8537	0	927	42,7270	0	757
-0,0906	0	-18	7,3105	0	162	25,2812	0	354	37,7121	0	677
10,8114	0	1023	6,6540	0	149	66,7824	0	874	-2,7553	0	-57
8,6468	0	856	12,8559	0	265	48,4737	0	642	2,6382	0	51
2,9872	0	359	1,6538	0	41	42,7514	0	571	0,9677	0	19
5,2449	0	570	19,2737	0	374	49,1959	0	651	-3,6104	0	-76
5,0994	0	557	7,3614	0	163	37,4100	0	505	4,0252	0	77
9,7589	0	943	4,9405	0	114	7,7541	0	121	35,4698	0	640
6,6247	0	690	11,7350	0	245	3,3013	0	54	40,3190	0	719
5,7087	0	611	17,3387	0	342	54,8618	0	722	27,1688	0	496
7,4612	0	760	12,4614	0	258	47,7507	0	633	-0,6000	0	-12
1,0990	0	157	16,3274	0	325	11,4418	0	173	3,6495	0	70
2,3714	0	297	2,4245	0	59	12,3167	0	185	42,4717	0	753
10,7847	0	1021	3,0875	0	74	65,2326	0	854	33,8656	0	613

Appendix E

Thermocouple Measurement with varying cold junction temperature											
Type R			Type T			Type E			Type J		
EMF (mV)	ITS-90 (mV)	T_hot	EMF (mV)	ITS-90 (mV)	T_hot	EMF (mV)	ITS-90 (mV)	T_hot	EMF (mV)	ITS-90 (mV)	T_hot
10,8381	10,838	1025	0,8299	0,83	21	-8,8988	-8,899	-203	13,7217	13,722	253
8,7729	8,773	866	3,9066	3,907	92	-2,7872	-2,787	-50	7,6790	7,679	144
10,2685	10,268	982	3,4484	3,448	82	-9,3314	-9,331	-223	-2,9384	-2,938	-61
10,3871	10,387	991	20,1934	20,193	389	-3,1520	-3,152	-57	5,0517	5,052	96
8,0979	8,098	812	7,5146	7,515	166	-7,8987	-7,899	-168	34,0426	34,043	616
1,0410	1,041	150	3,9066	3,907	92	-7,6996	-7,7	-162	-1,0437	-1,044	-21
1,4157	1,416	194	14,1680	14,168	288	-5,1919	-5,192	-99	35,2903	35,29	637
2,3908	2,391	299	0,3516	0,352	9	-9,2135	-9,214	-217	5,2146	5,215	99
-0,0906	-0,091	-18	14,0529	14,053	286	-8,5609	-8,561	-190	-0,7486	-0,749	-15
1,0990	1,099	157	11,2922	11,292	237	-8,3328	-8,333	-182	41,5180	41,518	738
2,6066	2,607	321	3,8604	3,86	91	73,8886	73,889	967	14,7204	14,72	271
0,0268	0,027	5	20,0704	20,07	387	53,3513	53,351	703	22,7308	22,731	416
7,6679	7,668	777	13,7661	13,766	281	8,1007	8,101	126	-2,8013	-2,801	-58
0,0654	0,065	12	0,5495	0,549	14	5,7145	5,714	91	22,0135	22,014	403
8,0979	8,098	812	0,0776	0,078	2	69,1705	69,171	905	36,3726	36,373	655
10,1110	10,111	970	20,0704	20,07	387	49,0355	49,035	649	2,4269	2,427	47
5,2449	5,245	570	20,5015	20,502	394	51,3573	51,357	678	-0,3012	-0,301	-6
1,7752	1,775	234	16,1501	16,15	322	25,4397	25,44	356	-3,4779	-3,478	-73
0,7692	0,769	116	10,0916	10,092	215	4,6565	4,656	75	-2,0081	-2,008	-41
3,0990	3,099	370	19,4570	19,457	377	5,5145	5,514	88	1,0191	1,019	20
5,5154	5,515	594	4,5133	4,513	105	23,7007	23,701	334	-3,0294	-3,029	-63
6,9922	6,992	721	2,4682	2,468	60	25,5983	25,598	358	0,0504	0,05	1
7,3765	7,376	753	3,4939	3,494	83	41,5383	41,538	556	22,8964	22,896	419
9,8238	9,824	948	14,5720	14,572	295	71,5394	71,539	936	41,2014	41,201	733
0,3030	0,303	51	20,5015	20,502	394	62,1924	62,192	815	28,3469	28,347	517
2,0834	2,083	267	3,9991	3,999	94	64,9995	65	851	23,7249	23,725	434
1,9141	1,914	249	3,4030	3,403	81	24,4898	24,49	344	37,8961	37,896	680

3,7530	3,753	433	4,3722	4,372	102	25,3604	25,36	355	38,3269	38,327	687
1,4421	1,442	197	19,8861	19,886	384	53,7492	53,749	708	13,0000	13	240
9,6163	9,616	932	6,2552	6,255	141	37,0863	37,086	501	13,0000	13	240
1,1661	1,166	165	15,9733	15,973	319	70,8537	70,854	927	42,7270	42,727	757
-0,0906	-0,091	-18	7,3105	7,31	162	25,2812	25,281	354	37,7121	37,712	677
10,8114	10,811	1023	6,6540	6,654	149	66,7824	66,782	874	-2,7553	-2,755	-57
8,6468	8,647	856	12,8559	12,856	265	48,4737	48,474	642	2,6382	2,638	51
2,9872	2,987	359	1,6538	1,654	41	42,7514	42,751	571	0,9677	0,968	19
5,2449	5,245	570	19,2737	19,274	374	49,1959	49,196	651	-3,6104	-3,61	-76
5,0994	5,099	557	7,3614	7,361	163	37,4100	37,41	505	4,0252	4,025	77
9,7589	9,759	943	4,9405	4,941	114	7,7541	7,754	121	35,4698	35,47	640
6,6247	6,625	690	11,7350	11,735	245	3,3013	3,301	54	40,3190	40,319	719
5,7087	5,709	611	17,3387	17,339	342	54,8618	54,862	722	27,1688	27,169	496
7,4612	7,461	760	12,4614	12,461	258	47,7507	47,751	633	-0,6000	-0,6	-12
1,0990	1,099	157	16,3274	16,327	325	11,4418	11,442	173	3,6495	3,65	70
2,3714	2,371	297	2,4245	2,425	59	12,3167	12,317	185	42,4717	42,472	753
10,7847	10,785	1021	3,0875	3,087	74	65,2326	65,233	854	33,8656	33,866	613
-0,1628	-0,163	-34	13,7661	13,766	281	10,5035	10,503	160	0,4050	0,405	8

Appendix F.1

```

function [y1] = Type_J_ThermoFcn(x1)
%TYPE_J_THERMOFCN neural network simulation function.
%
% 30-Aug-2018 23:34:44.%
% [y1] = Type_J_ThermoFcn(x1) takes these arguments:
% x = 2xQ matrix, input #1
% and returns:
% y = 1xQ matrix, output #1
% where Q is the number of samples.

%#ok<*RPMT0>

% ===== NEURAL NETWORK CONSTANTS =====

% Input 1
x1_step1.xoffset = [-9.35318363143181;-10];
x1_step1.gain = [0.0380062164930972;0.05];
x1_step1.ymin = -1;

% Layer 1
b1 = [-3.1957204495991407;-
2.9561682397139184;0.72406991335542414;1.4764589964920209;-
1.0684648875328424];
IW1_1 = [8.4116059433555943 0.24998504166793462;7.7618821407004583
0.23574223459283775;-0.14035704796217244 -
0.0054324299249743366;0.82730426660487533 0.032056168605518416;-
1.2435151945493277 -0.048195510008488311];

% Layer 2
b2 = [0.42584797930671148;-3.2422037231362473;-5.0079814593219369];
LW2_1 = [-3.2592248341409715 2.2017835885621695 -2.5112480782549529 -
0.67782740082033965 4.235815603877473;-0.0044378596620069837
0.0052114000124296733 -1.8138312924548463 4.8301396746704075
0.86805536390299598;1.1797553923805919 -6.2642707212977484 -
6.3061012104616241 0.71269149372791518 12.067872446705174];

% Layer 3
b3 = -0.12383316880726142;
LW3_2 = [-0.10316553920758917 3.0758300748226701 -1.9743852642515622];

% Output 1
y1_step1.ymin = -1;
y1_step1.gain = 0.00206185567010309;
y1_step1.xoffset = -210;

% ===== SIMULATION =====

% Dimensions
Q = size(x1,2); % samples

% Input 1
xp1 = mapminmax_apply(x1,x1_step1);

```

```

% Layer 1
a1 = tansig_apply(repmat(b1,1,Q) + IW1_1*xp1);

% Layer 2
a2 = tansig_apply(repmat(b2,1,Q) + LW2_1*a1);

% Layer 3
a3 = repmat(b3,1,Q) + LW3_2*a2;

% Output 1
y1 = mapminmax_reverse(a3,y1_step1);
end

% ===== MODULE FUNCTIONS =====

% Map Minimum and Maximum Input Processing Function
function y = mapminmax_apply(x,settings) y =
bsxfun(@minus,x,settings.xoffset);
    y = bsxfun(@times,y,settings.gain);
    y = bsxfun(@plus,y,settings.ymin);
end

% Sigmoid Symmetric Transfer Function
function a = tansig_apply(n,~)
    a = 2./ (1 + exp(-2*n)) - 1;
end

% Map Minimum and Maximum Output Reverse-Processing Function
function x = mapminmax_reverse(y,settings)
    x = bsxfun(@minus,y,settings.ymin);
    x = bsxfun(@rdivide,x,settings.gain);
    x = bsxfun(@plus,x,settings.xoffset);
end

```

Appendix F.2

```

function [y1] = Type_R_ThermoFcn(x1)
%TYPE_R_THERMOFCN neural network simulation function.
%
% 30-Aug-2018 20:10:09.%
% [y1] = Type_R_ThermoFcn(x1) takes these arguments:
% x = 2xQ matrix, input #1
% and returns:
% y = 1xQ matrix, output #1
% where Q is the number of samples.

%#ok<*RPMT0>

% ===== NEURAL NETWORK CONSTANTS =====

% Input 1
x1_step1.xoffset = [-9.35318363143181;-10];
x1_step1.gain = [0.0380062164930972;0.05];
x1_step1.ymin = -1;

% Layer 1
b1 = [0.49110613148313864;-4.0707722788709537;1.9797028855858321;-
2.3165560518494255;-2.2055564599678346];
IW1_1 = [0.31756876627275338 0.01216907736405304;-3.6797725027626158 -
0.14185490933283307;1.1785736977275978 -4.9090941640648795;-
1.4819669703057956 5.9633719976856225;-3.7576298845825868 -
0.14612140978604474];

% Layer 2
b2 = [0.71924886413673217;-1.5759933848585985;-0.07306204948841391];
LW2_1 = [1.3495705439189611 -0.75386232300268097 -0.98800277306787065
1.1646431325674504 -3.3222629615457904;1.7747436964417933 -
0.31393552275786507 -0.0011326026167509586 -0.00096054874905617893 -
0.011937529858994116;1.9013329012609581 -3.8441975310260439 -
0.030751405385407653 -0.026987787597518954 0.017389523966172531];

% Layer 3
b3 = -0.59529427355521891;
LW3_2 = [4.7285274175129939e-05 2.6393798712208327 1.7880404997411612];

% Output 1
y1_step1.ymin = -1;
y1_step1.gain = 0.00206185567010309;
y1_step1.xoffset = -210;

% ===== SIMULATION =====

% Dimensions
Q = size(x1,2); % samples
% Input 1
xp1 = mapminmax_apply(x1,x1_step1);
% Layer 1
a1 = tansig_apply(repmat(b1,1,Q) + IW1_1*xp1);
% Layer 2

```

```

a2 = tansig_apply(repmat(b2,1,Q) + LW2_1*a1);
% Layer 3
a3 = repmat(b3,1,Q) + LW3_2*a2;
% Output 1
y1 = mapminmax_reverse(a3,y1_step1);
end
% ===== MODULE FUNCTIONS =====
% Map Minimum and Maximum Input Processing Function
function y = mapminmax_apply(x,settings) y =
bsxfun(@minus,x,settings.xoffset);
y = bsxfun(@times,y,settings.gain);
y = bsxfun(@plus,y,settings.ymin);
end
% Sigmoid Symmetric Transfer Function
function a = tansig_apply(n,~)
a =2./ (1 + exp(-2*n)) - 1;
end
% Map Minimum and Maximum Output Reverse-Processing Function
function x = mapminmax_reverse(y,settings)
x = bsxfun(@minus,y,settings.ymin);
x = bsxfun(@rdivide,x,settings.gain);
x = bsxfun(@plus,x,settings.xoffset);
end

```

Appendix F.3

```

function [y1] = Type_T_ThermoFcn(x1)
%TYPE_T_THERMOFCN neural network simulation function.
%
% 03-November-2018 20:10:09.%
% [y1] = Type_R_ThermoFcn(x1) takes these arguments:
% x = 2xQ matrix, input #1
% and returns:
% y = 1xQ matrix, output #1
% where Q is the number of samples.

%#ok<*RPMT0>

% ===== NEURAL NETWORK CONSTANTS =====

% Input 1
x1_step1.xoffset = [-0.914346271382696;-10];
x1_step1.gain = [0.0904612998867249;0.05];
x1_step1.ymin = -1;

% Layer 1
b1 = [2.3695910760103582327;0.36978754244053091416;-
0.85569827983045865238;2.7819030466314016437;-3.0197540598338892259];
IW1_1 = [-1.5586173768715507748 -3.7040889002138772668;-
0.3750257030376670242 -0.024954342663195065721;2.5849882613984238589
2.5003595047438778032;0.97733814772277016747 0.065662195869926803793;-
0.18957122958990110795 0.28721656119632360538];

% Layer 2
b2 = [2.2060719753030353374;0.27278875960066123474;-3.0178356737378679853];
LW2_1 = [-0.00017855947179871590872 -1.1502730738210269479 -
2.7086743883620576406e-05 -1.2287381804824089038 1.3239839141695035618;-
0.00030133687465747565444 1.6449737756686595436 -0.00016034916663146178131
-2.2243481202138939423 -0.30197205981002112063;-2.7975767060876730596 -
1.4293430186634754619 2.3294233919455429316 0.16572495894353161949
2.7799778295614858692];

% Layer 3
b3 = -1.1688218164800976417;
LW3_2 = [1.6553222656154626957 -2.9687339126940814893 -
0.000339931044445808800364];

% Output 1
y1_step1.ymin = -1;
y1_step1.gain = 0.005;
y1_step1.xoffset = 0;

% ===== SIMULATION =====

% Dimensions
Q = size(x1,2); % samples
% Input 1
xp1 = mapminmax_apply(x1,x1_step1);
% Layer 1
a1 = tansig_apply(repmat(b1,1,Q) + IW1_1*xp1);

```

```

% Layer 2
a2 = tansig_apply(repmat(b2,1,Q) + LW2_1*a1);
% Layer 3
a3 = repmat(b3,1,Q) + LW3_2*a2;
% Output 1
y1 = mapminmax_reverse(a3,y1_step1);
end
% ===== MODULE FUNCTIONS =====
% Map Minimum and Maximum Input Processing Function
function y = mapminmax_apply(x,settings) y =
bsxfun(@minus,x,settings.xoffset);
y = bsxfun(@times,y,settings.gain);
y = bsxfun(@plus,y,settings.ymin);
end
% Sigmoid Symmetric Transfer Function
function a = tansig_apply(n,~)
a =2./ (1 + exp(-2*n)) - 1;
end
% Map Minimum and Maximum Output Reverse-Processing Function
function x = mapminmax_reverse(y,settings)
x = bsxfun(@minus,y,settings.ymin);
x = bsxfun(@rdivide,x,settings.gain);
x = bsxfun(@plus,x,settings.xoffset);
end

```

Appendix F.4

```

function [y1] = Type_E_ThermoFcn(x1)
%TYPE_E_THERMOFCN neural network simulation function.
%
% 03-November-2018 20:10:09.%
% [y1] = Type_R_ThermoFcn(x1) takes these arguments:
% x = 2xQ matrix, input #1
% and returns:
% y = 1xQ matrix, output #1
% where Q is the number of samples.

%#ok<*RPMT0>

% ===== NEURAL NETWORK CONSTANTS =====

% Input 1
x1_step1.xoffset = [-0.914346271382696;-10];
x1_step1.gain = [0.0904612998867249;0.05];
x1_step1.ymin = -1;

% Layer 1
b1 = [-0.31720603283965898012;2.1743939450111993139;-
0.18750284754824272926;2.6346429925536472005;4.0772235424854645913];
IW1_1 = [-0.082718985387574398005 -0.0017797274698325242764;
0.20307244842051216938 -0.68564276033515336728;0.11342447437015074074
0.0042783761702323858805;0.44844206616140036559 -
0.62857019254671364639;2.1093442743122237104 0.053246869763761577043];
% Layer 2
b2 = [-0.79485331974848705272;-0.70391048004113487835;-
0.46256252123350632965];
IW2_1 = [-0.90309850188499263268 -0.16546676903881518683
1.3156174168202814379 0.36692737126083313504 -0.44380467096548142925;
-1.5397599934107104591 0.087035532084973707412 0.64518315821542837618 -
0.28230905642625969687 -0.056434885334206902341;-5.223420270828670553
0.54886124833387295308 2.9166625646602191146 -0.69794018270488922262
1.6839783587996524084];
% Layer 3
b3 = 0.99012204847402307539;
IW3_2 = [2.8737621175139338447 4.3652518920400620317
3.6850914744647327304];

% Output 1
y1_step1.ymin = -1;
y1_step1.gain = 0.005;
y1_step1.xoffset = 0;

% ===== SIMULATION =====

% Dimensions
Q = size(x1,2); % samples
% Input 1
xp1 = mapminmax_apply(x1,x1_step1);
% Layer 1

```

```

a1 = tansig_apply(repmat(b1,1,Q) + IW1_1*xp1);
% Layer 2
a2 = tansig_apply(repmat(b2,1,Q) + LW2_1*a1);
% Layer 3
a3 = repmat(b3,1,Q) + LW3_2*a2;
% Output 1
y1 = mapminmax_reverse(a3,y1_step1);
end
% ===== MODULE FUNCTIONS =====
% Map Minimum and Maximum Input Processing Function
function y = mapminmax_apply(x,settings)
    y = bsxfun(@minus,x,settings.xoffset);
    y = bsxfun(@times,y,settings.gain);
    y = bsxfun(@plus,y,settings.ymin);
end
% Sigmoid Symmetric Transfer Function
function a = tansig_apply(n,~)
    a =2./ (1 + exp(-2*n)) - 1;
end
% Map Minimum and Maximum Output Reverse-Processing Function
function x = mapminmax_reverse(y,settings)
    x = bsxfun(@minus,y,settings.ymin);
    x = bsxfun(@rdivide,x,settings.gain);
    x = bsxfun(@plus,x,settings.xoffset);

end

```

Appendix G

Neural Network Layer	Function
Input 1	<code>xp1 = mapminmax_apply(x1,x1_step1);</code>
Layer 1	<code>a1 = tansig_apply(repmat(b1,1,Q) + IW1_1*xp1);</code>
Layer 2	<code>a2 = tansig_apply(repmat(b2,1,Q) + LW2_1*a1);</code>
Layer 3	<code>a3 = repmat(b3,1,Q) + LW3_2*a2;</code>
Layer 4	<code>a4 = repmat(b4,1,Q) + LW4_3*a3;</code>
Output 1	<code>y1 = mapminmax_reverse(a3,y1_step1);</code>

```

% ===== MODULE FUNCTIONS =====
% Map Minimum and Maximum Input Processing Function
function y = mapminmax_apply(x, settings)
    y = bsxfun(@minus, x, settings.xoffset);
    y = bsxfun(@times, y, settings.gain);
    y = bsxfun(@plus, y, settings.ymin);
end
% Sigmoid Symmetric Transfer Function
function a = tansig_apply(n, ~)
    a = 2 ./ (1 + exp(-2*n)) - 1;
end
% Map Minimum and Maximum Output Reverse-Processing Function
function x = mapminmax_reverse(y, settings)
    x = bsxfun(@minus, y, settings.ymin);
    x = bsxfun(@rdivide, x, settings.gain);
    x = bsxfun(@plus, x, settings.xoffset);
end

```

Appendix H

Neural Network Signal Conditioning of Thermocouples															
Type R				Type T				Type E				Type J			
EMF (mV)	Tref	Augmented ITS-90 T_hot	Neural Network T_hot	EMF (mV)	Tref	Augmented ITS-90 T_hot	Neural Network T_hot	EMF (mV)	Tref	Augmented ITS-90 T_hot	Neural Network T_hot	EMF (mV)	Tref	Augmented ITS-90 T_hot	Neural Network T_hot
6,3952	-1	670	669,99	13,2139	1	272	272,01	35,3660	14	490	489,97	23,3708	7	434	434,03
6,3686	4	670	669,99	12,3582	24	273	273,00	35,8264	9	492	491,97	23,1671	11	434	434,03
6,3245	12	670	669,99	13,0366	7	273	273,01	35,4285	17	493	492,97	24,2808	-10	435	435,05
6,2787	24	672	671,99	12,6003	18	273	273,01	36,8120	-5	494	493,99	23,5321	6	436	436,03
6,4446	-6	672	671,98	12,6803	16	273	273,01	36,5784	-1	494	493,99	23,5366	7	437	437,03
6,2904	24	673	672,99	12,1541	29	273	273,01	35,5696	16	494	493,97	23,3840	10	437	437,03
6,2959	27	675	674,99	12,3175	25	273	273,00	35,1056	25	495	494,98	23,5455	9	439	439,02
6,4863	-5	676	675,99	12,2929	27	274	274,01	36,8929	-5	495	494,99	23,9052	3	440	440,03
6,4225	7	676	675,99	12,2929	27	274	274,01	35,0033	28	496	496,00	24,5683	-8	442	442,03
6,4772	-1	677	676,99	12,2111	29	274	274,01	35,0229	29	497	497,01	23,3024	17	442	442,04
6,5184	-9	677	676,97	13,4052	-1	274	274,01	36,3118	9	498	497,98	23,3024	17	442	442,04
6,5199	-7	678	677,98	12,6973	17	274	274,01	36,0342	15	499	498,97	24,6236	-8	443	443,03
6,3608	22	678	678,00	12,2111	29	274	274,01	35,7329	20	499	498,97	24,1217	2	443	443,03
6,3724	20	678	678,00	13,5209	-4	274	274,01	35,2043	30	500	500,02	24,0206	4	443	443,02
6,3548	25	679	679,00	13,8078	-10	275	275,00	37,0863	0	501	500,99	24,6844	-7	445	445,03
6,4132	17	680	680,00	12,6740	19	275	275,01	37,5527	-8	501	500,99	24,6344	-6	445	445,03
6,5317	2	683	683,00	12,2680	29	275	275,01	37,0497	2	502	501,99	23,6733	13	445	445,03
6,4599	15	683	683,00	12,2680	29	275	275,01	36,9755	6	504	503,99	23,4684	17	445	445,04
6,5763	-2	685	684,99	13,6163	-5	275	275,01	35,8340	25	504	503,99	24,4893	-2	446	446,03
6,6123	-9	685	684,98	13,0499	11	276	276,01	37,4100	0	505	505,00	24,0390	8	447	447,02
6,6290	-10	686	685,97	13,6733	-5	276	276,01	36,3599	19	506	505,98	24,5948	-3	447	447,03
6,4070	30	686	685,98	13,3249	4	276	276,01	37,7832	-5	506	506,00	23,6858	16	448	448,03
6,5680	4	687	687,00	12,9707	13	276	276,01	36,0357	27	508	508,00	24,7557	-4	449	449,02
6,6064	-1	688	688,00	13,3037	6	277	277,01	38,0842	-6	509	509,00	24,2560	7	450	450,01
6,6272	-5	688	687,99	13,1070	11	277	277,01	36,6837	19	510	509,98	24,7158	-1	451	451,02
6,6033	4	690	690,00	12,5048	26	277	277,00	37,2449	11	511	510,98	23,6463	20	451	451,01
6,6247	0	690	690,00	12,5861	24	277	277,00	38,5589	-10	512	511,99	23,8560	17	452	452,03
6,4899	26	691	691,00	13,4000	5	278	278,01	38,1748	-2	513	513,00	24,4175	6	452	452,01
6,5136	24	692	692,00	12,7646	21	278	278,01	37,7257	7	514	513,99	23,7017	20	452	452,01
6,6547	1	693	693,00	13,7490	-4	278	278,01	37,2484	15	514	513,98	23,8086	19	453	453,02
6,6706	-2	693	693,00	12,8452	19	278	278,01	37,6284	10	515	514,99	25,0774	-6	453	453,02
6,6450	5	694	694,00	13,4390	4	278	278,01	37,6879	9	515	514,99	25,0774	-6	453	453,02
6,6069	14	695	695,01	13,8642	-7	278	278,01	37,4703	14	516	515,98	25,1883	-6	455	455,02
6,6073	16	696	696,01	13,5741	2	279	279,01	37,6497	11	516	515,99	24,4821	8	455	455,01
6,6577	7	696	696,00	13,9597	-8	279	279,00	37,7307	11	517	516,99	24,0735	16	455	455,03
6,5725	26	698	698,00	13,2212	11	279	279,01	38,2051	3	517	517,00	25,0432	-2	456	456,02
6,6489	17	700	700,01	13,8062	-4	279	279,01	38,6380	-3	518	518,01	24,8417	2	456	456,01
6,7622	3	703	703,00	13,9214	-7	279	279,01	38,8356	-5	519	519,00	24,5930	8	457	457,01
6,7888	-2	703	703,00	13,9402	-6	280	280,01	38,0757	12	522	521,99	24,6485	8	458	458,01
6,6612	21	703	703,01	13,9018	-5	280	280,01	39,1238	-3	524	524,01	24,2440	17	459	459,02
6,6197	28	703	703,00	13,4752	6	280	280,01	39,0878	-1	525	525,01	25,5654	-8	460	460,01
6,6197	28	703	703,00	13,3751	10	281	281,01	37,4317	28	526	526,03	25,3654	-4	460	460,01
6,6905	18	704	704,01	13,7661	0	281	281,01	37,6133	29	529	529,04	25,4763	-4	462	462,01
6,6791	22	705	705,01	13,8435	-2	281	281,01	39,7843	-6	530	530,01	24,7730	11	463	463,00
6,8484	-9	705	704,99	13,9206	-4	281	281,01	37,9388	25	530	530,01	24,7220	12	463	463,01
6,8347	-4	706	706,00	13,2564	13	281	281,01	37,9568	30	534	534,06	24,9814	8	464	464,00
6,7658	11	707	707,01	12,5697	30	281	281,01	40,0368	-2	536	536,02	25,6930	-5	465	465,00
6,7783	13	709	709,01	13,7661	0	281	281,01	38,4644	27	538	538,03	25,3509	4	467	467,00
6,8014	11	710	710,01	14,2078	-10	282	282,00	39,2932	16	540	540,00	25,2495	6	467	467,00
6,8518	4	711	711,01	13,9008	-2	282	282,01	40,7678	-9	540	540,01	25,2495	6	467	467,00
6,7736	18	711	711,02	13,5685	8	283	283,01	40,3099	3	543	543,02	24,6408	19	468	468,00
6,8992	-5	711	711,00	14,1121	-6	283	283,00	40,4276	1	543	543,02	24,5893	20	468	467,99
6,8039	23	716	716,02	14,2651	-10	283	283,00	38,8276	29	544	544,05	25,4718	6	471	470,99
6,8791	12	717	717,01	13,5291	9	283	283,01	40,2728	5	544	544,02	26,2758	-10	471	471,01
6,8099	24	717	717,02	13,0508	21	283	283,00	41,2304	-10	545	545,01	25,5322	7	473	472,99
6,8735	13	717	717,02	12,8480	26	283	283,00	41,1146	-8	545	545,02	26,3870	-10	473	473,01
6,9825	-5	718	718,00	13,9768	-1	284	284,00	40,6925	2	547	547,03	25,3331	12	474	474,00
6,8099	26	718	718,01	14,0154	-2	284	284,00	40,3593	9	548	548,02	25,1454	20	478	477,98
6,9922	0	721	721,01	12,9867	24	284	284,00	40,2436	15	551	551,01	26,4714	-5	479	478,99
6,9816	2	721	721,01	13,0678	22	284	284,00	40,8393	5	551	551,02	26,3209	-2	479	478,99
6,8754	23	722	722,02	13,0847	23	285	285,00	41,5383	0	556	556,03	25,3553	17	479	479,00
6,8636	27	723	723,01	13,1656	21	285	285,00	41,9923	-5	558	558,03	25,8661	7	479	478,98
6,9903	7	724	724,01	13,6620	10	286	286,01	41,6635	2	559	559,03	25,8710	8	480	479,98
6,9052	22	724	724,02	14,0529	0	286	286,00	41,3088	8	559	559,03	25,3597	18	480	479,99
6,9913	9	725	725,01	14,0142	1	286	286,00	41,4490	7	560	560,03	26,0282	6	481	480,98
6,9872	14	727	727,02	13,2230	21	286	286,00	40,7513	20	561	561,02	26,0332	7	482	481,98
7,0652	2	728	728,01	13,8584	5	286	286,00	40,5286	25	562	562,03	26,3873	0	482	481,99